De Novo and Bi-allelic Pathogenic Variants in *NARS1* Cause Neurodevelopmental Delay Due to Toxic Gain-of-Function and Partial Loss-of-Function Effects

Andreea Manole,[1,50] Stephanie Efthymiou,[1,50] Emer O'Connor,[1,50] Marisa I. Mendes,[2,50] Matthew Jennings,[3,50] Reza Maroofian,[1] Indran Davagnanam,[47] Kshitij Mankad,[4] Maria Rodriguez Lopez,[5] Vincenzo Salpietro,[1] Ricardo Harripaul,[6,7] Lauren Badalato,[8] Jagdeep Walia,[8] Christopher S. Francklyn,[9] Alkyoni Athanasiou-Fragkouli,[1] Roisin Sullivan,[1] Sonal Desai,[10] Kristin Baranano,[10] Faisal Zafar,[11] Nuzhat Rana,[11] Muhammed Ilyas,[12] Alejandro Horga,[1] Majdi Kara,[13] Francesca Mattioli,[16] Alice Goldenberg,[15] Helen Griffin,[3] Amelie Piton,[16] Lindsay B. Henderson,[17] Benyekhlef Kara,[18] Ayca Dilruba Aslanger,[18] Joost Raaphorst,[19,20] Rolph Pfundt,[19] Ruben Portier,[21] Marwan Shinawi,[22] Amelia Kirby,[23] Katherine M. Christensen,[23] Lu Wang,[24] Rasim O. Rosti,[24] Sohail A. Paracha,[25] Muhammad T. Sarwar,[25] Dagan Jenkins,[49] SYNAPS Study Group,[26] Jawad Ahmed,[25] Federico A. Santoni,[27,28] Emmanuelle Ranza,[27,29,30] Justyna Iwaszkiewicz,[31] Cheryl Cytrynbaum,[32] Rosanna Weksberg,[32] Ingrid M. Wentzensen,[17] Maria J. Guillen Sacoto,[17] Yue Si,[17] Aida Telegrafi,[17]

(Author list continued on next page)

Aminoacyl-tRNA synthetases (ARSs) are ubiquitous, ancient enzymes that charge amino acids to cognate tRNA molecules, the essential first step of protein translation. Here, we describe 32 individuals from 21 families, presenting with microcephaly, neurodevelopmental delay, seizures, peripheral neuropathy, and ataxia, with *de novo* heterozygous and bi-allelic mutations in asparaginyl-tRNA synthetase (*NARS1*). We demonstrate a reduction in *NARS1* mRNA expression as well as in NARS1 enzyme levels and activity in both individual fibroblasts and induced neural progenitor cells (iNPCs). Molecular modeling of the recessive c.1633C>T (p.Arg545Cys) variant shows weaker spatial positioning and tRNA selectivity. We conclude that *de novo* and bi-allelic mutations in *NARS1* are a significant cause of neurodevelopmental disease, where the mechanism for *de novo* variants could be toxic gain-of-function and for recessive variants, partial loss-of-function.

Introduction

The attachment of tRNA to cognate amino acids is essential for protein translation. Aminoacyl-tRNA synthetases (ARSs) are a group of enzymes encoded by ancient genes which are ubiquitously expressed and highly conserved.[1–3] These enzymes play a fundamental role in the esterification of proteinogenic amino acids to cognate tRNA. In total, 37 genes encoding ARS enzymes have been described. Of these, 20 encode enzymes that function in

[1]Department of Neuromuscular Disorders, University College London (UCL) Institute of Neurology, Queen Square, London, WC1N 3BG, UK; [2]Metabolic Unit, Department of Clinical Chemistry, Amsterdam University Medical Centers, Vrije Universiteit Amsterdam, Amsterdam Neuroscience, Amsterdam Gastroenterology and Metabolism, Amsterdam, 1081 the Netherlands; [3]Department of Clinical Neurosciences, University of Cambridge, Cambridge, CB2 0QQ UK; [4]Department of Neuroradiology, Great Ormond Street Hospital for Children, London, WC1N 3JH, UK; [5]Institute of Healthy Ageing, Department of Genetics, Evolution and Environment, University College London (UCL), London, WC1E 6BT, UK; [6]Campbell Family Mental Health Research Institute, Centre for Addiction and Mental Health, ON, M5T 1R8, Canada; [7]Institute of Medical Science and Department of Psychiatry, University of Toronto, Toronto, ON, M5T 1R8, Canada; [8]Department of Pediatrics, Queen's University, Kingston, ON, K7L 2V7, Canada; [9]Department of Biochemistry, University of Vermont College of Medicine, Burlington, VT 05405, USA; [10]Department of Neurology and Pediatrics, Johns Hopkins School of Medicine, Baltimore, MD 21205, USA; [11]Department of Pediatrics, Multan Hospital, Multan, 60000, Pakistan; [12]University of Islamabad, Islamabad, 45320, Pakistan; [13]Department of Pediatrics, Tripoli Children's Hospital, Tripoli, Libya; [14]University of Strasbourg, CNRS, GMGM UMR 7156, Strasbourg, 67083, France; [15]Département de Génétique, centre de référence anomalies du développement et syndromes malformatifs, CHU de Rouen, Inserm U1245, UNIROUEN, Normandie Université, Centre Normand de Génomique et de Médecine Personnalisée, Rouen, 76031, France; [16]Institute for Genetics and Molecular and Cellular Biology (IGBMC), University of Strasbourg, CNRS UMR7104, INSERM U1258, Illkirch, 67404, France; [17]GeneDx, 207 Perry Parkway Gaithersburg, MD 20877, USA; [18]Bezmiâlem Vakıf Üniversitesi, Istanbul, 34093, Turkey; [19]Department of Human Genetics, Donders Institute for Brain, Cognition and Behaviour, Radboud University Medical Center, 6500HB Nijmegen, the Netherlands; [20]Department of Neurology, Amsterdam Neuroscience Institute, Amsterdam University Medical Center, 1105AZ Amsterdam, the Netherlands; [21]Department of Neurology, Medisch Spectrum Twente, 7512KZ Enschede, the Netherlands; [22]Department of Pediatrics, Divisions of Genetics and Genomic Medicine, Washington University School of Medicine, St. Louis, MO, 63110, USA; [23]Division of Medical Genetics, SSM Health Cardinal Glennon Children's Hospital, Saint Louis University School of Medicine, St. Louis, MO 63104, USA; [24]Howard Hughes Medical Institute, University of California San Diego and Rady Children's Hospital, La Jolla, CA 92130, USA; [25]Institute of Basic Medical Sciences, Khyber Medical University, 25100 Peshawar, Pakistan; [26]SYNAPS Study Group, see Supplemental Information for the study group members who contributed clinical cases and data; [27]Department of Genetic Medicine and Development, University of Geneva, 1206 Geneva, Switzerland; [28]Department of Endocrinology, Diabetes, and Metabolism, University Hospital of Lausanne, 1011 Lausanne, Switzerland; [29]Service of Genetic Medicine, University Hospitals of Geneva, 1205 Geneva, Switzerland; [30]Medigenome, The Swiss Institute of Genomic Medicine, Geneva, CH-1207, Switzerland; [31]Swiss Institute of Bioinformatics, Molecular Modeling Group, Batiment Genopode, Unil Sorge, Lausanne, CH-1015, Switzerland; [32]Hospital for Sick

(Affiliations continued on next page)

Marisa V. Andrews,[22] Dustin Baldridge,[22] Heinz Gabriel,[33] Julia Mohr,[33] Barbara Oehl-Jaschkowitz,[34] Sylvain Debard,[14] Bruno Senger,[14] Frédéric Fischer,[14] Conny van Ravenwaaij,[35] Annemarie J.M. Fock,[35] Servi J.C. Stevens,[36] Jürg Bähler,[5] Amina Nasar,[8] John F. Mantovani,[45] Adnan Manzur,[49] Anna Sarkozy,[49] Desirée E.C. Smith,[2] Gajja S. Salomons,[2] Zubair M. Ahmed,[46] Shaikh Riazuddin,[37] Saima Riazuddin,[46] Muhammad A. Usmani,[46] Annette Seibt,[38] Muhammad Ansar,[27,48] Stylianos E. Antonarakis,[27,29,39] John B. Vincent,[6,7] Muhammad Ayub,[8] Mona Grimmel,[40] Anne Marie Jelsig,[41] Tina Duelund Hjortshøj,[41] Helena Gásdal Karstensen,[41] Marybeth Hummel,[42] Tobias B. Haack,[40,43] Yalda Jamshidi,[44] Felix Distelmaier,[38] Rita Horvath,[3] Joseph G. Gleeson,[24] Hubert Becker,[14,50] Jean-Louis Mandel,[16,50] David A. Koolen,[19,50] and Henry Houlden[1,50,*]

the cytoplasm, and the remainder relate exclusively to mitochondrial enzymes. Despite the essential canonical function and ubiquitous expression of ARS enzymes, mutations in these genes have been implicated in a variety of human diseases with both recessive and dominant inheritance patterns.[2,4–6] These mutations result in neurological disorders, ranging from mild late-onset peripheral neuropathy to severe multi-systemic neurodevelopmental disorders[4,5,7–9] (Table S1).

Mutations in cytoplasmic ARS-encoding genes cause peripheral nervous system degeneration resulting in Charcot-Marie-Tooth neuropathies (*GARS1* and *AARS1* [MIM: 601065]) and brain stem and spinal cord hypomyelination (*DARS1* [MIM: 603084]). ARSs, and ARSs interacting genes, including *DARS1*, *RARS1* (MIM: 107820), *AIMP1* (MIM: 603605), and *AARS1*, have been implicated in neurodevelopmental disorders and epilepsies. Furthermore, mitochondrial *ARS2* mutations are often associated with leukoencephalopathy (*AARS2* [MIM: 615889] and *DARS2* [MIM: 611105]) or pontocerebellar hypoplasia (*RARS2* [MIM: 611524]). More recently, recessive mutations in *FARSA* (MIM: 602918), *VARS1* (MIM: 192150), *CARS1* (MIM: 123859), and *TARS1* (MIM: 187790), with subsequent partial loss of the ARS protein, have been linked to neurodevelopmental phenotypes.[10–14] Modes of inheritance can be dominant or recessive; in cases such as *AARS1, YARS1* (MIM: 603623), *MARS1* (MIM: 156560), *HARS1* (MIM: 142810), and *GARS1,* both patterns can occur.[6]

The loss of function associated with mutations in ARSs is attributed to decreased aminoacylation efficiency or misfolding, causing protein instability with lower steady-state levels.[13] However, in some cases (*GARS1, YARS1,* and *AARS1*), it has not been possible to ascribe the phenotype to a loss of primary aminoacylation.[15–17] Overall, the physiological functions of ARS genes and previously identified disease associations indicate an essential biological role for these proteins, implying that defects in all ARSs incur disease.[6]

Asparaginyl-tRNA^{Asn} is generated by asparaginyl-tRNA synthetase (*NARS1* (MIM: 108410; RefSeq accession number NM_004539.4] in a reaction involving two steps. NARS1 first catalyzes the ATP-dependent activation of asparagine (Asn) into Asn∼AMP with the release of pyrophosphate, and then transfers the activated Asn onto tRNA^{Asn} with the release of AMP (Figure 1A). Here, we report the clinical phenotypes associated with *de novo* dominant and bi-allelic, autosomal recessive mutations in *NARS1* in 32 affected individuals from 21 families. We provide genetic proof for these mutations and analyze their impact through the use of individual cell lines, neural progenitor cells, and molecular modeling.

Subjects and Methods

Study Participants

Individuals were recruited via an international collaborative network of research and diagnostic sequencing laboratories. Samples and clinical information were obtained, with informed consent, from each institution using local institutional review board (IRB) ethics for functional analysis of human DNA and biomaterial. Clinical data collection involved a detailed review of medical records, photographs, videos, and phone interviews, as well as a clinical re-evaluation by a neurologist. Tables S2–S4 summarize the clinical and demographic details of the included cases.

Children, Division of Clinical and Metabolic Genetics, 555 University Ave., Toronto, M5G 1X8, Canada; [33]CeGaT GmbH and Praxis für Humangenetik Tuebingen, Tuebingen, 72076, Germany; [34]Biomedical Centre Cardinal-Wendel-Straße 14, 66424 Hamburg, Germany; [35]University of Groningen, University Medical Center Groningen, Department of Neurology, Groningen, 9713, the Netherlands; [36]Department of Clinical Genetics, Maastricht University Medical Centre, Maastricht, 6211, the Netherlands; [37]Jinnah Burn and Reconstructive Surgery Center, Allama Iqbal Medical College, University of Health Sciences, Lahore 54550, Pakistan; [38]Department of General Pediatrics, Heinrich-Heine-University, Moorenstr. 5, 40225 Düsseldorf, Germany; [39]iGE3 Institute of Genetics and Genomics of Geneva, 1211 Geneva, Switzerland; [40]Institute of Medical Genetics and Applied Genomics, University of Tuebingen, 72076 Tübingen, Germany; [41]Department of Clinical Genetics, University Hospital of Copenhagen, Rigshospitalet, 2100, Denmark; [42]Department of Pediatrics, Section of Medical Genetics, West Virginia University, Morgantown, WV 26506-9600, USA; [43]Centre for Rare Diseases, University of Tuebingen, 72076 Tübingen, Germany; [44]Genetics Centre, Molecular and Clinical Sciences Institute, St George's University of London, London, SW17 0RE, UK; [45]Division of Child Neurology, Washington University School of Medicine, St. Louis, MO, 63110, USA; [46]Department of Biochemistry and Molecular Biology, Johns Hopkins School of Medicine, Baltimore, MD 21205, USA; [47]Department of Brain Repair and Rehabilitation, UCL Institute of Neurology, Queen Square, London, WC1N 3BG, UK; [48]Institute of Molecular and Clinical Ophthalmology Basel, Basel Switzerland; [49]Institute of Child Health, Guilford Street and Dubowitz Neuromuscular Centre, Great Ormond Street Hospital for Children, London, WC1N 3JH, UK
[50]These authors contributed equally to this work
*Correspondence: h.houlden@ucl.ac.uk
https://doi.org/10.1016/j.ajhg.2020.06.016.

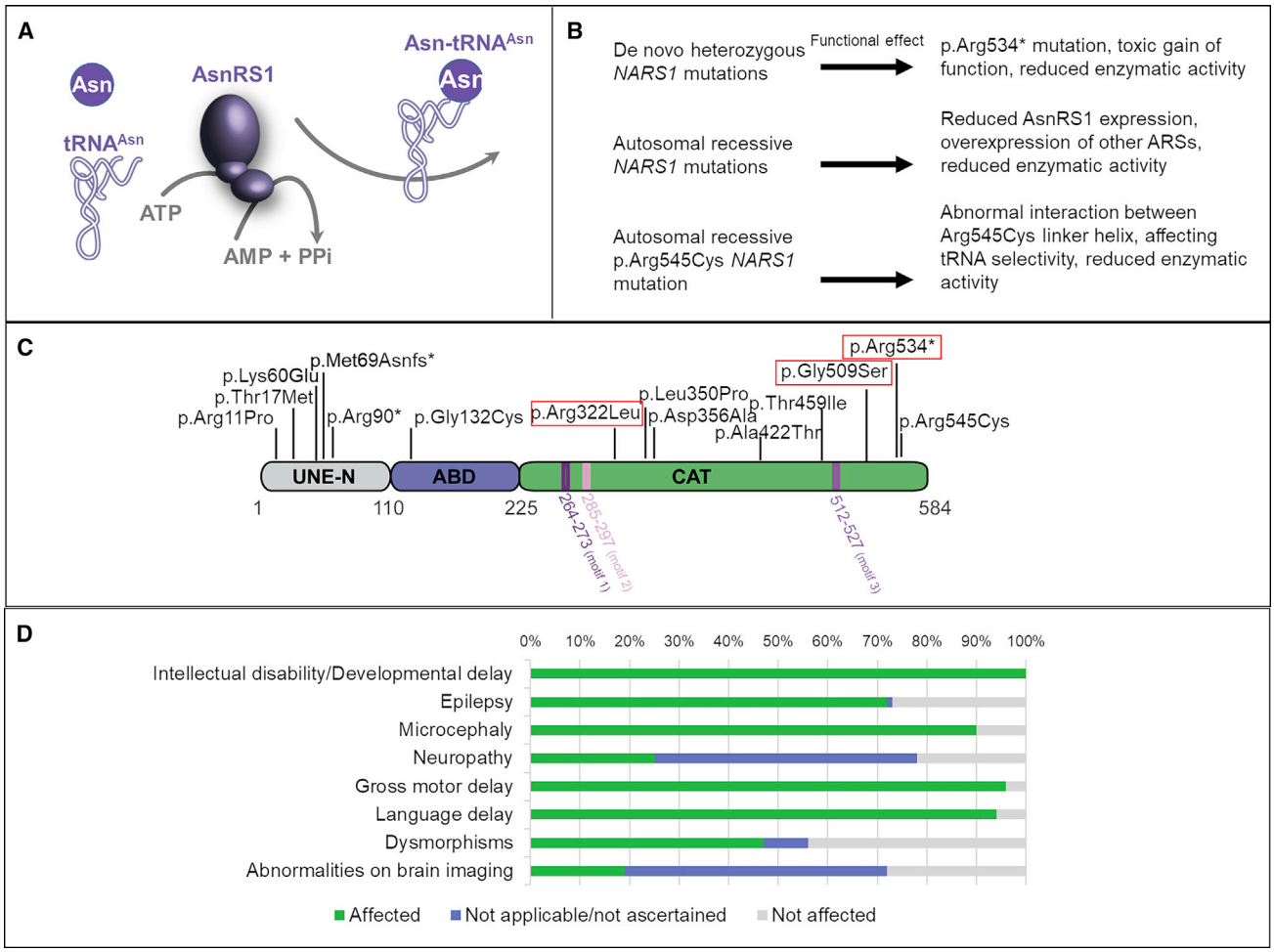

Figure 1. *AsnRS1* Protein Structure and Function
(A) AA asparagine (Asn) is ligated to $tRNA^{Asn}$ and catalyzed by AsnRS1 and ATP to produce Asn-tRNA (Asn), AMP, and pyrophosphate.
(B) *NARS1* mutations and their predicted functional effect.
(C) Schematic representation of human ARS1 primary structure. Three main domains are depicted: the unique domain (UNE-N), the anticodon binding domain (ABD), and the catalytic domain (CAT). The nature and position of the mutants are shown above the primary structure, *de novo* boxed in red, and the positions of the domains are indicated below, including motif 1 (involved in *AsnRS1* dimerization) and motifs 2 and 3 (which form the active site).
(D) Bar graph summarizing proportions of various clinical findings affecting individuals with *NARS1* mutations.

Sequencing

Exome sequencing was carried out using a number of methods in different centers with different analysis platforms and pipelines used (see Supplemental Methods, Section 2).

Bioinformatic Analysis

cDNA and protein sequence variants are described in accordance with the recommendations of the Human Genome Variation Society using Ensembl ENSG00000134440 and ENST00000256854.10 as the reference sequences. Evolutionary conservation of nucleotides was assessed using PhyloP (46 vertebrate species) and genomic evolutionary rate profiling (GERP) scores.[18] These were accessed through the University of California—San Francisco (UCSC) Genome Browser[19] using genomic coordinates from GRCh37/hg19. Grantham scores were used to assess the physicochemical nature of the amino acid (AA) substitutions. *In silico* analyses of sequence variants were performed using the pathogenicity prediction tools SIFT, PolyPhen-2, and Mutation Taster version 2.

Our bioinformatics filtering strategy screened for exonic and donor/acceptor splicing variants. In accordance with the pedigree and phenotype, priority was given to rare variants (<0.01% in public databases, including 1000 Genomes Project; National Heart, Lung, and Blood Institute [NHLBI] Exome Variant Server; Complete Genomics 69; and Exome Aggregation Consortium [ExAC v0.2]) fitting a recessive (homozygous or compound heterozygous) or a *de novo* model and/or variants in genes previously linked to epilepsy, developmental delay, intellectual disability, and other neurological disorders. Upon whole-exome sequencing (WES) analysis of the index family (F9), the *NARS1* variant c.1633C>T (p.Arg545Cys) was picked up according to its frequency and prediction tool scores (SIFT—damaging [score = 1], PolyPhen—damaging [score = 1], GERP—5.5, Mutation Taster—0.999992). All the candidate variants were further verified through the use of Sanger sequencing.

Generation of the nrs1 Vector

The pJR1-41XU-*nrs1* expression vector was used to express *Schizo-Saccharomyces pombe nrs1* by amplifying the coding sequence of *nrs1* from *S. pombe* DNA with the Nrs1-PJR-F and Nrs1-PJR-R primers (all primers are provided in Table S5) through the use of Phusion HF polymerase from New England Biolabs (NEB). The PCR product was cloned into XhoI digested pJR1-41XU[20] through the use of CloneEZ from Genscript. Plasmids were sequenced to confirm the correct insertion of the fragment.

Deletion of *nrs1* Gene in *S. pombe* Cells

JB775 (*h- ade6-M216 ura4-D18 leu1-32*) cells were synchronized, made competent, and transformed as previously described.[21] Cells were transformed using the plasmid containing the *nrs1* gene, pJR1-41XU-nrs1, and transformants were selected according to growth in Edinburgh minimal medium (EMM) + ade + leu, generating the strain MR397. The *nrs1* gene was deleted in MR397 cells through the use of the standard method via homologous recombination with the NatMx6 cassette[22,23] using the primers Nrs1DelFw and Nrs1DelRv (Table S5). Transformants were selected in EMM + Nat with no thiamine to promote the expression of the *nrs1* gene from the plasmid. Deletions were checked via PCR using primers Nrs1ck-L and kanR and Nrs1ck-R and kanF (Table S5). The strain generated was named MR409. MR409 cells were synchronized, made competent, and transformed as previously described.[21] The plasmids of the pJR-41XL series contained either the empty vector, wild-type *NARS1*, or the *NARS1* variants described. Transformants were selected in EMM + ade strains.

Cell Culture

Fibroblasts of affected individuals carrying the homozygous c.50C>T (p.Thr17Met), c.32G>C (p.Arg11Pro), and c.1633C>T (p.Arg545Cys) and compound heterozygous c.1067A>C (p.Asp356Ala) and c.203dupA (p.Met69Aspfs*4), as well as of corresponding controls, were grown in high-glucose Dulbecco's modified Eagle's medium (Sigma) supplemented with 10% fetal bovine serum and 1% penicillin and streptomycin.

Semiquantitative RT-PCR for Individual Lymphoblasts

Using TRIzol (Zymo research), as per manufacturer's instructions, total RNA was extracted from immortalized lymphoblasts available from P2 and parents. The concentration and purity of RNA was determined spectrophotometrically. 1 μg of RNA was reverse transcribed to first strand cDNA through the use of random primers and Moloney murine leukemia virus reverse transcriptase (Promega). GoTaq® Green Master Mix (Promega) was used and PCR reactions were performed with the following protocol: 95°C—2 min (95°C—30 s, 60°C—30 s, 73°C—1 min) for 35 cycles, 73°C—5 min, and 4°C hold. Two exponential curves representing the product formation were determined for both primer pairs. Cycles 28 and 29 were chosen for *NARS1* and *GAPDH*, respectively,we so that amplification rates were in the linear range for semiquantitative comparisons. Reactions were repeated in triplicate.

Western Blotting

For western blotting analysis, protein lysates were obtained from cultured fibroblasts and total protein concentration was measured by means of a Bradford assay. Aliquots of total protein (15 μg) were loaded on 4%–12% sodium dodecyl sulfate (SDS)-polyacrylamide gels (NuPAGE 4%–12% Bis-Tris Protein Gels, ThermoFisher Scientific), transferred to polyvinylidene fluoride membranes, and blocked and incubated overnight with a polyclonal antibody recognizing AsnRS1 (anti-rabbit 1:1000; Proteintech). Secondary antibody was added for 1 h, and signal was detected using enhanced chemiluminescence (ECL) reagents (Amersham Biosciences). Anti-beta-actin antibody (Sigma Aldrich, A3853; 1 in 5,000) was used as a loading control. Blots were repeated in triplicate and statistics were performed using Prism 6. Data are presented as mean ± standard error of the mean (SEM). The significance between the variables was shown based on the p value obtained (ns indicates $p > 0.05$, *$p < 0.05$, **$p < 0.005$, ***$p < 0.0005$, ****$p < 0.00005$).

Blue Native Polyacrylamide Gel Electrophoresis (BN-PAGE)

Fibroblast pellets were lysed using 10mM Tris (pH 8), 150mM NaCl, 0.1% NP40 with physical agitation for 30 min, centrifuged at 8,000xg to remove debris. The supernatant was removed, and total protein was quantified with the Bradford assay. Protein concentrations were equalized and prepared to 20μl at 1μg/μl using Native-PAGE sample buffer (Thermo) and 1ul of NuPAGE 5% G-250 Sample Additive (Thermo), and then loaded to a NativePAGE 3%–12% Bis-Tris Protein Gel (Thermo). Proteins were transferred to polyvinylidene fluoride (PVDF) membrane through the use of an iBlot2 PVDF Mini transfer stack (ThermoFisher Scientific) and probed with anti-NARS1 monoclonal antibody (Abcam ab129162, 1:5000) and glyceraldehyde 3-phosphate dehydrogenase (GAPDH; Santa Cruz). Blots were repeated in triplicate, and differences were analyzed using Welch-corrected t test.

Induced Neuronal Progenitor Cell (iNPC) Conversion

Based on the protocol published by Meyer et al.,[24] iNPCs were generated from primary fibroblasts by transduction with *Oct4-*, *Klf4,* and *c-Myc*-Sendai virus, followed by culturing in neuronal progenitor cell (NPC) induction media (1:1 DMEM/F-12: Neurobasal, 2× N2, 2× B27, 1% GlutaMAX, 10ng/mL hLIF, 3μM CHIR99021, and 2 μM SB431542). Neuroepithelial colonies were formed after 3–4 weeks of culturing. These were then isolated and expanded before we extracted total RNA from individual fibroblasts, age and sex matched healthy control fibroblasts, and iNPCs cells using the mirVana miRNA Isolation Kit (Ambion) for gene expression analysis by qPCR to confirm iNPC lineage and RNAseq in control and individual iNPCs in order to identify differentially expressed genes.

qPCR

Cell pellets from individual fibroblasts and iNPCs were lysed using a Trizol reagent. Following the addition of chloroform, the aqueous phase was transferred to RNeasy spin column (QIAGEN) for RNA isolation and resuspension. cDNA was generated using the reverse transcriptase kit (Applied Biosystems) and qPCR (Applied Biosystems 7900HT) was performed in triplicates using SYBR Green PCR Master Mix (Invitrogen, 4309155). Samples were normalized to expression of GAPDH and β-actin and repeated in triplicate.

RNaseq

Libraries were prepared using Illumina TruSeq Stranded Total RNA with Ribo-Zero Human kit and were sequenced on an Illumina HiSeq 2500 using a paired-end protocol. Quality of sequencing reads were ensured using FastQC. Reads were aligned using STAR aligner, and variants were called using the two-pass protocol outlined in the GATK documentation (see Web Resources). The numbers of

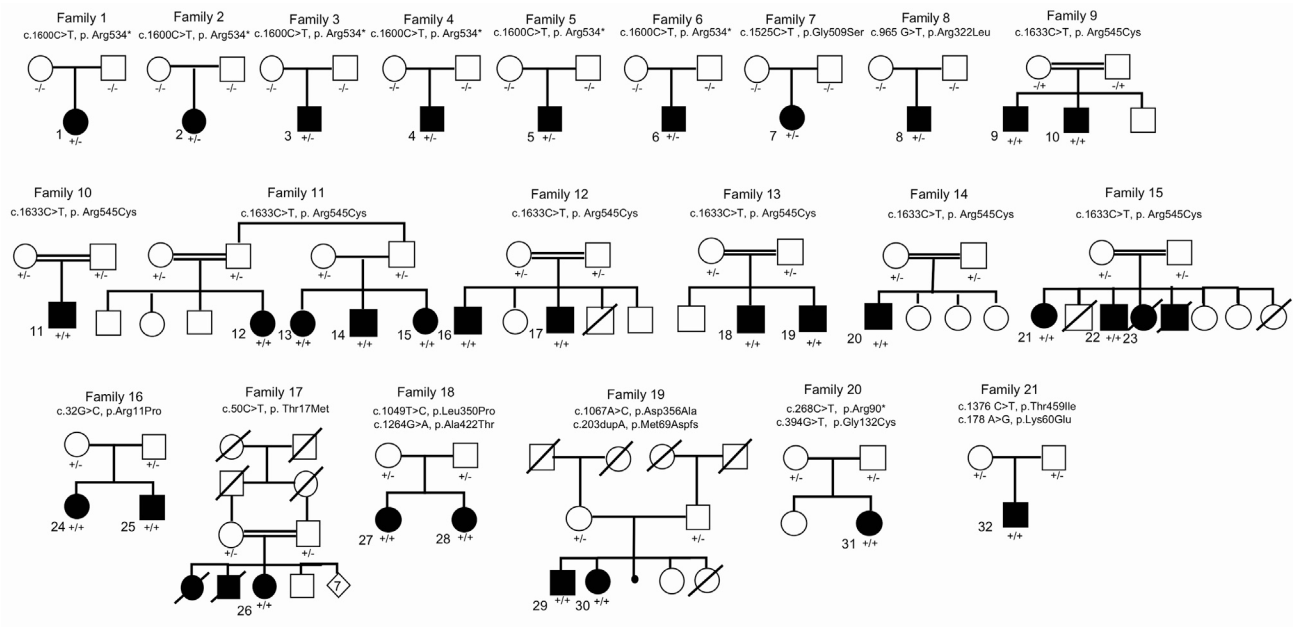

Figure 2. Pedigrees of the 21 Families and 32 Affected Individuals Identified in This Study with *de novo* and Bi-allelic Mutations in *NARS1*

Filled symbols represent affected individuals and double bars represent consanguinity in the family. −/−, +/−, and +/+ represent wild-type, heterozygous, and homozygous variants, respectively.

reads were counted using HTSeq-count.[25] Differentially expressed genes were identified using the DESeq2 Bioconductor package.[26] Differentially expressed genes with a false discovery rate of ≤ 0.1 and a $\log_2$ (fold change) ≥ 1 were considered significant. Gene set enrichment analysis was performed using the CPDB web tool.

NARS1 Enzyme Assay

Aminoacylation was assessed by measuring *NARS1* activity in cultured fibroblasts and lymphoblasts. Cell lysates (cytosolic fraction) were incubated in triplicate at 37°C for 10 min in a reaction buffer containing 50mmol/L Tris buffer pH 7.5; 12mmol/L $MgCl_2$; 25mmol/L KCl; 1 mg/mL bovine serum albumin; 0.5mmol/L spermine; 1mmol/L ATP; 0.2mmol/L yeast total tRNA; 1 mmol/L dithiothreitol; and 0.3mmol/L [$^{15}N_2$]-asparagine, [$^{13}C_4$,^{15}N]-threonine, [D_2]-glycine, [$^{15}N_2$]-arginine, and [D_4]-lysine. The reaction was terminated using trichloroacetic acid. Ammonia was then added to release the labeled AAs from the tRNAs. [$^{13}C_2$,^{15}N]-glycine and [$^{13}C_6$]-arginine were added as internal standards, and the labeled AAs were quantified via LC-MS/MS. Intra-assay variation was determined as <15% of TARS1, GARS1, RARS1 KARS1 activity which were simultaneously detected as control enzymes. AsnRS1 activities were measured blind, and testing was repeated in triplicate. Data are presented as mean ± SEM. The statistical significance of the difference of AsnRS1 activity between controls and affected individuals and/or carriers was determined using a Student's t test with a 95% confidence interval through the use of SPSS 26.

Molecular Modeling Analysis

The crystal structure of *Brugia malayi* AsnRS1 with a 65% identity to human AsnRS1, stored under the 2XGT code in the Protein Data Bank, was used for the molecular modeling analysis. The homology model of the dimeric human AsnRS1 overlapped with the *S. cerevisiae* DARS-tRNAAsp ligase, co-crystallized with tRNA molecule PDB 4WJ4, thus having a similar domain organization and sharing 27.5% of sequence identity with human AsnRS1. The protein was visualized with the University of California–San Francisco Chimera software.[27]

Results

Genetic Analysis

We identified 21 families (F1–F21) and 32 affected individuals (P1–P32) with mutations in *NARS1* (Figure 1B shows *NARS1* variant schematic and Figure 2 illustrates pedigrees). Eight families had *de novo* heterozygous variants; six had c.1600C>T (p.Arg534*) (F1–F6, P1–P6); one had c.1525G>A (p.Gly509Ser) (F7, P7); and one had c.965G>T (p.Arg322Leu) (F8, P8). These variants were not present in our 652 normal brain series or in the gnomAD database.

Bi-allelic variants were found in thirteen families. Seven have homozygous c.1633C>T (p.Arg545Cys) variants (F9–F15, P9–P23); one has homozygous c.50C>T (p.Thr17Met) (F17, P26); and one has two siblings with homozygous c.32G>C (p.Arg11Pro) (F16, P24 and 25). For compound variants, one family has two siblings with compound heterozygous c.1067A>C (p.Asp356Ala) and c.203dupA (p.Met69Aspfs*4) (F19, P29 and P30). Two siblings had compound heterozygous c.1049T>C (p.Leu350Pro) and c.1264G>A (p.Ala422Thr) variants (F18, P27 and P28). There was one case with the compound heterozygous variants c.268C>T (p.Arg90*) and c.394G>T (p.Gly132Cys) (F20, P31) and a final individual with compound heterozygous c.1376C>T (p.Thr459Ile) and

c.178A>G (p.Lys60Glu) variants (F21, P32). In gnomAD, c.1264G>A (p.Ala422Thr) is present in six heterozygote individuals, whereas c.1633C>T (p.Arg545Cys) and c.50C>T (p.Thr17Met) were present in five and four heterozygotes, respectively. The c.100 A>T (p.Met34Leu), c.203dupA (p.Met69Aspfs*4), and c.1049T>C (p.Leu350Pro) variants were absent, while c.32G>C (p.Arg11Pro) was present in one individual. The c.1067A>C (p.Asp356Ala) variant in family 19 was present in 264 heterozygotes, suggesting that this variant may modify the phenotype and be pathogenic only when in *trans* with a severe variant such as c.203dupA (p.Met69Aspfs*4).

Clinical Characteristics

Table 1 summarizes the core clinical features of affected individuals with *NARS1* defects (see Tables S2–S4 for additional details). All individuals had global developmental delay (GDD) and intellectual disability, which varied in severity from moderate to profound. They had marked delays in language development. Motor development was also severely impaired, and one individual never acquired autonomous ambulation. Microcephaly was observed in the majority of cases (90%). These cases predominantly presented with primary microcephaly; however, secondary microcephaly was also noted. Epilepsy was highly associated with the phenotype, affecting 23 cases (74.2%), with six individuals experiencing seizures below the age of one. The semiology of these attacks varied, with a mixture of partial, myoclonic, and generalized tonic-clonic seizures described. An ataxic gait, poor balance, and dysarthria were frequently detected on examination; this suggests an additional neurodegenerative process; however, no structural abnormality of the cerebellum was observed on imaging. A demyelinating peripheral neuropathy occurred in eight individuals (25%) who had distal leg muscle atrophy. Dysmorphic features described included abnormal hands (e.g., clinodactyly, fetal finger pad, two-to-three-toe syndactyly, slender fingers) and/or feet (e.g., small feet, toe syndactyly, slender feet). Upslanting palpebral fissures was the most common facial dysmorphism reported. A broad forehead, wide mouth, wide-set teeth, and low-set ears with overfolded helices were also described. Skeletal abnormalities including scoliosis, pronounced thoracic kyphosis, and *pes-cavus* were also noted. Behavioral traits associated with the phenotype included impulsivity, stereotypies with repetitive speech and/or hand movements, and selective feeding rituals.

Genotype-Phenotype Correlations

Family 16, with the homozygous variant c.32G>C (p.Arg11Pro), had a particularly severe clinical picture comprised of severe developmental delay, progressive microcephaly, refractory seizures from infancy, and arrested myelination with pronounced cerebral atrophy on MRI (see Supplemental Note, Table S3, and Figure 3).

Otherwise, imaging was normal apart from microcephaly. There was no common structural change across all cases. Individuals with the *de novo* c.1600C>T (p.Arg534*) variant showed severe microcephaly. In one family with this variant (F6), mild atrophy was observed (see Supplemental Information, Tables S2–S4, and Figure 3).

Individuals homozygous for c.1633C>T (p.Arg545Cys) demonstrated hypotonia and predominantly distal weakness. Spasticity was observed in individuals with the c.32G>C (p.Arg11Pro) or *de novo* variants.

A demyelinating polyneuropathy was documented in individuals homozygous for the c.1633C>T (p.Arg545Cys) variant (P9, P10, and P20), and in one case, this was confirmed with a sural nerve biopsy (F9, P9). It was also described in individuals with the *de novo* c.1600C>T (p.Arg534*) variant (P1, P2, and P5) and in the family with the compound heterozygous c.1049T>C (p.Leu350Pro) and c.1264G>A (p.Ala422Thr) variants (F18, P27 and P28).

Pathogenicity of *NARS1* Variants

NARS1 is intolerant to loss of function (missense variants constraint is $Z = 0.87$). We identified *de novo NARS1* mutations in eight families (F1–F8, P1–P8) with similar phenotypes. A variant at codon 534 recurred in six families (F1–F6, P1–P6). The two other *de novo* variants altered codons 322 and 509. The c.1600C>T (p.Arg534*) variant is located 15 AAs from the end of the 548-AA protein, representing a potential hotspot for pathogenic mutations. Arginine at codons 534 and 545 IS universally conserved in AsnRS1 from all three major taxonomic groupings, implying a significant structural or functional role.

The homozygous c.1633C>T (p.Arg545Cys) variant was observed in seven families with recessive disease. This variant affects the same C-terminal catalytic stretch as does c.1600C>T (p.Arg534*), and therefore it might have a comparable mechanistic effect to c.1600C>T (p.Arg534*).

The c.1067A>C (p.Asp356Ala) variant was found in *trans* with the only recessive truncating allele observed thus far at c.203dupA (p.Met69Aspfs*4) (P29 and P30). Two missense variants (c.965G>T [p.Arg322Leu] and c.653T>C, p.Asn218Ser) were found in P8; however, because c.965G>T (p.Arg322Leu) occurred *de novo*, it could not be determined whether these variants were in *cis* or *in trans*. Moreover, the frequency of c.653T>C (p.Asn218Ser) in the gnomAD database (78 heterozygotes) suggests it is unlikely to be associated with a severe phenotype, leaving c.965G>T (p.Arg322Leu) as the most likely disease-causing variant. The Arg322 residue is essential for enzymatic activity and therefore is predicted to cause impaired enzyme activity. Both the c.50C>T (p.Thr17Met) and c.32G>C (p.Arg11Pro) variants are in the N-terminal UNE-N appended domain of AsnRS1, which is specific to eukaryotes, and has recently been shown to have chemokine activity.[28]

Functional Characterization

Western Blotting and RT-PCR

Given the potential loss of function in homozygous *NARS1* individuals, we investigated gene expression levels

Table 1. Summary of *NARS1* Variants and Clinical Features of Affected Individuals

Variant: Nucleotide, Protein	c.1600C>T, p.Arg534*	c.1525G>A, p.Gly509Ser	c.965G>T, p.Arg322Leu	c.1633 >T, p.Arg545Cys	c.32G>C, p.Arg11Pro	c.50C>T, p.Thr17Met	c.1049T>C c.1264G>A, p.Leu350Pro p.Ala422Thr	c.1067A>C c.203dupA, p.Asp356Ala p.Met69Aspfs*4	c.268 C>T c.394G>T, p.Arg90* p.Gly132Cys	c.1376 C>T, c.178 A>G, p.Thr459Ile, p.Lys60Glu
Variant type	de novo heterozygous	de novo heterozygous	de novo heterozygous	homozygous	homozygous	homozygous	compound heterozygous	compound heterozygous	compound heterozygous	compound heterozygous
Inheritance	AD *de novo*	AD *de novo*	AD *de novo*	AR	AR	AR	AR	AR	AR	AR
Family	1–6	7	8	9–15	16	17	18	19	20	21
Affected Individual(s)	1–6	7	8	9–23	24–25	26	27–28	29–30	31	32
Ethnicity/country of origin	European	UK	European	Pakistan/North India	Kosovo	Libya	German	Turkey	Canada	USA
Age at onset	birth	birth	birth	childhood	childhood	birth	birth	birth	birth	childhood
Consanguinity	no	no	no	yes	no	yes	No	no	no	no
Presentation	severe GDD	severe GDD	severe GDD	severe GDD	seizures	seizures	mod GDD	mod GDD	severe GDD	severe GDD
ID	yes	yes	yes	yes	yes	yes	yes	yes	yes	yes
Microcephaly	yes	no	NA	yes	yes	yes	yes	yes	yes	yes
Dysmorphic	yes	yes	yes	yes	no	NA	no	no	yes	no
Seizures Affected Individuals	yes 1, 2, 4, 5, 6	yes	yes	yes 9, 14, 15, 18, 19, 21, 22, 23	yes all individuals	yes	yes 27	yes all individuals	yes	yes
Spasticity Affected Individuals	yes 3, 4, 6	no	yes	no hypotonia in 9, 10, 16, 17	yes 24	na	no hypotonia	na	no hypotonia	yes
Neuropathy Affected Individuals	Yes 1, 2, 5	NA	NA	yes 9, 10, 20	NA	NA	yes	NA	NA	NA
Ataxia Affected Individuals	yes all individuals	NA	Yes	yes 9–12, 21	NA	NA	yes	NA	yes	yes

AD = autosomal dominant, AR = autosomal recessive, GDD = global developmental delay, ID = intellectual disability Mod = moderate, NA = not available.

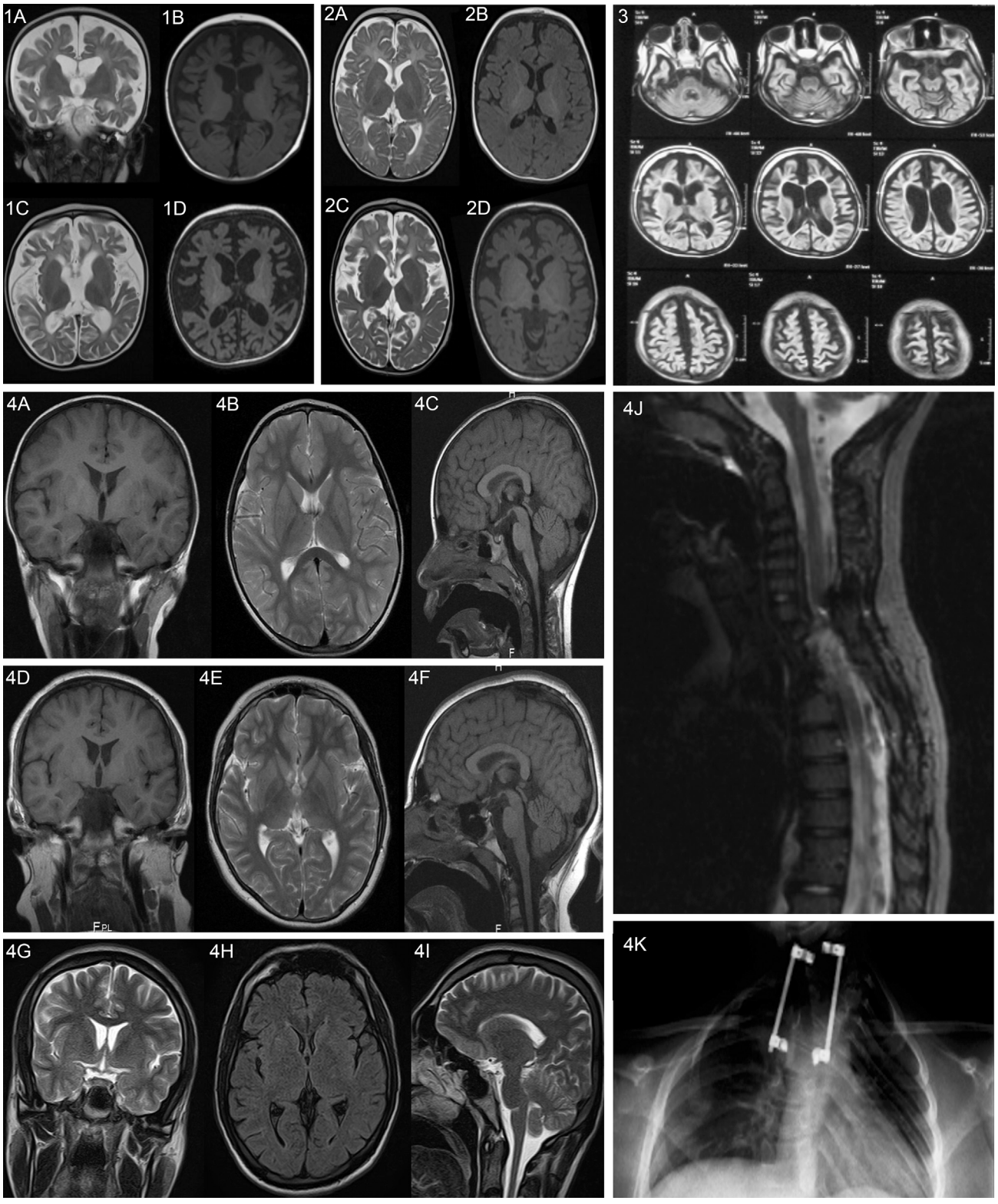

Figure 3. Radiological Findings of Individuals in Our Cohort
Set 1: Individual homozygous for c.32G>C (p.Arg11Pro). Upper row images (coronal T2-WI [1A] and axial T1-WI [1B]) at the age of 10 months show severely delayed myelination and fronto-temporal atrophy. Lower row images (axial T2-WI [1C] and axial T1-WI [1D]) repeated at the age of 18 months show progressive and global brain atrophy with an emerging pattern of severe hypomyelination. Set 2: An additional homozygous c.32G>C (p.Arg11Pro) individual. Upper row images (axial T2-WI [2A] and axial T1-WI [2B]) at the age of 8 months show mild fronto-temporal underdevelopment and severely delayed myelination. Lower row images (axial T2-WI [2C] and axial T1-W1 [2D]) repeated at the age of 2 years shows progressive and global brain atrophy along with severe hypomyelination.

(legend continued on next page)

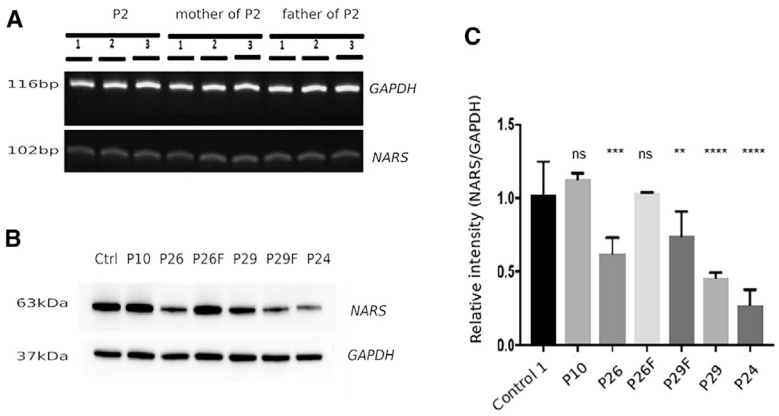

Figure 4. Protein Levels of AsnRS1 Are Reduced in Individual-Derived Cells
(A) RT-PCR of the *de novo* c.1600C>T (p.Arg534*) variant in P2 and parents (B) western blotting and (C) quantification graph of individuals with *NARS1* mutations compared with controls. Ctrl = control, P10 = homozygous c.1633C>T (p.Arg545Cys), P26 = homozygous c.50C>T (p.Thr17Met), P29 = compound heterozygous (c.1067A>C (p.Asp356Ala) and c.203dupA (p.Met69Aspfs*4) (F denotes father of individuals), P24 = homozygous c.32G>C (p.Arg11Pro).

through the use of semiquantitative PCR and protein levels through western blotting of AsnRS1 from lymphoblasts and fibroblasts from families harboring the p.Arg545Cys, p.Thr17Met, p.Asp356Ala, p.Met69Aspfs*4, and p.Arg11Pro variants. In all instances, both gene expression and protein levels are reduced (Figure 4A–4E).

iNPCs

iNPC colonies were produced and isolated from fibroblasts from P26 (c.50C>T), P29 (c.1067A>C), and P30 (c.203dupA). From the isolated colonies, gene expression was determined by using qPCR to select iNPC populations which presented decreased expression of fibroblast markers *COL1A1*, *COL3A1*, *TWIST2*, and *DKK3*, as well as increased numbers of NPC markers *NES*, *SOX1*, and *MSI1*, and the iNPC population was expanded to be subsequently used for RNA sequencing (RNaseq). RNaseq showed normal *NARS1* expression in iNPCs from affected individuals carrying the c.50C>T and c.1067A>C mutations, and decreased expression of the c.203dupA *NARS1* allele in the P29 cells. Interestingly, iNPCs from affected individuals show increased expression of several other ARSs (*DARS1, GARS1, RARS1, SARS1, TARS1, WARS1,* and *YARS1*) (Figure 5). This could be explained by the fact that the *NARS1* mutant(s) are inducing the integrated stress response (ISR), which activated a number of ARS genes as a result of the loss-of-function homozygous recessive variants. Impaired synthetase function may reduce the amount of charged tRNA available for translation elongation, with a possible increase in the levels of uncharged tRNA. Uncharged tRNAs produced as a result of AA deprivation have been reported to bind GCN2, leading to the activation of the ISR.[29]Analysis of the cellular pathways (Reactome, Gene Ontology) associated with genes with significantly altered mRNA levels showed that upregulated genes were enriched (adjusted p value < 0.01) for pathways heavily associated with protein translation and processing such as endoplasmic reticulum (ER) and Golgi protein processing and ribosomal homeostasis. In addition, increased action of VEGFR1/2 (upregulated by ATF4, which is one of the key transcription factors in the ISR) was suggested.

Blue-Native Polyacrylamide Gel Electrophoresis (BN-PAGE)

Similar to most other disease-associated ARSs, AsnRS1 functions as a class II homodimer.[30] We showed severely reduced dimer formation in P26 (c.50C>T [p.Thr17Met]) and P29 (c.1067A>C [p.Asn356Ala] and c.203dupA [p.Met69Aspfs*4]) compared to healthy controls (Figure 5E). The unaffected parents carrying one heterozygous mutation each also appeared to show a decreased level of the AsnRS1 dimer. P10 (c.1633C>T [p.Arg545Cys]) showed an AsnRS1 dimer amount comparable to that healthy controls. The decreased AsnRS1 dimer formation observed in fibroblasts from P26 and P29 shown by BN-PAGE accounts for the apparent deficit in aminoacylation capacity, despite showing no consistent decrease in the levels of AsnRS1 monomers. This idea is further supported by the molecular model simulation (Figure 6) that predicts an unstable dimer for the p.Asn356Ala mutant because this substitution is located at the interface between the two AsnRS1 monomers.

ARS Enzymatic Assays

In comparison with controls, AsnRS1 enzymatic activity was reduced in proband-derived fibroblasts and lymphoblasts. The most dramatic decrease was observed for P2 (*de novo* c.1600C>T [p.Arg534*]), and the mildest decrease was observed for P24 (c.32G>C [p.Arg11Pro], 80% of the controls). AA residue Arg11 is located in the 5′ end of the non-canonical UNE-N domain (Figure 7 and Figure S11), which has recently been shown to elicit cell migration of human immune cells via migration of CC chemokine

Set 3: Individual homozygous for c.50C>T (p.Thr17Met). Axial fluid-attenuated inversion recovery (FLAIR) images at the age of 9 months show global atrophy involving the cerebral and cerebellar hemispheres along with severe hypomyelination.
Set 4: MRI images of an individual with the homozygous c.1633C>T (p.Arg545Cyc) variant. Coronal T1-WI (4A), axial T2-WI (4B), and sagittal T1-WI (4C) at the age of 4 years; coronal T1-WI (4D), axial T2-WI (4E), and sagittal T1-WI (4F) at the age of 11 years; and coronal T2-WI (4G), axial FLAIR (4H), and sagittal T2-WI (4I) at the age of 20 years. These demonstrate normal intracranial appearances across the three different ages. This individual had an upper thoracic scoliosis, which was operatively corrected at the age of 4, demonstrated on the sagittal T2-WI of the spine (4J) and frontal projection radiograph of the chest/thoracic spine (4K).

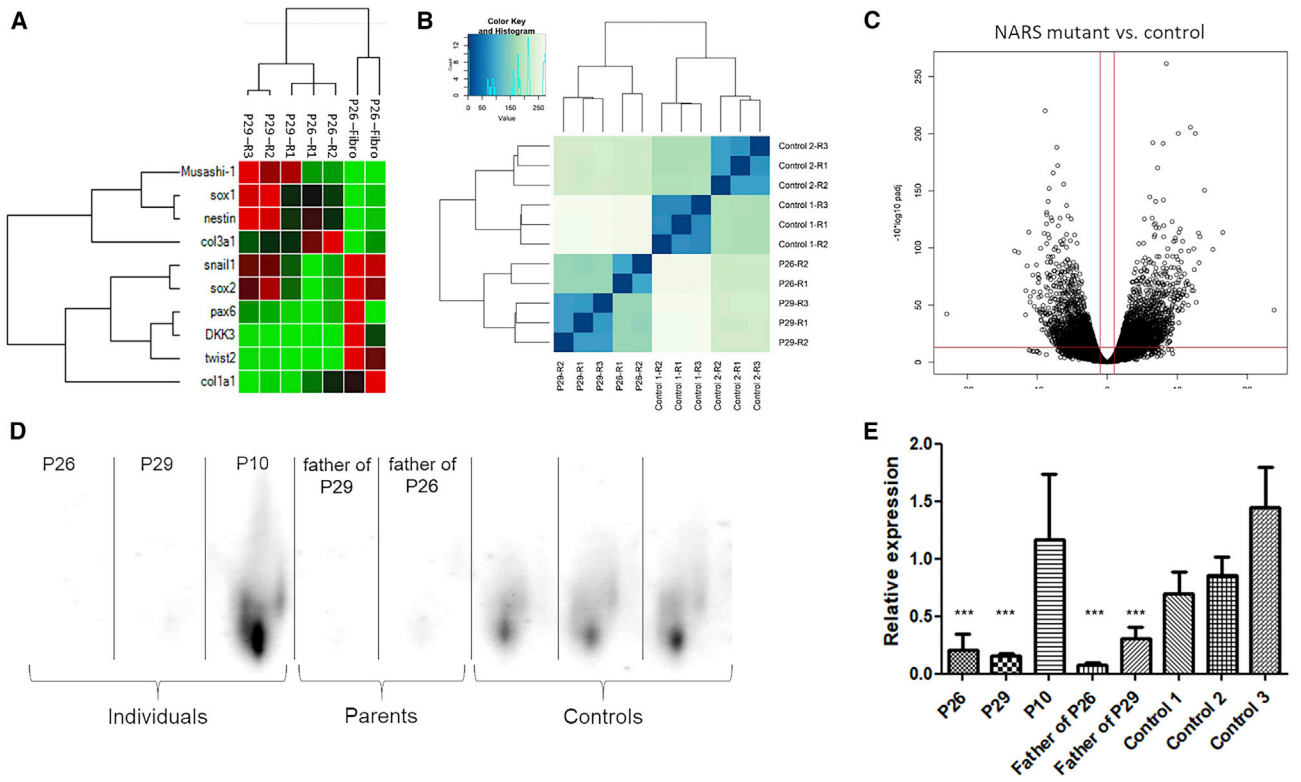

Figure 5. BN-PAGE and iNPC RNA-Sequencing

(A) iNPCs from P26 (c.50C>T [p.Thr17Met]) and P29 (c.203dupA [p.Met69Aspfs*4] and c.1067A>C [p.Asp356Ala]) exhibit increased expression of most iNPC markers (sox1, sox2, nestin, snail1, pax6, DKK3, twist2, and Musashi-1) compared to fibroblast (fbb) as measured by qPCR, shown with hierarchal clustering.

(B) Heatmap with hierarchal clustering generated using all gene counts from RNaseq distinction of control (Ctrl1 a–c, Ctrl2 a–c) and individual-derived (P26 a–b, P29 a–c) iNPCs.

(C) Volcano plot showing log2 of fold change in NARS mutant iNPCs compared to controls and −log10 (adjusted p value).

(D) BN-PAGE western blot showing reduced levels of the AsnRS1 dimer in individuals P26 and P29 and fathers compared to control, but not for individual P10.

(E) Quantification of BN-PAGE western blot AsnRS1 dimer formation, showing significantly (***$p < 0.001$) reduced levels of the AsnRS1 in individuals P26 and P29 and fathers compared to control but not change for P10.

P26 = homozygous c.50C>T (p.Thr17Met), P29 = c.203dupA (p.Met69Aspfs*4), c.1067A>C (p.Asp356Ala), P10 = c.1633C>T (p.Arh545Cys), father of P26 = heterozygous c.50C>T (p.Thr17Met), father of P29 = c.1067A>C (p.Asp356Ala).

receptor 3 (CCR3) in an autoimmune disease associated with ARS genes.[28]

Discussion

We identified *de novo* heterozygous and bi-allelic mutations in *NARS1* in 32 individuals with a neurodevelopmental phenotype. Mutations included recessive mutation hotspots affecting AA residues Arg534 and Arg545, respectively, both located in the last 40 AAs of the protein. Two homozygous variants identified at the 5′ end, c.32G>C (p.Arg11Pro) and c.50C>T (p.Thr17Met), were associated with a severe clinical phenotype. Other mutations in *NARS1* were spread throughout and did not cluster in any particular region of the gene.

The clinical phenotypes associated with homozygous variants c.32G>C (p.Arg11Pro) and c.50C>T (p.Thr17Met) correlate with reduced protein levels and could reflect impaired protein stability as suggested by the structural modeling of c.1633C>T (p.Arg545Cys) (Figure 6). Interestingly, MRI imaging of individuals harboring the c.32G>C (p.Arg11Pro) and c.50C>T (p.Thr17Met) variants showed atrophy and white matter abnormalities. In contrast, no such changes were identified in individuals with the p.Arg545Cys variant. The clustering of variants and associated phenotypes at the N and C termini suggests these regions are functionally important and disrupt the protein homodimer and ATP-binding and/or catalytic domain in *NARS1*. These two variants produced elevated AsnRS1 enzyme activity, which can be attributed to their location in the N-terminal extension domain. This domain has additional non-translational functions, enabling enzymatic activity of the modified protein. When we examine protein expression, protein synthesis, and the aminoacetylation activity, it is clear that the non-translational functions of such ARS proteins, regulated by the newly evolved appended domains such as UNE-N, don't seem necessary for ARS activity (Figure 7 and Figure S11).

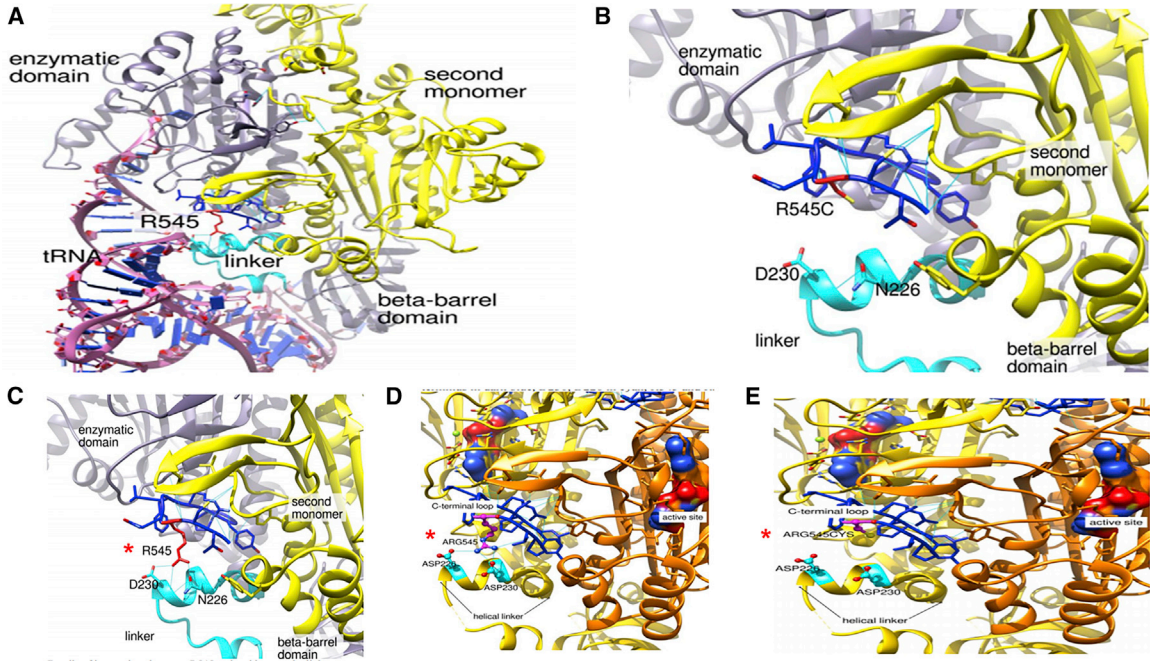

Figure 6. Molecular Modeling of the NARS1 p.Arg545Cys Homozygous Variant
The crystal structure is based on *B.malayi* AsnRS1. AsnRS1 is a homodimer; one AsnRS1 monomer is given in yellow and one in orange. Analog of the transition state presented in the surface representation, C terminus in dark blue, Asp230 and Asp226 in cyan, Arg545 and Arg545Cys in magenta.
(A) Interaction between *AsnRS1* and tRNA with residues on the helical linker.
(B–E) Zoom in on the C terminus helical linker region, (B) and (E) show loss of molecular interaction and folding of the p.Arg545Cys variant (*).

Our functional data, including fibroblasts and iNPCs transcriptomics, suggest that the majority of *NARS1* mutations cause a loss of the enzymatic protein by reduced expression and disruption of dimer formation. This results in abnormal protein synthesis and processing with a compensatory increase in expression of other ARSs (Figures 4, 5, and 7 and Figure S11). The increased activity of VEGFR1 and VEGFR 2 was of interest considering the reported actions of other ARSs, as in *GARS* and *EPRS* via GAIT complex, *SARS1*, *TARS1*, and mini *WARS1* on VEGF-related signaling.[31] Pathways associated with downregulated genes were typically associated with cell cycle progression, DNA repair and replication such as G2/M checkpoint, homology directed repair, and telomere maintenance pathways; this suggests that this alteration of cellular proliferation could be a result of decreased protein synthesis (Figures S5–S10). In general, the mutations in *NARS1* resulted in loss of function in both studied iNPC cell lines (P26 and P29), leading to a transcriptomic signature of induced ISR, upregulation of protein translation and processing in the ER and Golgi, and altered ribosomal homeostasis. This is similar to the results of other studies in cells with reduced aminoacylation activity in disease-associated mutations in other cytosolic ARSs.[5,31,32]

The recurrent homozygous c.1633C>T (p.Arg545Cys) variant in the western blot (Figure 4) and yeast model (Figure S12) showed near normal protein levels and an increased yeast growth suggestive of a gain-of-function mechanism. However, protein modeling of this variant demonstrated loss of the helix linker, and this indicates reduced tRNA interaction and catalytic activity. This loss-of-function effect was evidenced by the reduced aminoacylation activity to 40% compared to controls (Figure 7 and Figure S11). This effect could potentially be more harmful for cells of the nervous system than for a unicellular organism. One of the possibilities is that the *NARS1* mutant mischarges a tRNA in the human cells that might be less conserved in fungi. Thus, the mischarging would be reduced in yeast, hence the better growth without side effects. Molecular modeling has shown that the p.Arg545Cys variant lies within a region that probably interacts with the sugar-phosphate backbone of the tRNA (at positions 68–69), close to the active site of the enzyme.[33] Replacing the bulky arginine with a cysteine does not seems to perturb the enzyme's overall structure (Figure 6). However, by disrupting the tRNA-enzyme contact, this variant may alter the enzyme selectivity toward tRNA, decreasing the overall affinity for tRNA. AsnRS1 enzyme activity for individuals homozygous for this variant (P9 and P20) showed decreased activity (Figure 7 and Figure S11). Similarly, the *de novo* c.1600C>T (p.Arg534*) variant, located adjacent to the end of the protein, has a gain-of-function effect that interferes with normal protein function. It is likely a protein that lacks the 15 AAs containing the ATP-binding domain is produced. This region is crucial for enzymatic function, and it escapes

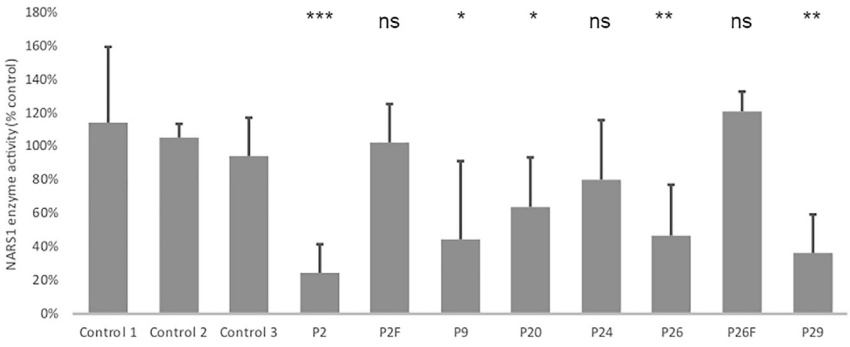

Figure 7. Reduced Asparaginyl-tRNA Synthetase Activity in Individuals with Homozygous *NARS1* Variants

c.1600C>T (p.Arg534*) (P2), c.1633C>T (p.Arg545Cys) (P9 and P20), c.32G>C (p.Arg11Pro) (P24), c.50C>T (p.Thr17Met) (P26), and c.1067A>C (p.Asp356Ala)/c.203dupA (p.M69Aspfs*4) (P29) *NARS1* variants in comparison to the average of three unrelated fibroblast cell lines. (All cell lines are fibroblast except P2, which is a lymphoblast cell line. Control values for lymphoblast are similar to fibroblasts.) n = 9, p value FDR < 0.01.

mRNA decay, as shown by semiquantitative RT-PCR from family 2 (Figure 4A). We further developed a zebrafish model of this variant (Figure S13) which elicits a dominant negative effect on the wild-type allele, causing a dose-dependent phenotype, specifically cyclopia and gastrulation defects at 200–500pg. Similar cyclopia defects in zebrafish were reported for microcephaly gene *ORC1*.[34]

Given the essential function and constraint metrics of *NARS1*, in conjunction with the clinical phenotypes of included individuals, we propose that genotypes with dominant heterozygous variants produce a toxic gain of function. This is compared with the homozygous recessive variants that probably experience a loss of function, though this can perhaps be least partially compensated for by other ARS genes. Taking into consideration the aminoacylation assay and yeast model for *de novo* mutations, and the western blot, aminoacylation assay, and modeling for homozygous recessive mutations, we have confirmed the pathogenicity of all *NARS1* mutations mentioned. Similar effects are seen in Aicardi-Goutières syndrome, which is caused by pathogenic variants in *ADAR* . There are relatively frequent alleles that are pathogenic when *in trans* to a null, but are never found in individuals with the homozygous state.[35] For distal C terminus mutations, such as the homozygous c.1633C>T (p.Arg545Cys) variant, the mechanism is likely due to abnormal protein structure and catalytic activity (Figures 1C and 6 and Figures S1 and S2).

Affected individuals had both central and peripheral nervous system involvement and a broad neurodevelopmental phenotype characterized by GDD, microcephaly, ataxia, neuropathy, and seizures. This is reflective of high *NARS1* expression in the cortex, cerebellum, and brainstem as demonstrated in mouse brains[36,37] (Figure S3). Mutations have been reported for the majority of ARSs. AsnRS2, a mitochondrial ARS protein coded by *NARS2*, has recently been linked with an overlapping phenotype consisting of multisystem mitochondrial disorder (MID). Intellectual disability, epilepsy in childhood, hearing loss, and myopathy have also been seen in *NARS1* individuals.[38–41] In addition, ARS interacting multifunctional proteins 1–3 (AIMP1–3) participate together with nine cytosolic ARSs to constitute the so-called multi-synthetase complex, and have also been associated with a variety of human diseases.[42] In considering their critical cellular functions, we expect that all ARSs will have a disease association.[7–9] The *NARS1* data bring the number of characterized ARSs to 35 out of 37. On a modified Taylor's Venn diagram of AA properties, *NARS1* is placed in close proximity to other AAs with similar properties (*IARS1, LARS1, DARS1, EPRS1, NARS1, RARS1,* and *QARS1*) which also have more severe phenotypes[43] (Figure S4).

Our functional work supports the likelihood that there is a loss-of-function mechanism in homozygotes and has helped to further understand the role of *NARS1* mutations in disease. The development of CRISPR/Cas9 heterozygous knockin and homozygous knockout animal models is the next important step in understanding the molecular rationale of these *NARS1* variants. Considering the high number of individuals and variants identified here, the addition of *NARS1* to genetic testing panels for children and young adults presenting with NDD, epilepsy, and/or a demyelinating neuropathy may be of clinical benefit.

Data and Code Availability

The variants reported in this paper have been submitted to the Leiden Open Variation Database, and the accession numbers are: LOVD: 668185, LOVD: 668186, LOVD: 668187, LOVD: 668188, LOVD: 668189, LOVD: 668190, LOVD: 668191, LOVD: 668192, LOVD: 668193, LOVD: 668194, LOVD: 668195, LOVD: 668196, LOVD: 668197, and LOVD: 668198.

Supplemental Data

Supplemental Data can be found online at https://doi.org/10.1016/j.ajhg.2020.06.016.

Acknowledgments

We are grateful to individuals and families for taking part in our research project. We heartfully thank James Burns for reading and correcting our manuscript. We thank the Gene Expression Nervous System Atlas (GENSAT) Project, National Institute of Neurological Disorders and Stroke (NINDS) contracts N01NS02331 and HHSN271200723701C to The Rockefeller University (New York, NY). H.H. is grateful to the Medical Research Council (MRC), The Wellcome Trust Synaptopathies Award, MRC Centre grant

G0601943, Ataxia UK, the Rosetrees Trust, Brain Research UK, the University College London (UCL) Official Development Assistance (ODA) and Low and Middle Income Country (LMIC) award, the Multiple System Atrophy (MSA) Trust, Muscular Dystrophy (MDUK). and the Muscular Dystrophy Association (MDA). This research was also supported by the UCL/UCL Hospital (UCLH) National Institute for Health Research University College London Hospitals Biomedical Research Centre.

Declaration of Interests

Maria J. Guillen Sacoto, Lindsay B. Henderson, Yue Si, Aida Telegrafi, and Ingrid M. Wentzensen are employees of GeneDx. The other authors declare no competing interests.

Received: February 25, 2020
Accepted: June 23, 2020
Published: July 30, 2020

Web Resources

1000 Genomes Project, https://www.genome.gov/27528684/1000-genomes-project
Complete Genomics 69, https://www.completegenomics.com/public-data/69-genomes/
CPDB web tool, http://cpdb.molgen.mpg.de/
Ensembl, http://www.ensembl.org/i
FastQC, http://www.bioinformatics.babraham.ac.uk/projects/fastqc/
GATK documentation, https://software.broadinstitute.org/gatk/
Human Genome Variation Society, http://www.hgvs.org
Mutation Taster version 2, http://www.mutationtaster.org/
National Heart, Lung, and Blood Institute (NHLBI) Exome Variant Server, https://evs.gs.washington.edu/EVS/
Picard, http://broadinstitute.github.io/picard/
PolyPhen-2, http://genetics.bwh.harvard.edu/pph2/
SIFT, http://sift.jcvi.org/
University of California—San Francisco (UCSC) Genome Browser, https://genome.ucsc.edu/

References

1. Lee, E.Y., Kim, S., and Kim, M.H. (2018). Aminoacyl-tRNA synthetases, therapeutic targets for infectious diseases. Biochem. Pharmacol. *154*, 424–434.
2. Ognjenović, J., and Simonović, M. (2018). Human aminoacyl-tRNA synthetases in diseases of the nervous system. RNA Biol. *15*, 623–634.
3. Rajendran, V., Kalita, P., Shukla, H., Kumar, A., and Tripathi, T. (2018). Aminoacyl-tRNA synthetases: Structure, function, and drug discovery. Int. J. Biol. Macromol. *111*, 400–414.
4. Antonellis, A., and Green, E.D. (2008). The role of aminoacyl-tRNA synthetases in genetic diseases. Annu. Rev. Genomics Hum. Genet. *9*, 87–107.
5. Meyer-Schuman, R., and Antonellis, A. (2017). Emerging mechanisms of aminoacyl-tRNA synthetase mutations in recessive and dominant human disease. Hum. Mol. Genet. *26* (R2), R114–R127.
6. Oprescu, S.N., Griffin, L.B., Beg, A.A., and Antonellis, A. (2017). Predicting the pathogenicity of aminoacyl-tRNA synthetase mutations. Methods *113*, 139–151.
7. Francklyn, C.S., and Mullen, P. (2019). Progress and challenges in aminoacyl-tRNA synthetase-based therapeutics. J. Biol. Chem. *294*, 5365–5385.
8. Rogers, S.O. (2019). Evolution of the genetic code based on conservative changes of codons, amino acids, and aminoacyl tRNA synthetases. J. Theor. Biol. *466*, 1–10.
9. González-Serrano, L.E., Chihade, J.W., and Sissler, M. (2019). When a common biological role does not imply common disease outcomes: Disparate pathology linked to human mitochondrial aminoacyl-tRNA synthetases. J. Biol. Chem. *294*, 5309–5320.
10. Okur, V., Ganapathi, M., Wilson, A., and Chung, W.K. (2018). Biallelic variants in *VARS* in a family with two siblings with intellectual disability and microcephaly: case report and review of the literature. Cold Spring Harb. Mol. Case Stud. *4*, a003301.
11. Stephen, J., Nampoothiri, S., Banerjee, A., Tolman, N.J., Penninger, J.M., Elling, U., Agu, C.A., Burke, J.D., Devadathan, K., Kannan, R., et al. (2018). Loss of function mutations in VARS encoding cytoplasmic valyl-tRNA synthetase cause microcephaly, seizures, and progressive cerebral atrophy. Hum. Genet. *137*, 293–303.
12. Siekierska, A., Stamberger, H., Deconinck, T., Oprescu, S.N., Partoens, M., Zhang, Y., Sourbron, J., Adriaenssens, E., Mullen, P., Wiencek, P., et al.; C4RCD Research Group; and AR working group of the EuroEPINOMICS RES Consortium (2019). Biallelic VARS variants cause developmental encephalopathy with microcephaly that is recapitulated in vars knockout zebrafish. Nat. Commun. *10*, 708.
13. Friedman, J., Smith, D.E., Issa, M.Y., Stanley, V., Wang, R., Mendes, M.I., Wright, M.S., Wigby, K., Hildreth, A., Crawford, J.R., et al. (2019). Biallelic mutations in valyl-tRNA synthetase gene VARS are associated with a progressive neurodevelopmental epileptic encephalopathy. Nat. Commun. *10*, 707.
14. Krenke, K., Szczałuba, K., Bielecka, T., Rydzanicz, M., Lange, J., Koppolu, A., and Płoski, R. (2019). FARSA mutations mimic phenylalanyl-tRNA synthetase deficiency caused by FARSB defects. Clin. Genet. *96*, 468–472.
15. Forrester, N., Rattihalli, R., Horvath, R., Maggi, L., Manzur, A., Fuller, G., Gutowski, N., Rankin, J., Dick, D., Buxton, C., et al. (2020). Clinical and Genetic Features in a Series of Eight Unrelated Patients with Neuropathy Due to Glycyl-tRNA Synthetase (GARS) Variants. J. Neuromuscul. Dis. *7*, 137–143.
16. Lee, A.J., Nam, D.E., Choi, Y.J., Nam, S.H., Choi, B.O., and Chung, K.W. (2020). Alanyl-tRNA synthetase 1 (AARS1) gene mutation in a family with intermediate Charcot-Marie-Tooth neuropathy. Genes Genomics *42*, 663–672.
17. Williams, K.B., Brigatti, K.W., Puffenberger, E.G., Gonzaga-Jauregui, C., Griffin, L.B., Martinez, E.D., Wenger, O.K., Yoder, M.A., Kandula, V.V.R., Fox, M.D., et al. (2019). Homozygosity for a mutation affecting the catalytic domain of tyrosyl-tRNA synthetase (YARS) causes multisystem disease. Hum. Mol. Genet. *28*, 525–538.
18. Cooper, G.M., Stone, E.A., Asimenos, G., Green, E.D., Batzoglou, S., Sidow, A.; and NISC Comparative Sequencing Program (2005). Distribution and intensity of constraint in mammalian genomic sequence. Genome Res. *15*, 901–913.
19. Kuhn, R.M., Karolchik, D., Zweig, A.S., Wang, T., Smith, K.E., Rosenbloom, K.R., Rhead, B., Raney, B.J., Pohl, A., Pheasant, M., et al. (2009). The UCSC Genome Browser Database: update 2009. Nucleic Acids Res. *37*, D755–D761.

20. Moreno, M.B., Durán, A., and Ribas, J.C. (2000). A family of multifunctional thiamine-repressible expression vectors for fission yeast. Yeast *16*, 861–872.
21. Rodríguez-López, M., Cotobal, C., Fernández-Sánchez, O., Borbarán Bravo, N., Oktriani, R., Abendroth, H., Uka, D., Hoti, M., Wang, J., Zaratiegui, M., and Bähler, J. (2017). A CRISPR/Cas9-based method and primer design tool for seamless genome editing in fission yeast. Wellcome Open Res. *1*, 19. https://doi.org/10.12688/wellcomeopenres.10038.3.
22. Bähler, J., Wu, J.Q., Longtine, M.S., Shah, N.G., McKenzie, A., 3rd, Steever, A.B., Wach, A., Philippsen, P., and Pringle, J.R. (1998). Heterologous modules for efficient and versatile PCR-based gene targeting in Schizosaccharomyces pombe. Yeast *14*, 943–951.
23. Sato, M., Dhut, S., and Toda, T. (2005). New drug-resistant cassettes for gene disruption and epitope tagging in Schizosaccharomyces pombe. Yeast *22*, 583–591.
24. Meyer, J., Novak, M., Hamel, A., and Rosenberg, K. (2014). Extraction and analysis of cortisol from human and monkey hair. J. Vis. Exp. *83*, e50882.
25. Anders, S., Pyl, P.T., and Huber, W. (2015). HTSeq–a Python framework to work with high-throughput sequencing data. Bioinformatics *31*, 166–169.
26. Love, M.I., Huber, W., and Anders, S. (2014). Moderated estimation of fold change and dispersion for RNA-seq data with DESeq2. Genome Biol. *15*, 550.
27. Pettersen, E.F., Goddard, T.D., Huang, C.C., Couch, G.S., Greenblatt, D.M., Meng, E.C., and Ferrin, T.E. (2004). UCSF Chimera–a visualization system for exploratory research and analysis. J. Comput. Chem. *25*, 1605–1612.
28. Park, J.S., Park, M.C., Lee, K.Y., Goughnour, P.C., Jeong, S.J., Kim, H.S., Kim, H.J., Lee, B.J., Kim, S., and Han, B.W. (2018). Unique N-terminal extension domain of human asparaginyl-tRNA synthetase elicits CCR3-mediated chemokine activity. Int. J. Biol. Macromol. *120* (Pt A), 835–845.
29. Dong, J., Qiu, H., Garcia-Barrio, M., Anderson, J., and Hinnebusch, A.G. (2000). Uncharged tRNA activates GCN2 by displacing the protein kinase moiety from a bipartite tRNA-binding domain. Mol. Cell *6*, 269–279.
30. Vijayakumar, R., and Tripathi, T. (2018). Soluble expression and purification of a full-length asparaginyl tRNA synthetase from Fasciola gigantica. Protein Expr. Purif. *143*, 9–13.
31. He, W., Bai, G., Zhou, H., Wei, N., White, N.M., Lauer, J., Liu, H., Shi, Y., Dumitru, C.D., Lettieri, K., et al. (2015). CMT2D neuropathy is linked to the neomorphic binding activity of glycyl-tRNA synthetase. Nature *526*, 710–714.
32. Boczonadi, V., Meyer, K., Gonczarowska-Jorge, H., Griffin, H., Roos, A., Bartsakoulia, M., Bansagi, B., Ricci, G., Palinkas, F., Zahedi, R.P., et al. (2018). Mutations in glycyl-tRNA synthetase impair mitochondrial metabolism in neurons. Hum. Mol. Genet. *27*, 2187–2204.
33. McClain, W.H., Schneider, J., Bhattacharya, S., and Gabriel, K. (1998). The importance of tRNA backbone-mediated interactions with synthetase for aminoacylation. Proc. Natl. Acad. Sci. USA *95*, 460–465.
34. Bicknell, L.S., Bongers, E.M., Leitch, A., Brown, S., Schoots, J., Harley, M.E., Aftimos, S., Al-Aama, J.Y., Bober, M., Brown, P.A., et al. (2011). Mutations in the pre-replication complex cause Meier-Gorlin syndrome. Nat. Genet. *43*, 356–359.
35. Schmelzer, L., Smitka, M., Wolf, C., Lucas, N., Tüngler, V., Hahn, G., Tzschach, A., Di Donato, N., Lee-Kirsch, M.A., and von der Hagen, M. (2018). Variable clinical phenotype in two siblings with Aicardi-Goutières syndrome type 6 and a novel mutation in the ADAR gene. Eur. J. Paediatr. Neurol. *22*, 186–189.
36. Melé, M., Ferreira, P.G., Reverter, F., DeLuca, D.S., Monlong, J., Sammeth, M., Young, T.R., Goldmann, J.M., Pervouchine, D.D., Sullivan, T.J., et al.; GTEx Consortium (2015). Human genomics. The human transcriptome across tissues and individuals. Science *348*, 660–665.
37. Consortium, G.T.; and GTEx Consortium (2015). Human genomics. The Genotype-Tissue Expression (GTEx) pilot analysis: multitissue gene regulation in humans. Science *348*, 648–660.
38. Seaver, L.H., DeRoos, S., Betz, B., and Rajasekaran, S. (2019). Reply to Finsterer Regarding Lethal NARS2-Related Disorder Associated With Rapidly Progressive Intractable Epilepsy and Global Brain Atrophy. Pediatr. Neurol. *93*, 65.
39. Simon, M., Richard, E.M., Wang, X., Shahzad, M., Huang, V.H., Qaiser, T.A., Potluri, P., Mahl, S.E., Davila, A., Nazli, S., et al. (2015). Mutations of human NARS2, encoding the mitochondrial asparaginyl-tRNA synthetase, cause nonsyndromic deafness and Leigh syndrome. PLoS Genet. *11*, e1005097.
40. Sofou, K., Kollberg, G., Holmström, M., Dávila, M., Darin, N., Gustafsson, C.M., Holme, E., Oldfors, A., Tulinius, M., and Asin-Cayuela, J. (2015). Whole exome sequencing reveals mutations in NARS2 and PARS2, encoding the mitochondrial asparaginyl-tRNA synthetase and prolyl-tRNA synthetase, in patients with Alpers syndrome. Mol. Genet. Genomic Med. *3*, 59–68.
41. Vanlander, A.V., Menten, B., Smet, J., De Meirleir, L., Sante, T., De Paepe, B., Seneca, S., Pearce, S.F., Powell, C.A., Vergult, S., et al. (2015). Two siblings with homozygous pathogenic splice-site variant in mitochondrial asparaginyl-tRNA synthetase (NARS2). Hum. Mutat. *36*, 222–231.
42. Boczonadi, V., Jennings, M.J., and Horvath, R. (2018). The role of tRNA synthetases in neurological and neuromuscular disorders. FEBS Lett. *592*, 703–717.
43. Taylor, W.R. (1986). The classification of amino acid conservation. J. Theor. Biol. *119*, 205–218.

The American Journal of Human Genetics, Volume *107*

Supplemental Data

De Novo and Bi-allelic Pathogenic Variants in *NARS1* Cause Neurodevelopmental Delay Due to Toxic Gain-of-Function and Partial Loss-of-Function Effects

Andreea Manole, Stephanie Efthymiou, Emer O'Connor, Marisa I. Mendes, Matthew Jennings, Reza Maroofian, Indran Davagnanam, Kshitij Mankad, Maria Rodriguez Lopez, Vincenzo Salpietro, Ricardo Harripaul, Lauren Badalato, Jagdeep Walia, Christopher S. Francklyn, Alkyoni Athanasiou-Fragkouli, Roisin Sullivan, Sonal Desai, Kristin Baranano, Faisal Zafar, Nuzhat Rana, Muhammed Ilyas, Alejandro Horga, Majdi Kara, Francesca Mattioli, Alice Goldenberg, Helen Griffin, Amelie Piton, Lindsay B. Henderson, Benyekhlef Kara, Ayca Dilruba Aslanger, Joost Raaphorst, Rolph Pfundt, Ruben Portier, Marwan Shinawi, Amelia Kirby, Katherine M. Christensen, Lu Wang, Rasim O. Rosti, Sohail A. Paracha, Muhammad T. Sarwar, Dagan Jenkins, SYNAPS Study Group, Jawad Ahmed, Federico A. Santoni, Emmanuelle Ranza, Justyna Iwaszkiewicz, Cheryl Cytrynbaum, Rosanna Weksberg, Ingrid M. Wentzensen, Maria J. Guillen Sacoto, Yue Si, Aida Telegrafi, Marisa V. Andrews, Dustin Baldridge, Heinz Gabriel, Julia Mohr, Barbara Oehl-Jaschkowitz, Sylvain Debard, Bruno Senger, Frédéric Fischer, Conny van Ravenwaaij, Annemarie J.M. Fock, Servi J.C. Stevens, Jürg Bähler, Amina Nasar, John F. Mantovani, Adnan Manzur, Anna Sarkozy, Desirée E.C. Smith, Gajja S. Salomons, Zubair M. Ahmed, Shaikh Riazuddin, Saima Riazuddin, Muhammad A. Usmani, Annette Seibt, Muhammad Ansar, Stylianos E. Antonarakis, John B. Vincent, Muhammad Ayub, Mona Grimmel, Anne Marie Jelsig, Tina Duelund Hjortshøj, Helena Gásdal Karstensen, Marybeth Hummel, Tobias B. Haack, Yalda Jamshidi, Felix Distelmaier, Rita Horvath, Joseph G. Gleeson, Hubert Becker, Jean-Louis Mandel, David A. Koolen, and Henry Houlden

Supplementary data

Contents

Section 1: Supplementary Clinical Data

Family 1: Individual 1: *NARS1* de novo mutation, c.1600C>T, p.Arg534*

The proband was a Dutch female born to healthy non-consanguineous parents. She had an uneventful perinatal course and was born with a normal weight for gestational age. Feeding difficulties were immediately apparent, requiring tube feeding in neonatal period. As an infant, she had global development delay (GDD), failing to meet developmental milestones in multiple areas of functioning. In terms of motor milestones, sitting was achieved aged 18 months and she began walking aged 36 months. She had severe delay in language development, speaking first words aged 2 year, and at follow-up aged 17 years, her vocabulary is limited to approximately 10 words. She was also found to have progressive microcephaly with an occipital frontal circumference (OFC) of 45.8 cm (2_{nd} percentile, -2.1 SD) at 3.5 years and 49 cm ($<1_{st}$ percentile, -5 SD) at 16 years. She had an MRI aged 4 years, which was otherwise unremarkable. Recurrent febrile seizure were reported aged of 11, 16, 23 and 33 months. As she grew older, she continued to exhibit signs of severe intellectual disability with limitations across all adaptive domains. Her examination was notable for a number of dysmorphic features including brachycephaly, deep-set eyes, upslanting palpebral fissures, short philtrum, long slender fingers and persistent fetal finger pads. She had bilateral pes cavus requiring surgical correction and a unilateral foot-drop. She was unable to fully co-operate in a neurological examination, but there was evidence of wasting distally in the upper and lower limbs, she also appeared ataxic on mobilising and had absent ankle reflexes bilaterally.

Family 2: Individual 2: *NARS1* de novo mutation, c.1600C>T, p.Arg534*

A Dutch female born to non-consanguineous parents. She presented with global developmental delay with failure to meet age-appropriate milestones, first sitting aged 16 months old and walking at 26 months. She spoke her first words aged 2 years and 6 months and continued to show profound speech delay. Now, as an adult, she speaks only a few words with a nasal pitch and has severe intellectual disability. Microcephaly was confirmed on examination with an OFC measuring 46.8 cm ($<1_{st}$ percentile, -4.3 SD) aged 8 years and 11 months. She has epilepsy, experiencing her first GTC seizure aged 3 years, with epileptiform discharges confirmed on EEG in the posterior temporal regions. On examination, she has several dysmorphic features including mild upslanting palpebral fissures, wide set teeth, a broad jaw, clinodactyly and marked thoracic kyphosis. She has severe bilateral foot drop with atrophy of the lower legs and intrinsic foot muscles. She is hypotonic with muscle weakness, which is more pronounced distally. Vibration and sensation are impaired to the level of the ankles. Her coordination is grossly normal but she has a slight intention tremor in the right upper limb. She has had several investigations including an MRI brain, aged 9 years, which was reported as normal. Nerve conduction studies confirmed a demyelinating polyneuropathy and muscle ultrasound indicated hyperechogenecity distally in lower limbs bilaterally.

Family 3: Individual 3: *NARS1* de novo mutation, c.1600C>T, p.Arg534*

The proband was a Dutch male born to healthy non-consanguineous parents. His pre-natal course was remarkable for inter-uterine growth retardation and oligohydramnios. At birth, he was found to have a low weight and OFC for gestational age. GDD was evident from early infancy as he failed to reach several milestones including gross motor parameters, walking for the first time aged 30 months. In particular, his speech was severely delayed. Now, aged 10 years his language is limited to short sentences with a notably nasal quality. Dysmorphic features were evident on follow-up examination including medial eyebrow flare, a short upturned nose, retrognathia and clinodactyly of his fifth fingers. He was notably dysarthric and had a bilateral tremor with occasional myoclonus. He was hypertonic with clonus at the knee and ankle. Power was reduced with weakness in a pyramidal distribution in the upper and lower limbs. He was hyperreflexic with upgoing plantar reflexes bilaterally.

Family 4: Individual 4: *NARS1* de novo mutation c.1600C>T, p.Arg534*

Caucasian male born to healthy non-consanguineous parents. He presented with his first seizure aged 4 months old, suffering from both partial and myoclonic seizures with associated EEG abnormalities. In addition, he has a dilated aortic root, which was diagnosed in infancy. He suffered from GDD. Gross motor skills were severely delayed, first sitting aged 16 months and never acquiring the ability to walk unaided. His speech was also profoundly delayed and is now limited to 1-2 words at the age of 13 years. On examination, he had a dysmorphic appearance with arachnodactyly, pectus excavatum, dolichostenomelia, long palpebral fissures and hypertelorism. He exhibited stereotypies with hand and mouth repetitive movements. He had microcephaly with an OFC of 49cm aged 13 years old ($<1_{st}$ percentile, -4.7 SD). His neurological examination was notable for severe spasticity in upper and lower limbs and impaired co-ordination.

Family 5: Individual 5: *NARS1* de novo mutation c.1600C>T, p.Arg534*

Female born to healthy non-consanguineous parents. Characterised by severe global developmental delay, with profound speech delay. Now aged 16 using she has only 1-2 word phrases. She first walked age 3 years. She had feeding difficulties in infancy requiring G-tube feeding. In terms of epilepsy, she had an initial seizure at 3 months of age continued to have both partial and generalized seizures throughout her childhood, which was well managed with levetiracetam. An EEG at 15 years was consistent with chronic static encephalopathy. Her examination was notable for microcephaly with a sloping forehead, slanting eyes, low set ears with fleshy helices, widely spaced teeth and small hands with tapered fingers. She walked with a broad based ataxic gait. There was wasting distally especially involving the extensor digitorum brevis. She was hypotonic in upper and lower limbs with distal weakness and hyporeflexia. She had impaired sensation to pinprick in the upper and lower limbs. Nerve conduction studies showed findings consistent with a demyelinating neuropathy.

Family 6: Individual 6: *NARS1* de novo mutation c.1600C>T, p.Arg534*

Male proband born to healthy non-consanguineous parents. He presented in infancy with neurodevelopmental delay (NDD), walking for the first time aged 23 months. His speech development was severely delayed and, now aged 8 years, he has a vocabulary limited to approximately 20 words. He began having seizures at 11 months, which were initially considered febrile seizures; however, these occurred recurrently throughout childhood and were classified as atypical febrile seizure. At this time, he underwent an EEG which failed to capture epileptiform activity. On examination he had microcephaly (<1st percentile, -3.25SD) and several dysmorphic features including a long philtrum, a thin upper lip, an everted lower lip, a wide mouth, midface hypoplasia and low set ears with overfolded helices. He also had syndactyly of his toes and short first toe bilaterally. His physical examination was notable for a broad-based ataxic gait and increased tone in the lower limbs bilaterally with hyperreflexia and clonus. MRI brain showed mild cortical atrophy with enlargement of the CSF space at 8 months however subsequent imaging aged 3 years was unremarkable for structural abnormalities.

Family 7: Individual 7: *NARS1* de novo mutation c.1525G>A, p.Gly509Ser

The proband was a British female born to non-consanguineous parents. Of note, exome sequencing also revealed a complex X chromosome rearrangement. She first presented at 9 months with focal seizures with secondary generalisation. She subsequently underwent EEG, which failed to capture epileptiform discharges. She had GDD, failing to reach a number of developmental milestones, resitting for the first time aged 12 months and walking aged 27 months with severe delays in speech. She persisted to have learning difficulties throughout her childhood and suffered with chronic constipation. On examination, she was normocephalic. Dysmorphic features included broad forehead, large ears, tented upper lip, long and slender fingers, slender feet, hypermetropia and a unilateral convergent squint. She was hypotonic with brisk DTR and down-going plantars. She unexpectedly died while sleeping aged 10 years 8 months. Autopsy showed a normally formed brain with focal calcification of basal ganglia and dentate nucleus.

Family 8: Individual 8: *NARS1* de novo mutation c.965 G>T, p.Arg322Leu

The proband is a 15 year old male of mixed race (German-Irish / English-Native American/ Russian-Polish heritage) born to healthy parents. In infancy, he had feeding difficulties and was slow to reach motor milestones, sitting aged 8 months and walking at 35 months. His speech was profoundly delayed speaking first words aged 8-9 years old. He has intractable epilepsy characterised by both absence and myoclonic seizures, confirmed on EEG with slow wave bursts with spike & poly-spike bursts. On examination, dysmorphic features included a prominent nose and broad forehead. He is dysarthric with limited speech, which mostly consists of repetitive phrases. He had increased tone in the lower limbs bilaterally and hyperreflexia throughout. Vibration and sensation were intact. Co-ordination was impaired with both appendicular and axial ataxia. MRI was unremarkable for structural abnormalities.

Family 9: Individual 9 and 10: *NARS1* Homozygous mutation c.1633C>T, p.Arg545Cys

The proband, individual 9, is a 33 year old male of Indian descent, born to consanguineous parents. He had a normal prenatal course and uncomplicated birth. He failed to meet developmental milestones in infancy, with severe delays in speech and fine motor skills. He began having generalised tonic-clonic seizures aged one year, which were poorly controlled with anti-epileptic agents and persisted into adulthood. Contractures in his lower limbs required him to undergo a tendon lengthening procedure aged 14 years. Additionally, he has severe sensory and motor neuropathy with NCV showing complete absence of sensory action potentials in the upper limbs, and absent motor action potentials in the upper and lower limbs. On examination, he is microcephalic and has bilateral foot drop with a left sided foot deformity consistent with a Charcot joint. He wears AFOs to enable ambulation and has a broad-based ataxic gait. There are contractures of his fingers bilaterally and evidence of muscle atrophy distally. He is hypotonic with reduced power proximally (3/5) with a pronounced weakness distally (2/5). He is areflexic and has impaired sensation to pinprick to the level of elbows and ankles in the upper and lower limbs respectively. His younger brother, individual 10, is similarly affected. He also had an unremarkable prenatal course and birth

but failed to meet expected developmental milestones. As an older child, he had learning difficulties requiring special schooling. He has no history of seizures. He has scoliosis, a broad based gait and difficulty walking. Nerve conduction velocities revealed a demyelinating neuropathy in upper and lower limbs.

Family 10: Individual 11: *NARS1* Homozygous mutation c.1633C>T, p. Arg545Cys

The proband, is an 8 year old male born to consanguineous parents from Pakistan. As an infant, he initially had feeding difficulties, choking and regurgitating with feeds. He failed to meet developmental milestones with severe delays in gross motor skills, sitting at 12 months and walking at 24 months. Speech was also severely delayed and now, aged eight, his vocabulary is limited to a few sentences. On examination, he had severe microcephaly with an OFC of 46.5cm (<1p, -4.2 SD). He had fifth finger clinodactyly bilaterally and toe syndactyly of the right foot. Neurological examination was limited in a setting of intellectual disability. There was no evidence of wasting. He had a broad based gait and poor balance with difficulty running. Patellar reflexes were 3+ bilaterally; otherwise reflexes were normal with down-going plantars. His MRI was unremarkable for structural abnormalities.

Family 11: Individuals 12-15: *NARS1* Homozygous mutation c.1633C>T, p.Arg545Cys

The proband is 17-year-old female born to Pakistani parents. She has severe intellectual disability across all adaptive domains. As a child, she was slow to meet several developmental milestones, sitting for the first time at 12 months and walking at 20 months. She also had difficulty feeding, choking regularly. She has microcephaly with and OFC of 49.5 cm (<1p,-4.5 SD). She has no history of seizures. Her physical examination is notable for reduced power (3/5) in all muscle groups with and an ataxic gait. She has no evidence of wasting or impaired sensation. She has two siblings, an older brother and sister and a female cousin who are similarly affected with GDD in childhood and severe intellectual disability. Additionally, her older brother and sister also have epilepsy characterised by generalised tonic clonic seizures and her eldest sibling is the most severely affected with profound intellectual disability.

Family 12: Individuals 16-17: *NARS1* Homozygous mutation c.1633C>T, p.Arg545Cys

The proband is a male born to consanguineous parents was reviewed aged 8 years. He has severe intellectual disability with a history of GDD, including severe delay in meeting motor milestones, walking for the first time age 6.5 years. He also had severe speech delay and at the time of follow-up had a limited vocabulary and difficulty forming sentences. His neurological examination was notable for hypotonia and lower limb weakness. His brother, now aged 21 years, is also affected with severe intellectual disability, wasting, and weakness in lower limbs.

Family 13: Individuals 18-19: *NARS1* Homozygous mutation c.1633C>T, p.Arg545Cys

Two siblings born to consanguineous parents from Pakistan. The proband is 6 months old male who presented in the neonatal period with microcephaly, seizures and failure to thrive. His older brother also has epilepsy, microcephaly and global developmental delay. He walked age 3 years. His speech is severely delayed and, at follow-up aged 6.5 years, he only speaks a few words and is unable to form sentences.

Family 14: Individuals 20: *NARS1* Homozygous mutation c.1633C>T, p.Arg545Cys

The proband is a 16 year old boy born to consanguineous parents from Pakistan. He was born following a normal pregnancy and perinatal course, but began to exhibit signs of moderate global developmental delay in infancy. He sat at 7 months, began walking at 2 years of age and had moderate delay in speech development. He had learning disabilities in school and persisted to have moderate intellectual disability. His examination was notable for bilateral pes cavus, weakness and wasting distally in upper and lower limbs, absent deep tendon reflexes and impaired sensation. Nerve conduction velocities revealed severe sensorimotor polyneuropathy with primary axonal degeneration. His MRI Brain was unremarkable.

Family 15: Individuals 21-23: *NARS1* Homozygous mutation c.1633C>T, p.Arg545Cys

This family consists of eight siblings born to consanguineous Pakistani parents. Four siblings were affected with GDD, microcephaly and seizures. The eldest, a female, was reviewed aged 30 years. She presented with severe GDD in childhood, sitting for the first time at 4 years of age and walking first steps at 10 years. She did not speak at all until she was 4.5 years old and now has limited speech with difficulties communicating. At 4.5 years of age she fell downstairs, after which, she began having left sided focal seizures, which were controlled with sodium valproate. Her seizures stopped after 2 years, however she had persistent left sided weakness which was attributed to the fall. On examination, she had bilateral foot drop and several dysmorphic characteristics including; large dysplastic ears, a large nose with broad nares, a large mouth with widely spaced teeth, and syndactyly of the second and third toes bilaterally. She had normal tone with reduced power in lower limbs bilaterally particularly on dorsiflexion (1/5). She had an ataxic gait with absent ankle reflexes. She was unable to participate in sensory examination.

Her younger brother, who is now 16, is similarly affected but has less severe intellectual disability. He also has microcephaly and had delayed developmental milestones as child, sitting at 1 years of age, walking aged 2 years and speaking first words at 3 years of age. His speech remains limited, he is unable to speak in full sentences, and he has a tendency towards aggressive behaviour. He also had focal seizures in infancy, however they have now resolved and his last witnessed seizure occurred aged 2 years. Two other siblings, also affected, died in childhood. A girl, who was reviewed aged 13 years, also presented with GDD and microcephaly in infancy. She had severe intellectual disability and was unable to feed herself independently. She also had a history of delayed milestones in childhood, sitting aged two and walking aged three, and had poor language abilities and spoke only a few words. She began having generalised tonic clonic seizures aged 4 years which were treated with sodium valproate but poorly controlled. She died at the age of 16 years due to sepsis secondary to burns which she obtained following a fall into a stove. Her brother also died aged 6 years of age. He was unable to sit, stand or speak and had severe and seizures which commenced when he was 2 months old. His death was attributed to respiratory distress secondary to unrelated respiratory complications. Besides these siblings, these individuals also had six first degree relatives (not shown) that had GDD and died in early childhood.

Family 16: Individuals 24-25. *NARS1* siblings with homozygous mutation c.32G>C, p.Arg11Pro

Two affected siblings born to parents from Kosovo, who were not known to be related. The couple's first child (a girl) was unaffected. Their second child, a boy, was born at full term following an uneventful pregnancy. He had a normal postnatal course and birth parameters. No abnormalities were detected until he was 5 months old when he presented with generalised tonic-clonic seizures. Moreover, his motor development deteriorated with progressive muscle spasticity. CT imaging of his brain revealed widening of bifrontal subarachnoid spaces as well as small subdural hygroma. Laboratory work-up including CSF analysis was unhelpful. Brain MRI at the age of 10 months revealed prominent cerebral atrophy and delayed myelination. During the following year, he was treated with phenobarbital, levetiracetam and baclofen to control seizures and spasticity. Progressive microcephaly was noted OFC 43 cm (<1st percentile, -4 SD). Motor and cognitive milestones were not reached (e.g. no crawling, no sitting without support, no development of language, etc). Follow-up brain MRI at the age of 1 ½ years showed severe atrophy with no progression of myelination. At the age of 2 ½ year, the boy deteriorated with poor feeding, vomiting and dehydration. An MRI brain demonstrated basilar thrombosis and associated infarction in the cerebellum, pons and midbrain. His neurological function deteriorated further and he died aged 4 years in a palliative care setting with severe aspiration pneumonia. The third born, a girl, had normal pre- and postnatal development. She presented aged 8 months with status epilepticus. Physical examination revealed microcephaly, developmental delay and moderate spasticity of the extremities. Brain MRI showed comparable findings to her brother with severely delayed myelination. Follow-up brain MRI at the age of 2 years revealed progressive brain atrophy and arrest of myelination.

Family 17: Individual 26. *NARS1* siblings with homozygous c.50C>T, p.Thr17Met

The proband is a female born to Libyan parents who were first cousins. She was reviewed aged 7 years, at which point was found to have severe microcephaly 42cm (<1st percentile, -7.7 SD). She has severe intellectual disability. She presented with generalised tonic clonic seizure at 6 months and was diagnosed with GDD in infancy failing to meet age appropriate milestones. She has 2 additional siblings who were similarly affected but passed away in childhood.

Family 18: Individuals 27 and 28. *NARS1* siblings with compound heterozygous c.1049T>C, c.1264G>A, p.Leu350Pro, p.Ala422Thr

The proband is a 15-year-old female born to healthy non-consanguineous German parents. She presented in childhood with neurodevelopmental delay and progressive microcephaly. She failed to reach appropriate motor milestones sitting for the first time age 3 years. Speech developmental was also severely delayed and now aged 15 years her vocabulary is limited to a few words and she is unable to communicate effectively. She persisted to have severe intellectual disability and experiences frequent episodes of inappropriate laughter. She had her first generalised tonic clonic seizures at approximately 4 years of age, at which point she was documented as having an abnormal EEG. Her neurological examination was notable for an ataxic gait. She had muscle atrophy which is more pronounced in her lower limbs. She is hypotonic with reduced power distally and hyporeflexic in the lower limbs with upgoing plantars bilaterally. Sensation to sharp touch was impaired. A MRI brain ruled out any structural abnormalities and nerve conduction velocities confirmed demyelinating peripheral neuropathy. Her sister who is now 21 years of age and is clinically similar to her sister with severe intellectual disability, microcephaly and demyelinating peripheral neuropathy. However, she has never had seizures.

Family 19: Individual 29-30. *NARS1* siblings with compound heterozygous .1067A>C, c.203dupA, p.Asp356Ala, p.Met69Aspfs*

The proband is a male born to non-consanguineous Turkish parents. He was born with a low weight (-2.38 SD) and height (-3.76 SD) for gestational age. He failed to meet age appropriate developmental milestones in terms of motor skills and did not walk until 3 years of age. His speech was also severely delayed speaking his first words aged 4 years. He began having generalised tonic clonic seizures aged 6 years at which point he underwent an MRI brain, which revealed thickening of gyri. Examination at follow up at 14 years of age revealed severe microcephaly 49.2 cm (<1$_{st}$ percentile, -3.4 SD). His sister, also affected, is clinically identical with GDD and epilepsy.

Family 20: Individual 31. *NARS1* compound heterozygous variants c.268C>T, c.394G>T, p.Arg90*, p.Gly132Cys

The proband is an 8 year old Canadian female born to healthy non-consanguineous parents. She was born at 37 weeks and had feeding difficulties from the beginning with associated failure to thrive. Developmental milestones were profoundly delayed. She did not walk until 6 years and 10 months and did not speak until she was 5 years old. At follow-up aged 8 years, her speech was limited to 3 words and she was unable to form sentences. From 1 to 3 years of age, she experienced five generalised tonic-clonic seizures. She is now seizure free and does not require anti-epileptic drugs. On examination, she was small for age with a weight of 11kg (-5.6 SD) and height of 95.3 cm (-7.6 SD). She has severe microcephaly (-3SD) and several dysmorphic features including hypotelorism, deep set eyes, a prominent nasal bridge and thin upper lip with smooth philtrum. Skeletal abnormalities include a right sided hip dysplasia and bilateral varus deformities requiring de-rotational osteotomies. Due to severe intellectual disability, she struggled to co-operate with the neurological examination, however she appeared to be hypotonic and have impaired co-ordination. An MRI brain showed microcephaly with a thin corpus callosum and decreased white matter volume throughout.

Family 21: Individual 32. NARS compound heterozygous c.1376 C>T, c.178 A>G, p.Thr459Ile, p.Lys60Glu

The proband is a 3-year-old male born in the USA to healthy non-consanguineous parents. He is microcephalic on examination with a head circumference of 43.5cm (-5 SD). His history is notable for global developmental delay characterised by severe language delays and delays in gross motor milestones, sitting at 10 months and starting to walk at 3 years. He now walks with an ataxic gait and has evidence of spasticity on examination. He also has epilepsy and began having generalised tonic clonic seizures in infancy. MRI brain revealed a small arachnoid cyst involving the right middle cranial fossa but was otherwise within normal limits.

Section 2: Supplementary Figures S1-S13

Supplementary Figure 1

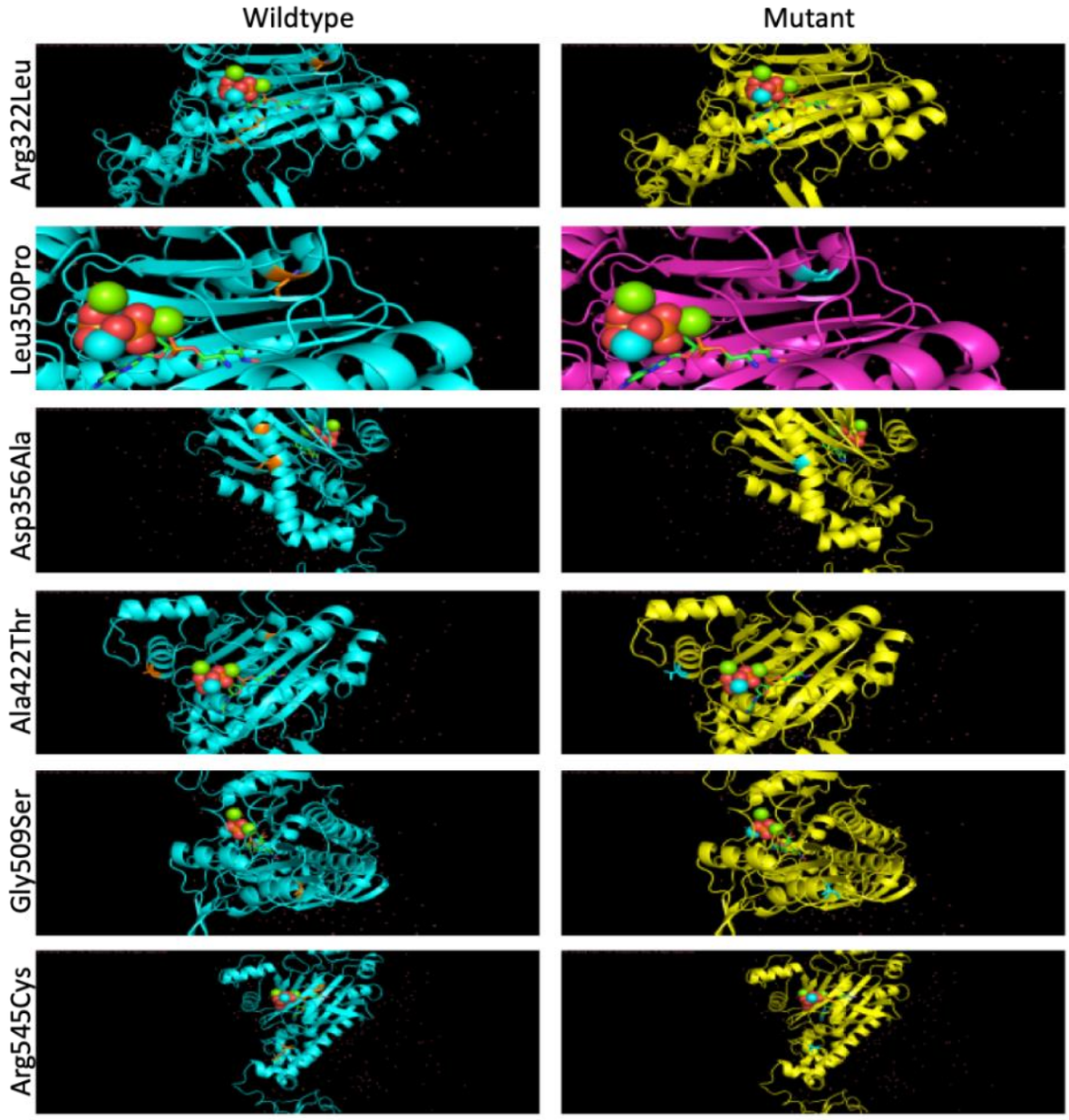

Figure S1. **Molecular modelling of *NARS1* mutations.** Wild type NARS1 and each mutation was modelled using the Phyre2 server1. We observed that each model gave rise to a "wild type" AsnRS1 enzyme indicating that none of the mutations completely destabilizes the protein structure (left panels). The Arg11Pro, Thr17Met and Met34Leu mutations could not be modelled because they lie in the unknown UNE-N domain. The substrate depicted with balls on the figure corresponds to the ATP:Mg and L-Asp-beta-NOHandenylate:PPi:Mg from the structure of *B. malayi* NARS1 that was superimposed to each model we obtained. They were superimposed with a very good concordance. From this study we propose that the mutations might have the following effects: Asn218Ser (affects the interaction between AsnRS1 and the anticodon arm of the tRNA), Arg322Leu (affects the stabilization of the aminoacyl-adenylate in the active site), Leu350Pro (little effect on AsnRS1 activity and dimer interface), Asn356Ala (might weaken the dimer stability), Ala422Thr (little effect on 3' tRNA end binding), Gly509Ser (slight interference on dimer interface), Arg545Cys (see Figure 6).

Supplementary Figure 2

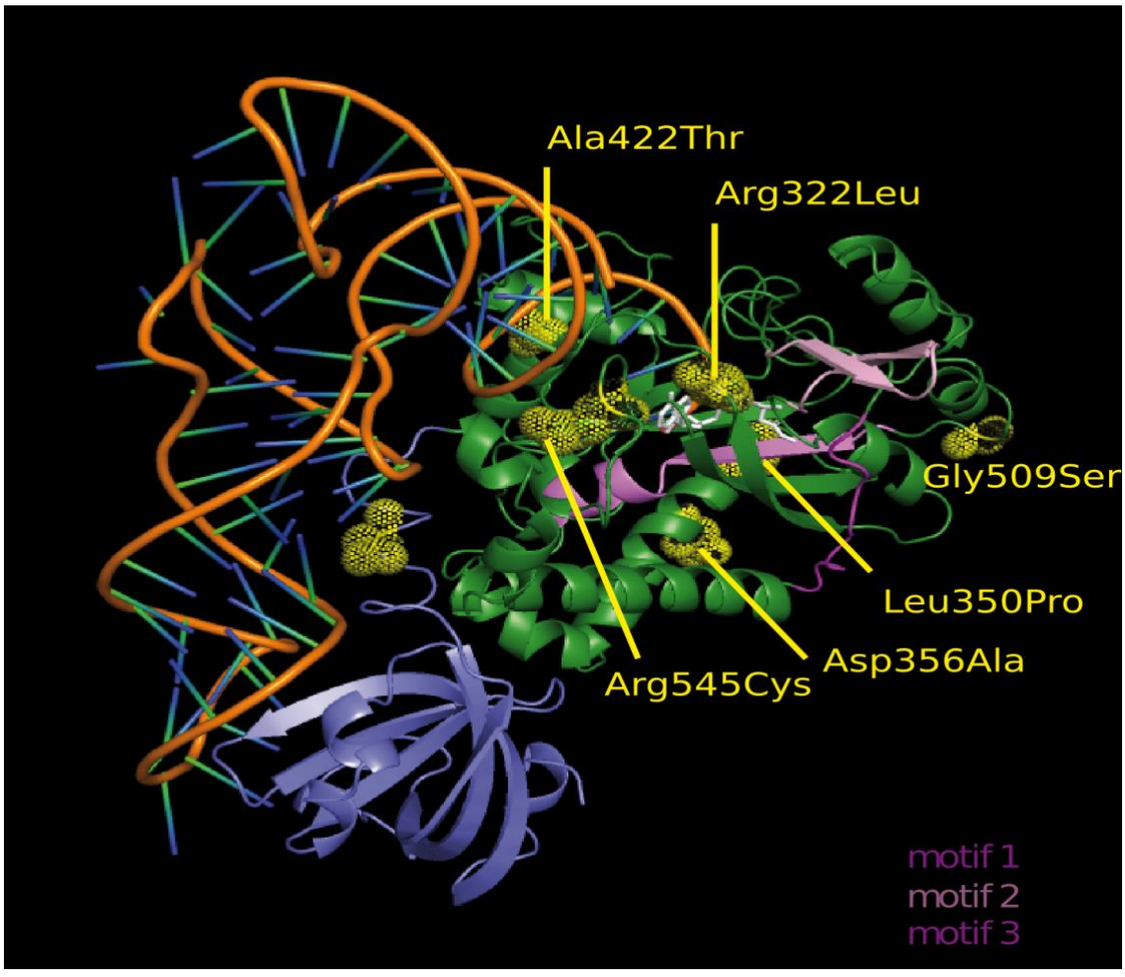

Figure S2. Model of human AsnRS1. This was obtained using the Phyre2 webserver. The latter was superposed with *Brugia malayi* AsnRS1 structure (2xti) complexed with ATP:Mg and L-Asp-ß-NOH adenylate:PPi:Mg (L-Asp-ß-NOH is shown in white color on the figure). The tRNA is $tRNA_{Asp}$ that results from the superposition of the AspRS/$tRNA_{Asp}$ complex from yeast with the human AsnRS1 model. Note that the UNE-N domain is absent from the modelled structure. The position of the mutations are indicated by yellow spheres.

Supplementary Figure 3

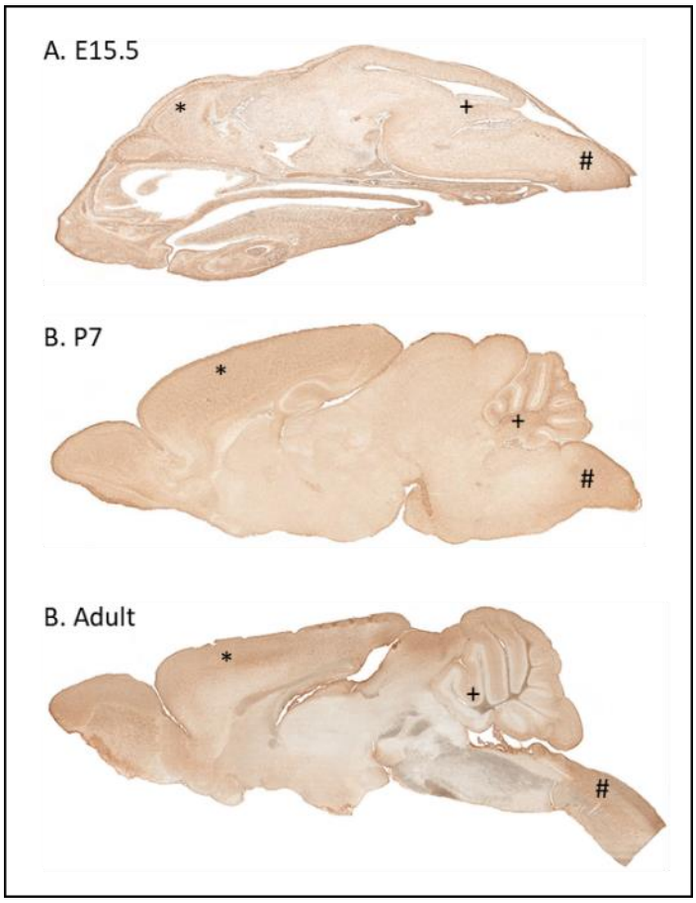

Figure S3. In-situ expression of the *NARS1* gene in mouse brain at three different ages, E15.5, P7 and adult. The *NARS1* probe used was GENSAT1-BX1431. Data from the Gene Expression Nervous System Atlas (GENSAT) Project. Expression was moderate in the brain, higher in the cortex (*), cerebellum (+) and brainstem (#).

Supplementary Figure 4

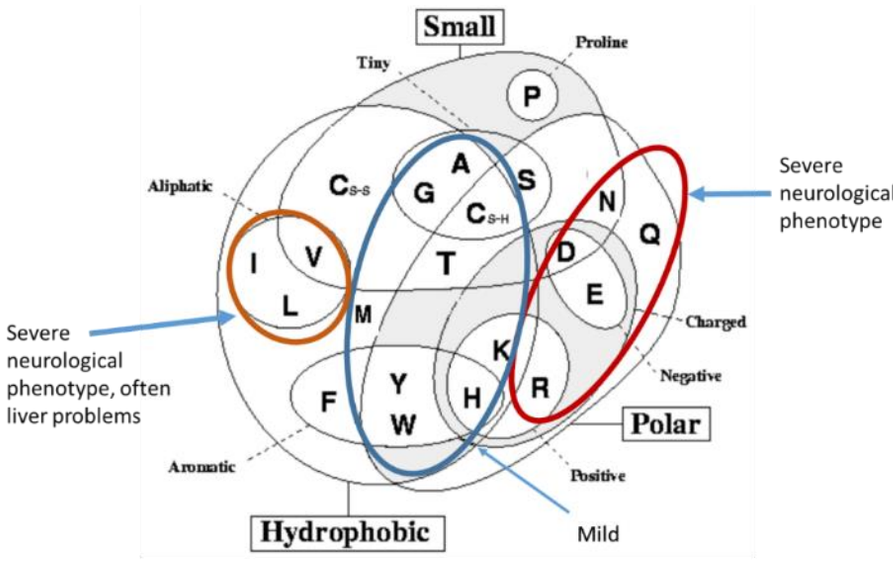

Figure S4. Modified Taylor's Venn diagram of amino acid properties, each amino acid is described by its physical or chemical properties (Taylor, TW, J, 1986, *Theor. Biol*. 119: 205-218). AARs clinical phenotype severity seem to cluster into two areas (red ovals) according to the amino acid that is targeted.

Supplementary Figure 5

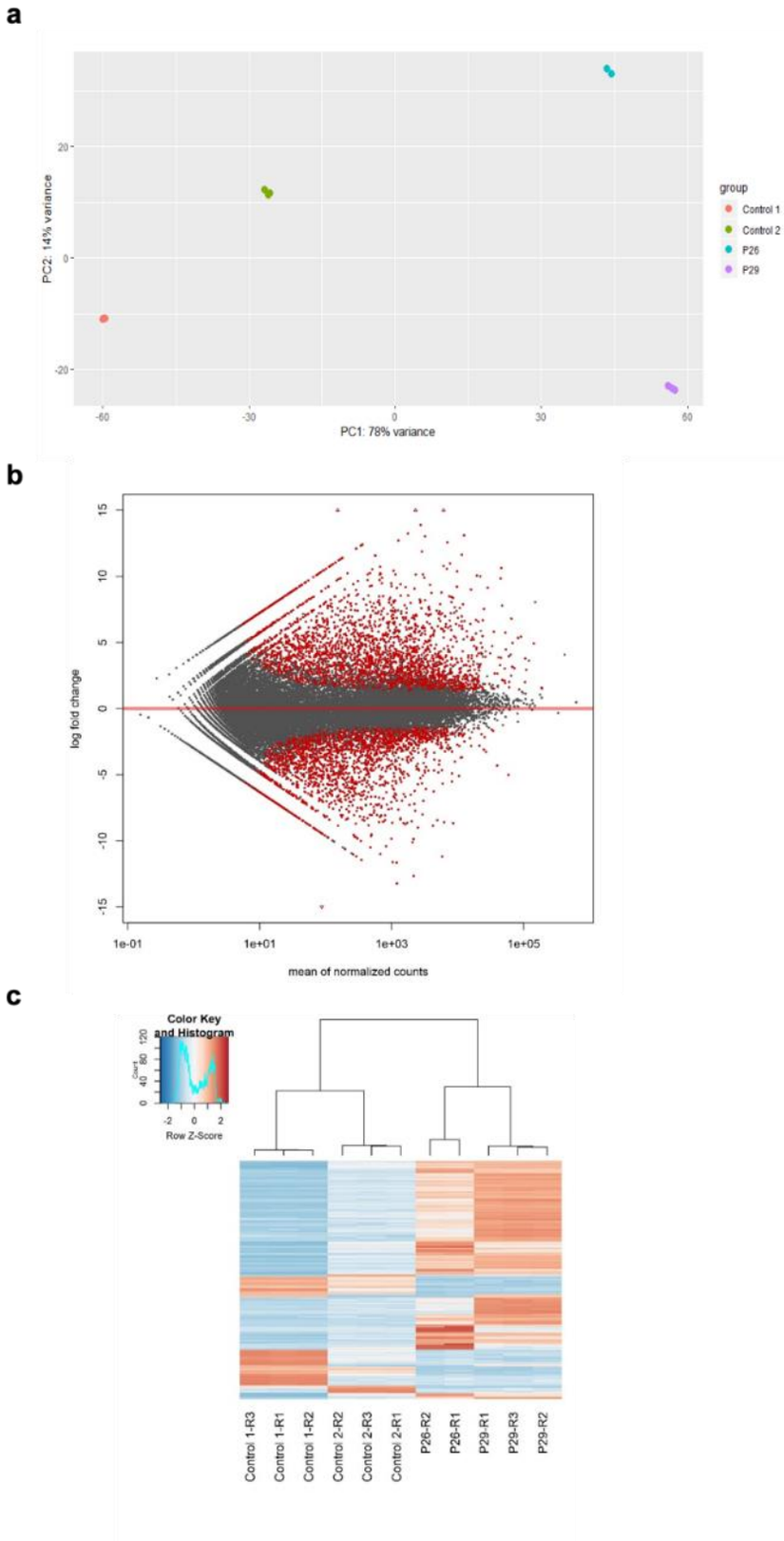

Figure S5. Transcriptomic gene expression analysis A. Principle component analysis of transcriptomic gene expression levels. B. MA plot showing normalised count number versus fold change, significantly differentially expressed gene shown in red. C. Cluster heatmap of top 750 most differentially expressed normalised gene counts.

Supplementary Figure 6

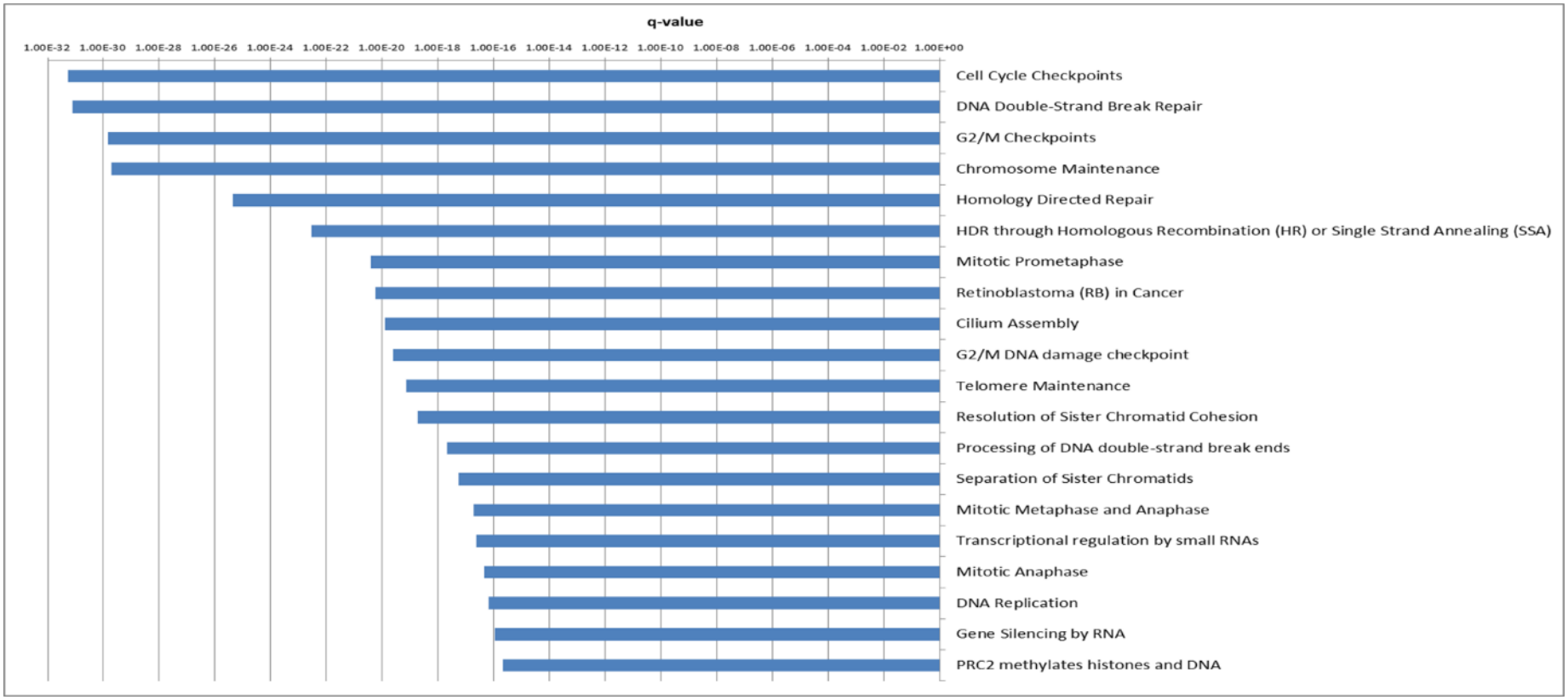

Figure S6. Supplementary iNPC data of top 20 (by significance) pathways associated with downregulated genes. (Filtered to <200 members)

Supplementary Figure 7

Figure S7. Supplementary iNPC data of top 20 (by significance) pathways associated with upregulated genes. (Filtered to <200 members)

Supplementary Figure 8

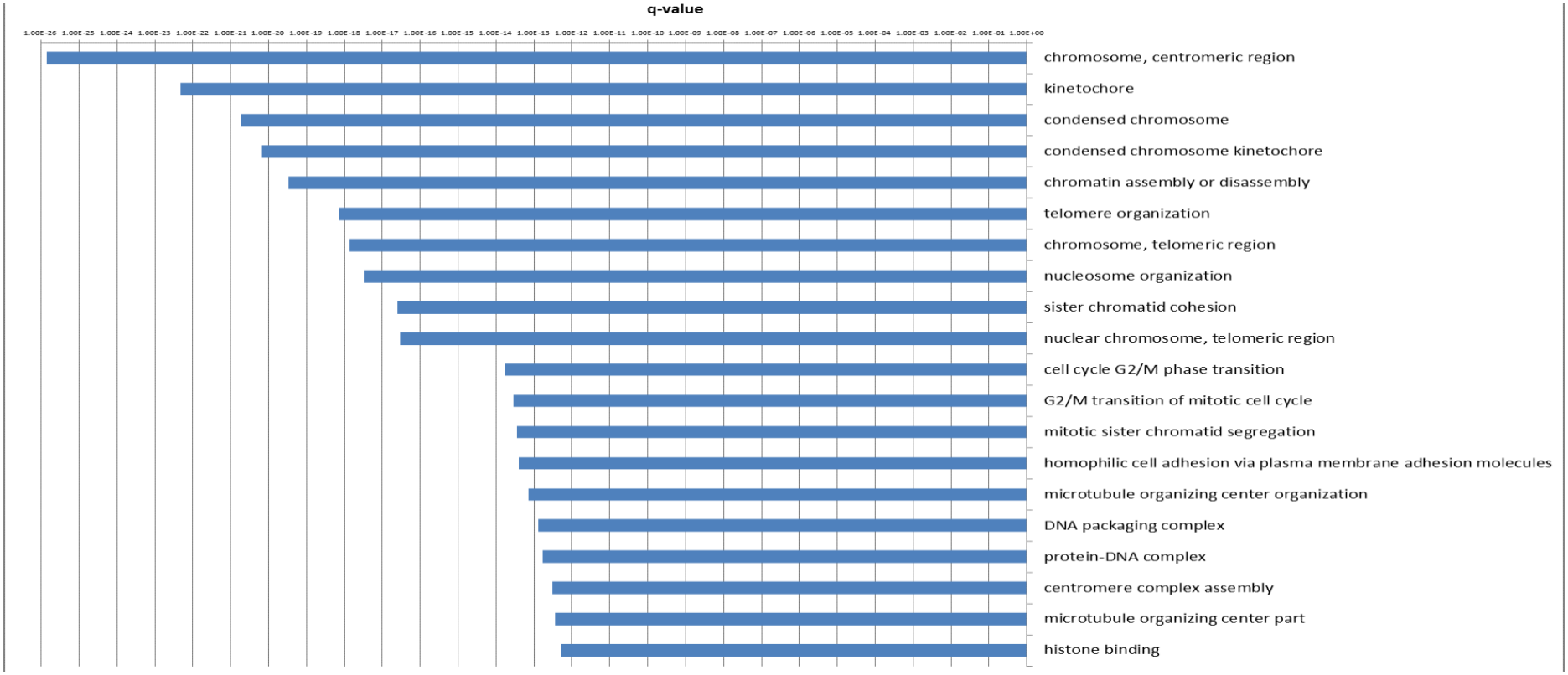

Figure S8. Supplementary iNPC data of top 20 (by significance) GO terms associated with downregulated genes. (Filtered to <200 members)

Supplementary Figure 9

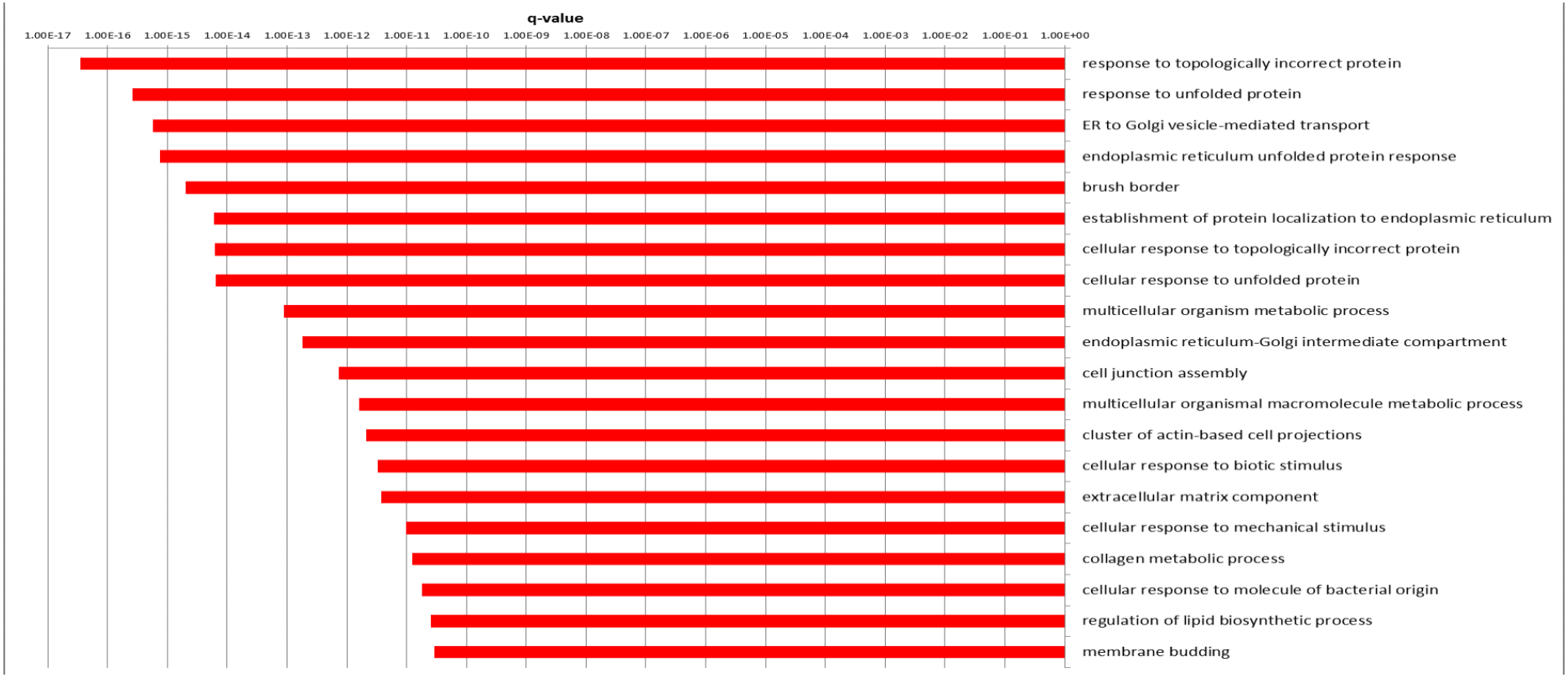

Figure S9. Supplementary iNPC data of top 20 (by significance) GO terms associated with upregulated genes. (Filtered to <200 members)

In summary, downregulated genes have been associated with DNA replication, whereas upregulated genes like VEGF are associated with protein synthesis and processing. NARS1 gene expression was unaltered (p=0.45), while other tRNA synthetase genes were upregulated (DARS, RARS, WARS, TARS, YARS, GARS, SARS). LARS was downregulated & others were not altered. In the compound heterozygous individual (P29), the frameshift mRNA (p.Met69Asp*fs*) is only expressed at a 1:9 ratio compared to the allele with a single base change (this can be visualised if desired), also confirmed by Western blotting showing decreased AsnRS1 expression.

Supplementary Figure 10

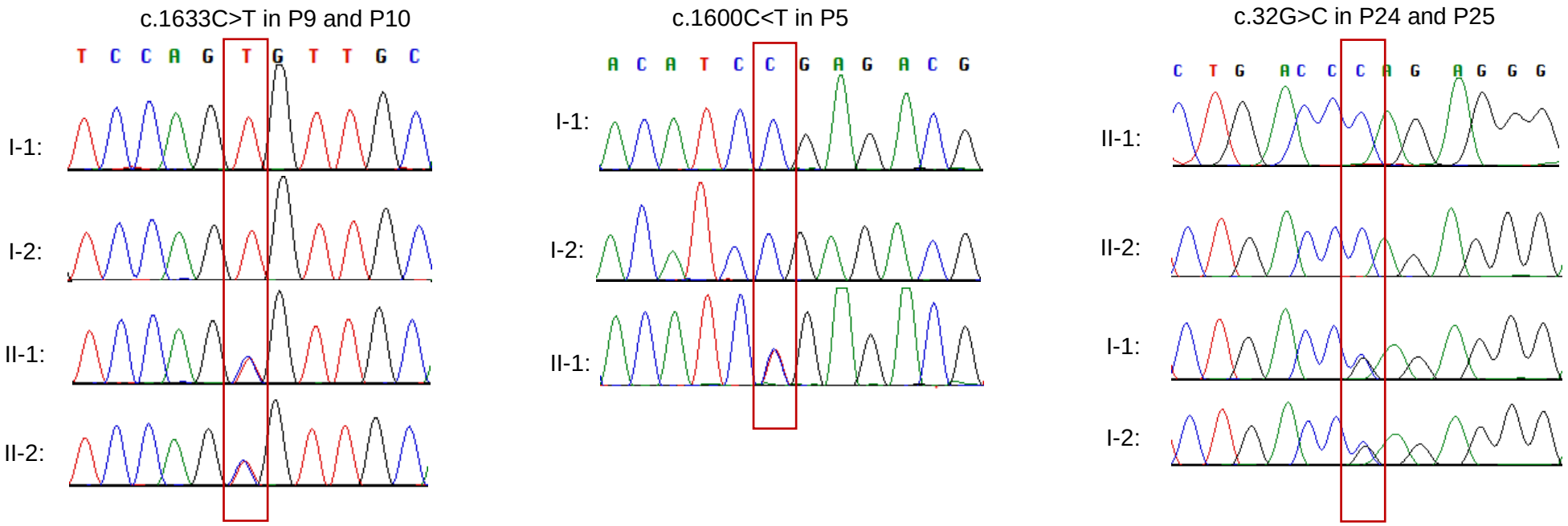

Figure S10. Segregation studies by Sanger sequencing. The top panels shows segregation of the c.1633C>T, p.Arg545Cys variant in individuals P9 and P10, and their parents. The middle panel shows segregation of the c.1600C>T, p.Arg534* variant in individual P5 and his parents. The bottom shows segregation of the c.32G<C, p.Arg11Pro variant in individuals P24 and P25 and their parents.

Supplementary Figure 11

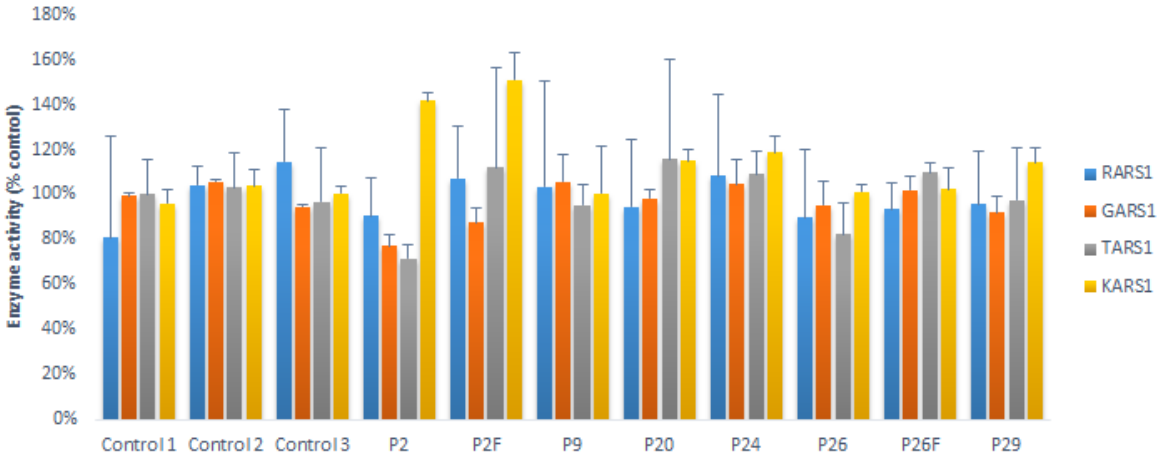

Figure S11. Individual derived fibroblast and lymphoblast cells displaying loss of *AsnARS1* activity compared to control. Asparaginyl-tRNA synthetase activity reduced significantly than other tRNA synthetase in individuals' and parents' cells (c.1600C>T, p.Arg534* (P2), c.1633C>T, p.Arg545Cys (P9, P20), c.32G>C, p.Arg11Pro (P24), c.50C>T, p.Thr17Met (P26) and c.1067A>C, p.Asp356Ala / c.203dupA, p.M69Aspfs*4 (P29); TARS: Threonyl-tRNA sythetase; KARS: lysyl-tRNA synthetase; GARS: Glycyl-tRNA synthetase and RARS: arginyl-tRNA synthetase were measured as control for AsnRS1 activity.

Supplementary Figure 12

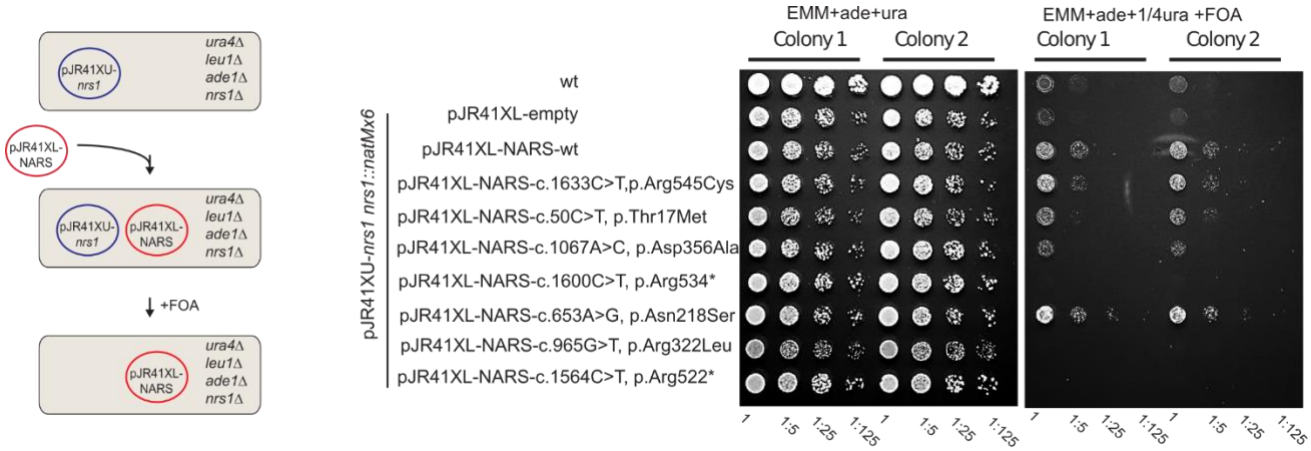

Figure S12. Human *NARS1* gene is able to complement fission yeast *nrs1.* Schematic of the yeast complementation assay. Fission yeast cells containing a plasmid expressing *nrs1* gene with uracil selectable marker whose genomic copy of the *nrs1* is deleted are transformed with plasmids containing the different variants of the human *NARS1* gene. These cells are promoted to lose the *nrs1*gene plasmids by incubating them in media with uracil for 24 hours. Five-fold serial dilutions of 2 different colonies of strains containing the different variants of *NARS1* gene wt, c.1633C>T, p.Arg545Cys; c.50C>T, p.Thr17Met; c.1067A>C, p.Asp356Ala; c.1600C>T, p.Arg534*; c.653A>T, p.Asn218Ser; c.965G>T, p.Arg322Leu; c.1564C>T, p.Arg522*, the empty vector and wt cells were plated in media containing uracil, or media containing FOA, which allows the growth of only those cells that have lost the yeast *nrs1* plasmid and whose *NARS1* variant is able to complement *nrs1*D.

Supplementary Figure 13

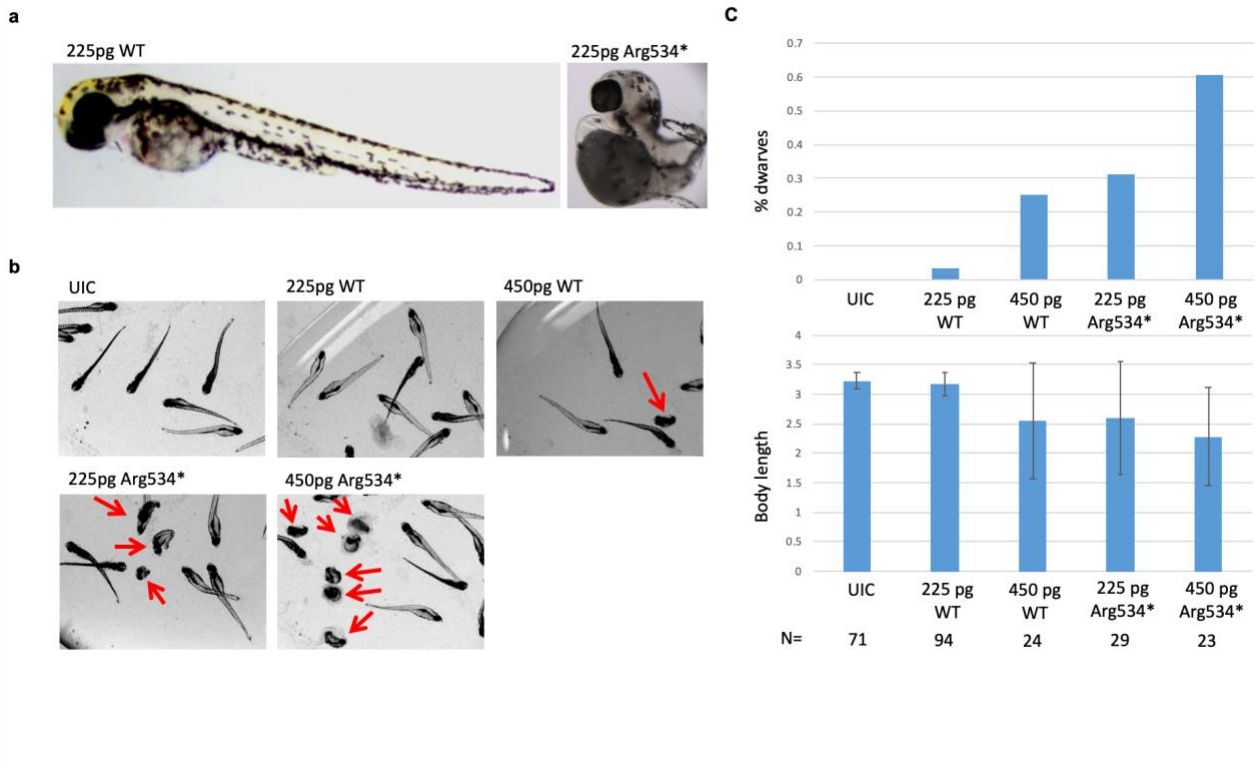

Figure S13. Microinjection of human *NARS1* RNA into zebrafish embryos. a. Microinjection of the indicated doses of wild-type (WT) or c.1600C>T, p.Arg534* mutant capped RNA encoding human *NARS1* into zebrafish embryos resulted in complete cyclopia and severe truncation of the body axis, a dwarf-like appearance. b. Low-power representative images of each experimental group at 5 days post-fertilisation. Dwarves are indicated by the red arrows. c. Quantification of animal body length and the proportion of animals exhibiting the dwarfic appearance for each experimental group, as indicated. Error bars are standard deviations.

Section 3: Supplementary Tables S1-S6

Table S1: *ARS* gene implicated in human disease

Gene	Locus	Location of Protein	Mode	Disease Phenotype(s)	Clinical severity	Ref
AARS1	16q22	Cytoplasm	AD	Charcot Marie Tooth disease type 2N	Mild	2-6
			AR	Epileptic encephalopathy, early infantile, 29	Moderate	
AARS2	6p21.1	Mitochondria	AR	Mitochondrial Infantile Cardiomyopathy	Moderate	7-11
				Leukoencephalopathy with ovarian failure	Moderate	
CARS1	11p15.4	Cytoplasm	AR	Microcephaly, DD, brittle hair and nails	Moderate	12
CARS2	13q34	Mitochondria	AR	Epilepsy encephalopathy, myoclonic epilepsy	Moderate	13-16
				Combined oxidative phosphorylation deficiency 27		
DARS1	2q21.3	Cytoplasm	AR	Hypomyelination, brainstem, spinal cord and leg spasticity	Moderate	17-19
DARS2	1q25.1	Mitochondria	AR	Hypomyelination, brainstem, spinal cord, elevated lactate	Severe	20-29
EPRS1	1q41	Cytoplasm	AR	Leukodystrophy, hypomyelinating, 15	Moderate	30
EARS2	16p12.2	Mitochondria	AR	Leukoencephalopathy and high lactate	Severe	31-36
				Combined oxidative phosphorylation deficiency 12		
FARSA	19p13.2	Cytoplasm	AR	Rajab interstitial lung disease with brain calcifications	Moderate	37
FARSB	2q36.1	Cytoplasm	AR	Rajab interstitial lung disease with brain calcifications	Moderate	38; 39
FARS2	6p25.1	Mitochondria	AR	Combined oxidative phosphorylation deficiency 14	Moderate	40-45
				Spastic paraplegia 77		
GARS1	7p15	Cytoplasm & Mitochondria	AD	Charcot Marie Tooth disease type 2D	Mild	3; 46-62
			AR	Distal SMA type V, myalgia, cardiomyopathy		
HARS1	5q31.3	Cytoplasm	AD	Charcot Marie Tooth disease type 2W	Mild	63; 64
			AR	Usher Syndrome 3B	Moderate	
HARS2	5q31.3	Mitochondria	AR	Perrault Syndrome 2	Mild	65; 66
IARS1	9q22.31	Cytoplasm	AR	ID, GR, muscular hypotonia, hepatopathy, cholestasis	Severe	67
IARS2	1q41	Mitochondria	AR	Cataracts, GH deficiency, deaf, neuropathy, bone dysplasia	Severe	68-70
				Leigh syndrome		
KARS1	16q23.1	Cytoplasm & Mitochondria	AR	Intermediate Charcot Marie Tooth disease type B	Moderate	71-74
				Autosomal recessive deafness-89		
				Visual impairment, microcephaly, DD, seizures		
				Leukoencephalopathy		
LARS1	5q32	Cytoplasm	AR	Infantile hepatopathy	Severe	75
LARS2	3p21.31	Mitochondria	AR	Perrault syndrome 4	Mild	76
				Hydrops, lactic acidosis and sideroblastic anaemia		
MARS1	12q13.3	Cytoplasm	AD	Charcot Marie Tooth disease type 2U	Mild	77-80
			AR	Interstitial lung and liver disease	Moderate	
MARS2	2q33.1	Mitochondria	AR	DD, sensorineural hearing loss, Spastic ataxia 3	Mild	81; 82
				Combined oxidative phosphorylation deficiency 25	Moderate	
NARS2	11q14.1	Mitochondria	AR	Alpers, Leigh syndrome, DD, ID, epilepsy, myopathy	Severe	83-88
				Combined oxidative phosphorylation deficiency 24		

PARS2	3p21.31	Mitochondria	AR	Infantile-onset developmental delay and epilepsy	Moderate	88
				Alpers syndrome		
QARS1	3p21.31	Cytoplasm	AR	Microcephaly, seizures, DD, cerebral cerebellar atrophy	Severe	89
RARS1	5q34	Cytoplasm	AR	hypomyelinating leukodystrophy 9	Severe	90-92
RARS2	6q16.1	Mitochondria	AR	Epileptic encephalopathy, lactic acidosis neurological symptoms, pontocerebellar hypoplasia 6	Severe	93-95
SARS1	1p13.3	Cytoplasm	AR	Ataxia, weakness, ID, microcephaly, speech impaired	Moderate	96
SARS2	19q13.2	Mitochondria	AR	Hyperuricemia, pulmonary HT, renal failure, alkalosis	Moderate	97
TARS1	5p13.3	Cytoplasm	AR	Trichothiodystrophy, ichthyosis, ID, decreased fertility	Moderate	98
TARS2	1q21.2	Mitochondria	AR	Axial hypotonia and severe psychomotor delay	Mild	99; 100
				Combined oxidative phosphorylation deficiency 21		
VARS1	6p21.33	Cytoplasm	AR	Severe DD, microcephaly, seizures, cortical atrophy	Moderate	101-104
VARS2	6p21.33	Mitochondria	AR	Microcephaly, epilepsy, encephalocardiomyopathy	Moderate	99; 105-108
				Combined oxidative phosphorylation deficiency 20		
WARS1	14q32.2	Cytoplasm	AD	Distal hereditary motor neuropathy	Mild	109
WARS2	1p12	Mitochondria	AR	Ataxia, weakness, microcephaly, speech impaired, ID	Moderate	96; 110-112
YARS1	1p35.1	Cytoplasm	AD	Dominant-intermediate Charcot Marie Tooth disease	Mild	106; 113
			AR	Multisystem disease, DD, failure to thrive	Moderate	
YARS2	12p11.2	Mitochondria	AR	myopathy, lactic acidosis, and sideroblastic anaemia	Moderate	114-116

ARS gene implicated in 36 human diseases from a total of 37 genes. The first letter of the ARSs' gene name corresponds to the amino acid specificity of the corresponding ARS (based on the amino acid one-letter code) and 2 indicates that the gene encodes a mitochondrial-restricted isoform 117-119. Clinical phenotype is bases upon publications. Key: ID = intellectual disability, GH = growth hormone, GR = growth retardation, DD = developmental delay, AR = autosomal recessive, AD = autosomal dominant, HT = hypertension, SMA = spinal muscular atropy

Table S2 : Detailed clinical features of individuals with *NARS1* de novo heterozygous mutations. Families 1-8.								
Family	1	2	3	4	5	6	7	8
Individual	1	2	3	4	5	6	7	8
Inheritance	de novo Heterozygous	de novo Heterozygous	de novo Heterozygous	de novo Heterozygous	de novo Heterozygous	de novo Heterozygous	de novo Heterozygous	de novo Heterozygous
Variant	c.1600C>T p.Arg534*	c.1600C>T p.Arg534*	c.1600C>T p.Arg534*	c.1600C>T p.Arg534*	c.1600C>T p.Arg534*	c.1600C>T p.Arg534*	c.1525G>A p.Gly509Ser	c.965 G>T p.Arg322Leu
Origin	Dutch	Dutch	Dutch	Caucasian	Hispanic, European	European	UK	European
Consanguinity	N	N	N	N	N	N	N	N
Gender / Age at follow-up	F/ 17	F / 22	M / 10	M /13	F / 16	M / 5y 8m	F / 2y 10m	M /15
Occipital Frontal Circumference (OFC)								
Birth	45.8cm <2p *(-2.1SD)*	NA	NA	33cm (10p)	NA	NA	NA	NA
Follow –up Percentile / SD	49cm <1p *(-5SD)*	46.8cm <1p*(-4.3 SD)*	50cm <1p *(-2.2 SD)*	49cm <1p *(-4.7SD)*	49.3cm at 13 y <1p *(-4.5 SD)*	47cm <1p *(-3.2SD)*	50 cm 86p	54cm 27p
Microcephaly	Y	Y	Y	Y	Y	Y	N	N
Developmental Delay								
GDD	Y	Y	Y	Y	Y	Y	Y	Y
Sitting (Months)	18	16	NA	16	11	NA	12	8
Walking (Years)	3	2y 2 m	2y 6m	N	3	23	2y 3m	2y 11m
Language	Severely Delayed	Severely Delayed	Severely Delayed	Severely Delayed	Severely Delayed	Severely Delayed	Severely Delayed	Severely Delayed
Neurological Findings								
Intellectual Disability	Severe	Severe	Severe	Profound	Profound	Severe	Severe	Severe
Seizures	GTC	GTC	NA	Myoclonic / Partial	GTC / Partial	GTC	GTC	Partial/Myoclonic
Peripheral Neuropathy	Y	Y	NA	N	Y	N	NA	NA
Ataxia	Y	Y	Y	Y	Y	Y	NA	Y
Imaging	NAD	NAD	NAD	NA	NA	Mild atrophy, CSF space enlargement	NA	NAD
Clinical Features								
Dysmorphic Features	Upslanting palpebral fissures Pes-cavus	Clinodactyly Upslanting palpebral fissures Thoracic Kyphosis Wide spaced teeth	Clinodactyly Retrognathia	Upslanting palpebral fissures Hypertelorism Arachnodactyly, Pectus Excavatum	Upslanting palpebral fissures Wide spaced teeth Low set ears Fleshy Helices	Low set ears Overfolded Helices Syndactyly	Large ears Long slender fingers	Broad Forehead
Tone	NAD	Reduced	Increased	Increased	Reduced	Increased	Reduced	Increased
Power	Reduced	Reduced	Reduced	NAD	Reduced	Reduced	NA	NAD
Sensation	NA	Reduced	NA	NAD	Reduced	NAD	NA	NA
Co-ordination	Ataxic gait	Unilateral Intention Tremor	Dysarthria	Ataxic gait	Ataxic gait	Ataxic gait	NA	Ataxia
Reflexes	Reduced	Reduced	Increased	Increased	Reduced	NAD	Increased	Increased
Other	N	N	Tremor /Myoclonus	Stereotypies	N	N	N	Stereotypies
Y = Yes, N= No, M= Male, F= Female, NA= Not Available, p = percentile, SD = standard deviation, NAD = No abnormalities detected, GTC = Generalised Tonic Clonic Seizures								

Table S3: Detailed clinical features of individuals with *NARS1* Homozygous mutation c.1633C>T, p.R545C including families 9-15.															
Family	9	9	10	11	11	11	11	12	12	13	13	14	15	15	15
Individual	9	10	11	12	13	14	15	16	17	18	19	20	21	22	23
Origin	North India	North India	North India	Pakistan	Pakistan	Pakistan	Pakistan	Pakistan	Pakistan	Pakistan	Pakistan	Pakistan	Pakistan	Pakistan	Pakistan
Consanguinity	Y	Y	Y	Y	Y	Y	Y	Y	Y	Y	Y	Y	Y	Y	Y
Gender / Age at follow-up	M / 33	M / 17	M / 8	F / 17	F / 17	M / 19	F / 23	M / 8	M /21	M / 6m	M / 6.5	M / 16	F / 30	M / 16	F / 13
Occipital Frontal Circumference (OFC)															
Birth	NA	NA	NA	NA	NA	NA	NA	NA	NA	NA	NA	NA	NA	NA	NA
Follow –up Percentile / SD	NA	NA	46.5cm <1p *(-4.2 SD)*	52cm 2p *(-2.2 SD)*	49.5cm <1p *(-4.5 SD)*	52cm 2p *(-2.1 SD)*	50.3cm <1p *(-3.8 SD)*	46cm <1p *(4.6SD)*	51cm <1p *(2.8SD)*	NA	49cm 2p *(-2.0SD)*	NA	50.8cm <1p *(-3.3SD)*	48.2cm <1p *(-4.5SD)*	48cm <1p *(-4.4SD)*
Microcephaly	Y	Y	Y	Y	Y	y	Y	Y	Y	Y	Y	N	Y	Y	Y
Developmental Milestones & Intellectual Disabilities															
GDD	Y	Y	Y	Y	Y	Y	Y	Y	Y	Y	Y	Y	Y	Y	Y
Sitting (Months)	12m	12m	12m	12m	14m	12m	12m	NA	NA	NA	NA	7m	4y	1y	2y
Walking (Years)	NA	NA	2y	1y 8m	2y 8m	2y 8m	2y 8m	6y 6m	3y	3y	3y	2y	10y	2y	3y
Language	Delayed	Delayed	Severely Delayed	Severely Delayed	Severely Delayed	Severely Delayed	Severely Delayed	Severely Delayed	Severely Delayed	Severely Delayed	Severely Delayed	Severely Delayed	Severely Delayed	Severely Delayed	Severely Delayed
Neurological Findings															
Intellectual Disability	Severe	Moderate	Severe	Severe	Severe	Severe	Profound	Severe	Severe	Severe	Severe	Moderate	Severe	Moderate	Moderate
Seizures	GTC	N	N	N	N	GTC	GTC	N	N	GTC	GTC	N	Partial	Partial	GTC
Ataxia	Y	Y	Y	Y	N	N	N	NA	NA	NA	NA	NA	Y	NA	NA
Peripheral Neuropathy	Y	Y	N	N	N	N	N	NA	NA	NA	NA	Y	NA	NA	NA
Imaging	NAD	NAD	NAD	NA	NA	NA	NA	NA	NA	NA	NA	NAD	NA	NA	NA
Clinical Findings															
Dysmorphic Features	Contractures	Scoliosis	Clinodactyly Syndactyly	Clinodactyly	NAD	Clinodactyly Short Limbs	NAD	NAD	NAD	NAD	NAD	NAD	Dysplastic ears Syndactyly	NA	NA
Tone	Reduced	Reduced	NAD	NAD	NAD	NAD	NAD	Reduced	Reduced	NA	NA	N	N	NA	NA
Power	Reduced	Reduced	NAD	NAD	Reduced	Reduced	Reduced	Reduced	Reduced	Reduced	Reduced	Reduced	Reduced	NA	NA
Sensation	Reduced	Reduced	NAD	NAD	NAD	NAD	NAD	NA	NA	NA	NA	Reduced	NA	NA	NA
Co-ordination	Ataxic	Ataxic	Ataxic	Ataxic	NAD	NAD	NAD	NA	NA	NA	NA	NA	Ataxic	NA	NA
Reflexes	NAD	NAD	NAD	Reduced	Reduced	NAD	Reduced	NA	NA	Reduced	Reduced	Reduced	Reduced	NA	NA
Y = Yes, N= No, M= Male, F= Female, NA= Not Available, p = percentile, SD = standard deviation, NAD = No abnormalities detected, GTC = Generalised Tonic Clonic Seizures															

Table S4: Detailed clinical features of individuals with *NARS1* mutations. Autosomal recessive inheritance. Families 16-20.									
Family	16	16	17	18	18	19	19	20	21
Individual	24	25	26	27	28	29	30	31	32
Inheritance	Homozygous	Homozygous	Homozygous	Compound Heterozygous	Compound Heterozygous	Compound Heterozygous	Compound Heterozygous	Compound Heterozygous	Compound Heterozygous
Variant	c.32G>C p. Arg11Pro	c.32G>C p. Arg11Pro	c.50C>T p.Thr17Met	c.1049T>C, p.Leu350Pro c.1264G>A, p.Ala422Thr	c.1049T>C, p.Leu350Pro c.1264G>A, p.Ala422Thr	c.1067A>C, p.Asp356Ala c.203dupA, p.Met69Aspfs*	c.1067A>C, p.Asp356Ala c.203dupA, p.Met69Aspfs*4	c.268C>T, p.Arg90* c.394G>T, p.Gly132Cys	c.1376 C>T, p.Thr459Ile c.178 A>G, p.Lys60Glu
Origin	Kosovo	Kosovo	Libya	German	German	Turkey	Turkey	Canada	USA
Consanguinity	N	N	Y	N	N	N	N	N	N
Gender / Age at follow-up	M / 2	F / 2y 6m	F/ 7	F / 15	F / 21	M/ 14y 2m	F / 7y 10m	F / 8	M/3
Occipital Frontal Circumference (OFC)									
Birth	34cm 20p	NA	NA	33cm 11p	NA	NA	NA	NA	NA
Follow –up Percentile / SD	43cm <1p *(-4SD)*	40.5cm <1p*(-5 SD)*	42cm <1p *(-7.7SD)*	NA	NA	49.2Cm <1p*(-3.4SD)*	47.5cm <1p*(-3.4SD)*	41 cm <1p *(-8.7SD)*	43.5cm <1p*(-5SD)*
Microcephaly	Y	Y	Y	Y	Y	Y	Y	Y	Y
Developmental Milestones & Intellectual Disabilities									
GDD	Y	Y	Y	Y	Y	Y	Y	Y	Y
Sitting (Months)	N	N	NA	NA	NA	NA	NA	NA	10m
Walking (Years)	N	N	NA	3	3	3	2	6y 10m	3y
Language	N	N	Severely Delayed	Severely Delayed	Severely Delayed	Severely Delayed	Severely Delayed	Severely Delayed	Severely Delayed
Neurological Findings									
ID	Profound	Severe	Severe	Severe	Severe	Severe	Severe	Severe	Severe
Seizures	Myoclonic / GTC	GTC	GTC	GTC	N	GTC	GTC	GTC	GTC
Peripheral Neuropathy	NA	NA	NA	Y	Y	NA	NA	NA	NA
Ataxia	NA	NA	NA	Y	Y	NA	NA	Y	Y
Imaging	Delayed Myelination	Delayed Myelination	NA	NAD	NA	Thickening of gyri	NA	Thin corpus callosum Decreased white matter	Arachnoid Cyst
Clinical Features									
Dysmorphic Features	NAD	NAD	NA	NAD	NAD	NAD	NAD	Hypotelorism	NAD
Tone	Increased	NAD	NA	Reduced	Reduced	NA	NA	Reduced	Increased
Power	Reduced	Reduced	NA	Reduced	Reduced	NA	NA	N	N
Sensation	NA	NA	NA	Reduced	Reduced	NA	NA	N	N
Co-ordination	NA	NA	NA	Ataxic gait	Ataxic gait	NA	NA	Ataxic	Ataxic
Reflexes	Reduced	Reduced	NA	Reduced	NA	NA	NA	N	Increased
Other	N	N	N	N	N	N	N	Hip dysplasia	N

Y = Yes, N= No, M= Male, F= Female, NA= Not Available, p = percentile, SD = standard deviation, NAD = No abnormalities detected, ID = Intellectual Disability, GTC = Generalised Tonic Clonic Seizures, ASD = Autistic Spectrum Disorder

Table S5: Primer sequences

Nrs1-PJR-F	TTTGTTAAATCATACCTCGAGATGGCGGGATTGGAATCAAAAGTTT
Nrs1-PJR-R	GCCTCGCGAGTCGACCTCGAGTTAAGGTGTGCAACGTTCAGTAAATCG
Nrs1DelFw	CTCTAACGAGACTATAAGTTATCCAAGGCCGGTTATTTGATATTTAACATTTTCACTAACTTCAAACTGTCCTTTTAAAACGGATCCCCGGGTTAATTAA
Nrs1DelRv	AAATTCTAAGTAAACAACATAGTTCGCCCACTGTTCAAACATTAAAAGCTACCCATTTCTTCGATATGGATAAACTTTGCGAATTCGAGCTCGTTTAAAC
Nrs1ck-L	ACTAGCCGAAATTTTGGAATCA
Nrs1ck-R	CTAACTGACTCGCACCTAGCCT
KanR	CGGATGTGATGTGAGAACTGTATCCTAGC
KanF	CGCTATACTGCTGTCGATTCG
NARS1_F	GCGTTAGAAGGATATAGAGGCCA
NARS1_R	ACCATCTCGCAACACCAGAAA
GAPDH_F	TGTGGGCATCAATGGATTTGG
GAPDH_R	ACACCATGTATTCCGGGTCAAT

Table S6. Missense mutations in *NARS1* with the description of protein affects.

Residue	**Predicted effect of the mutation on Asn*RS1* protein**
Arg11Pro	Unique domain of *AsnRS1* (UNE-N),
Thr17Met	Unique domain of *AsnRS1* (UNE-N),
Arg322Leu	Disturbance of the stabilization of aa-adenylate
Leu350Pro	Probably little effect on enzymatic activity and tRNA recognition, predictable effect on *AsnRS1* dimer formation.
Asp356Ala	Mutant at the interface between the two enzymes, loss of the side chain of Asp356 and therefore probably an interaction with the dimmer becoming more unstable
Ala422Thr	Affects the 3 'end of the acceptor arm
Gly509Ser	Disrupts the end of the interface between the two subunits of *AsnRS1*
Arg545Cys	Potential disruption of the interaction with the acceptor arm of the tRNA

Table S6: The substrate in the figures is the aminoacyl-adenylate of Brugia malayi Asparaginyl-tRNA synthetase complexed with ATP: Mg and L-Asp-beta-NOH adenylate: PPi: Mg. The models of wild, mutant and Brugia malayi structures were superimposed with very good agreement. Apart from the unique domain of *AsnRS1*, which cannot be modelled. The strongest effect in terms of catalysis would be expected for Arg322Leu and Asp356Ala.

Section 4: Supplemental methods

Next-generation sequencing methods

Families 5, 6, 8,10 were sequenced at GeneDx, where genomic DNA was extracted from the proband and parents (when available). The exonic regions and flanking splice junctions of the genome were captured using the Clinical Research Exome kit (Agilent Technologies, Santa Clara, CA) or the IDT xGen Exome Research Panel v1.0. Massively parallel (NextGen) sequencing was done on an Illumina system with 100bp or greater paired-end reads. Reads were aligned to human genome build GRCh37/UCSC hg19, and analysed for sequence variants using a custom-developed analysis tool. Additional sequencing technology and variant interpretation protocol has been previously described[120]. The general assertion criteria for variant classification are publicly available on the GeneDx ClinVar submission page (http://www.ncbi.nlm.nih.gov/clinvar/submitters/26957/)

Families 17 and 19, Agilent sequence capture was used, as described elsewhere[121]. They were subjected to exome capture with either the Agilent SureSelect Human All Exome 50 Mb kit (Agilent Technologies, Inc., USA) or the Illumina Rapid Capture 37 Mb Enrichment kit. Sequencing with 100-bp paired-end reads was performed using either the Illumina HiSeq2000 or HiSeq4000 instruments (Illumina, Inc., USA), resulting in >94% recovery at 10× coverage and >85% recovery at 20x coverage. GATK best practices pipeline was used for SNP and INDEL variant identification (http://www.broadinstitute.org/gatk/). Variants were annotated with in-house software1 and homozygous variant prioritization was done using custom Python scripts (available upon request) to keep variants with MAF.

The rest of the cases were sequenced based on the Nextera Rapid Capture Exome kit (Illumina) and run on the HiSeq 2500 platform (Illumina), the resulting 100 bp paired-end sequence reads were mapped against the human reference genome assembly 19 (GRCh37) with the Burrows-Wheeler Aligner package [122] and read duplicates were removed with Picard. Variant calling and indel realignments were performed with the Genome Analysis Toolkit (GATK) [123] and variants were submitted to ANNOVAR for annotation[124].

Zebrafish modeling

Zebrafish (*Danio rerio*) embryos were obtained from a wild-type strain and were raised at 28.5 °C. Microinjections (~1 nl) were performed at the one-cell stage. The expression vector used was *NARS1* (NM_004539) Human cDNA Clone (OriGene) cloned into pCS2+ (addgene) using CloneEZ from genescript as described above for the yeast studies. Plasmids where sequenced to confirm the correct insertion of the fragment. Mutant versions of this construct were generated using the QuikChange Site-Directed Mutagenesis kit (Stratagene). The sequences for all primers are available upon request. Capped RNA was synthesized using the mMESSAGE mMACHINE kit (Ambion). Live zebrafish were imaged on a Leica MZFL III stereo microscope, and body surface area was calculated using IPLab software (Biovision). All experiments with zebrafish were performed in compliance with local ethical and Home Office (UK) regulations, project license 70/6875.

Yeast complementation assay of *NARS*1 gene

The experiments were performed in an analogous way as described before[7]. In brief, cells were grown on EMM + ade+ ura to saturation (for 24 hours), to allow for the loss of the pJR-41XU-nrs1 plasmid. After this time, cell density was adjusted to 4 x 10^6 cells /ml, and five-fold dilutions were spotted onto EMM + ade + ura plates or EMM + ade + ¼ ura + FOA

plates to select for cells that have lost the plasmid expressing different *NARS1* variants. All mutants constructed using the human *NARS1* WT gene, are found in conserved amino acids identical to the yeast *NARS1* WT, with the exception of c.1067A>C, p.Asp356Ala, which translated to a similar amino acid. These experiments showed that a yeast strain carrying an nrs1 deletion was well complemented by the c.1633C>T, p.Arg545Cys mutation. Given the increased growth, it would therefore fit with a conformational effect present in higher species that would only change the code here likely by tRNA interaction (Figure S12).

Section 5: Supplementary References

1. Kelley, L.A., Mezulis, S., Yates, C.M., Wass, M.N., and Sternberg, M.J. (2015). The Phyre2 web portal for protein modeling, prediction and analysis. Nat Protoc 10, 845-858.
2. Latour, P., Thauvin-Robinet, C., Baudelet-Mery, C., Soichot, P., Cusin, V., Faivre, L., Locatelli, M.C., Mayencon, M., Sarcey, A., Broussolle, E., et al. (2010). A major determinant for binding and aminoacylation of tRNA(Ala) in cytoplasmic Alanyl-tRNA synthetase is mutated in dominant axonal Charcot-Marie-Tooth disease. Am J Hum Genet 86, 77-82.
3. Seburn, K.L., Nangle, L.A., Cox, G.A., Schimmel, P., and Burgess, R.W. (2006). An active dominant mutation of glycyl-tRNA synthetase causes neuropathy in a Charcot-Marie-Tooth 2D mouse model. Neuron 51, 715-726.
4. Lynch, D.S., Zhang, W.J., Lakshmanan, R., Kinsella, J.A., Uzun, G.A., Karbay, M., Tufekcioglu, Z., Hanagasi, H., Burke, G., Foulds, N., et al. (2016). Analysis of Mutations in AARS2 in a Series of CSF1R-Negative Patients With Adult-Onset Leukoencephalopathy With Axonal Spheroids and Pigmented Glia. JAMA Neurol 73, 1433-1439.
5. Dohrn, M.F., Glockle, N., Mulahasanovic, L., Heller, C., Mohr, J., Bauer, C., Riesch, E., Becker, A., Battke, F., Hortnagel, K., et al. (2017). Frequent genes in rare diseases: panel-based next generation sequencing to disclose causal mutations in hereditary neuropathies. J Neurochem 143, 507-522.
6. Sundal, C., Carmona, S., Yhr, M., Almstrom, O., Ljungberg, M., Hardy, J., Hedberg-Oldfors, C., Fred, A., Bras, J., Oldfors, A., et al. (2019). An AARS variant as the likely cause of Swedish type hereditary diffuse leukoencephalopathy with spheroids. Acta Neuropathol Commun 7, 188.
7. Dallabona, C., Diodato, D., Kevelam, S.H., Haack, T.B., Wong, L.J., Salomons, G.S., Baruffini, E., Melchionda, L., Mariotti, C., Strom, T.M., et al. (2014). Novel (ovario) leukodystrophy related to AARS2 mutations. Neurology 82, 2063-2071.
8. Gotz, A., Tyynismaa, H., Euro, L., Ellonen, P., Hyotylainen, T., Ojala, T., Hamalainen, R.H., Tommiska, J., Raivio, T., Oresic, M., et al. (2011). Exome sequencing identifies mitochondrial alanyl-tRNA synthetase mutations in infantile mitochondrial cardiomyopathy. Am J Hum Genet 88, 635-642.
9. Sommerville, E.W., Zhou, X.L., Olahova, M., Jenkins, J., Euro, L., Konovalova, S., Hilander, T., Pyle, A., He, L., Habeebu, S., et al. (2019). Instability of the mitochondrial alanyl-tRNA synthetase underlies fatal infantile-onset cardiomyopathy. Hum Mol Genet 28, 258-268.
10. Wang, X., Wang, Q., Tang, H., Chen, B., Dong, X., Niu, S., Li, S., Shi, Y., Shan, W., and Zhang, Z. (2019). Novel Alanyl-tRNA Synthetase 2 Pathogenic Variants in Leukodystrophies. Frontiers in neurology 10, 1321.
11. Kuo, M.E., Antonellis, A., and Shakkottai, V.G. (2020). Alanyl-tRNA Synthetase 2 (AARS2)-Related Ataxia Without Leukoencephalopathy. Cerebellum (London, England) 19, 154-160.
12. Kuo, M.E., Theil, A.F., Kievit, A., Malicdan, M.C., Introne, W.J., Christian, T., Verheijen, F.W., Smith, D.E.C., Mendes, M.I., Hussaarts-Odijk, L., et al. (2019). Cysteinyl-tRNA Synthetase Mutations Cause a Multi-System, Recessive Disease That Includes Microcephaly, Developmental Delay, and Brittle Hair and Nails. American journal of human genetics 104, 520-529.

13. Coughlin, C.R., 2nd, Scharer, G.H., Friederich, M.W., Yu, H.C., Geiger, E.A., Creadon-Swindell, G., Collins, A.E., Vanlander, A.V., Coster, R.V., Powell, C.A., et al. (2015). Mutations in the mitochondrial cysteinyl-tRNA synthase gene, CARS2, lead to a severe epileptic encephalopathy and complex movement disorder. J Med Genet 52, 532-540.
14. Samanta, D., Gokden, M., and Willis, E. (2018). Clinicopathologic Findings of CARS2 Mutation. Pediatr Neurol 87, 65-69.
15. Samanta, D. (2018). Cerebral Infarction in CARS2 Mutation. Pediatr Neurol.
16. Hallmann, K., Zsurka, G., Moskau-Hartmann, S., Kirschner, J., Korinthenberg, R., Ruppert, A.K., Ozdemir, O., Weber, Y., Becker, F., Lerche, H., et al. (2014). A homozygous splice-site mutation in CARS2 is associated with progressive myoclonic epilepsy. Neurology 83, 2183-2187.
17. Taft, R.J., Vanderver, A., Leventer, R.J., Damiani, S.A., Simons, C., Grimmond, S.M., Miller, D., Schmidt, J., Lockhart, P.J., Pope, K., et al. (2013). Mutations in DARS cause hypomyelination with brain stem and spinal cord involvement and leg spasticity. Am J Hum Genet 92, 774-780.
18. Frohlich, D., Suchowerska, A.K., Voss, C., He, R., Wolvetang, E., von Jonquieres, G., Simons, C., Fath, T., Housley, G.D., and Klugmann, M. (2018). Expression Pattern of the Aspartyl-tRNA Synthetase DARS in the Human Brain. Front Mol Neurosci 11, 81.
19. Frohlich, D., Suchowerska, A.K., Spencer, Z.H., von Jonquieres, G., Klugmann, C.B., Bongers, A., Delerue, F., Stefen, H., Ittner, L.M., Fath, T., et al. (2017). In vivocharacterization of the aspartyl-tRNA synthetase DARS: Homing in on the leukodystrophy HBSL. Neurobiol Dis 97, 24-35.
20. Scheper, G.C., van der Klok, T., van Andel, R.J., van Berkel, C.G., Sissler, M., Smet, J., Muravina, T.I., Serkov, S.V., Uziel, G., Bugiani, M., et al. (2007). Mitochondrial aspartyl-tRNA synthetase deficiency causes leukoencephalopathy with brain stem and spinal cord involvement and lactate elevation. Nature genetics 39, 534-539.
21. Yelam, A., Nagarajan, E., Chuquilin, M., and Govindarajan, R. (2019). Leucoencephalopathy with brain stem and spinal cord involvement and lactate elevation: a novel mutation in the DARS2 gene. BMJ Case Rep 12.
22. Shimojima, K., Higashiguchi, T., Kishimoto, K., Miyatake, S., Miyake, N., Takanashi, J.I., Matsumoto, N., and Yamamoto, T. (2017). A novel DARS2 mutation in a Japanese patient with leukoencephalopathy with brainstem and spinal cord involvement but no lactate elevation. Hum Genome Var 4, 17051.
23. Lan, M.Y., Chang, Y.Y., Yeh, T.H., Lin, T.K., and Lu, C.S. (2017). Leukoencephalopathy with brainstem and spinal cord involvement and lactate elevation (LBSL) with a novel DARS2 mutation and isolated progressive spastic paraparesis. J Neurol Sci 372, 229-231.
24. Kohler, C., Heyer, C., Hoffjan, S., Stemmler, S., Lucke, T., Thiels, C., Kohlschutter, A., Lobel, U., Horvath, R., Kleinle, S., et al. (2015). Early-onset leukoencephalopathy due to a homozygous missense mutation in the DARS2 gene. Mol Cell Probes 29, 319-322.
25. Yamashita, S., Miyake, N., Matsumoto, N., Osaka, H., Iai, M., Aida, N., and Tanaka, Y. (2013). Neuropathology of leukoencephalopathy with brainstem and spinal cord involvement and high lactate caused by a homozygous mutation of DARS2. Brain Dev 35, 312-316.
26. Miyake, N., Yamashita, S., Kurosawa, K., Miyatake, S., Tsurusaki, Y., Doi, H., Saitsu, H., and Matsumoto, N. (2011). A novel homozygous mutation of DARS2 may cause a severe LBSL variant. Clin Genet 80, 293-296.

27. Tzoulis, C., Tran, G.T., Gjerde, I.O., Aasly, J., Neckelmann, G., Rydland, J., Varga, V., Wadel-Andersen, P., and Bindoff, L.A. (2012). Leukoencephalopathy with brainstem and spinal cord involvement caused by a novel mutation in the DARS2 gene. J Neurol 259, 292-296.
28. Synofzik, M., Schicks, J., Lindig, T., Biskup, S., Schmidt, T., Hansel, J., Lehmann-Horn, F., and Schols, L. (2011). Acetazolamide-responsive exercise-induced episodic ataxia associated with a novel homozygous DARS2 mutation. J Med Genet 48, 713-715.
29. Lin, J., Chiconelli Faria, E., Da Rocha, A.J., Rodrigues Masruha, M., Pereira Vilanova, L.C., Scheper, G.C., and Van der Knaap, M.S. (2010). Leukoencephalopathy with brainstem and spinal cord involvement and normal lactate: a new mutation in the DARS2 gene. J Child Neurol 25, 1425-1428.
30. Mendes, M.I., Gutierrez Salazar, M., Guerrero, K., Thiffault, I., Salomons, G.S., Gauquelin, L., Tran, L.T., Forget, D., Gauthier, M.S., Waisfisz, Q., et al. (2018). Bi-allelic Mutations in EPRS, Encoding the Glutamyl-Prolyl-Aminoacyl-tRNA Synthetase, Cause a Hypomyelinating Leukodystrophy. American journal of human genetics 102, 676-684.
31. Steenweg, M.E., Ghezzi, D., Haack, T., Abbink, T.E., Martinelli, D., van Berkel, C.G., Bley, A., Diogo, L., Grillo, E., Te Water Naude, J., et al. (2012). Leukoencephalopathy with thalamus and brainstem involvement and high lactate 'LTBL' caused by EARS2 mutations. Brain 135, 1387-1394.
32. Gungor, O., Ozkaya, A.K., Sahin, Y., Gungor, G., Dilber, C., and Aydin, K. (2016). A compound heterozygous EARS2 mutation associated with mild leukoencephalopathy with thalamus and brainstem involvement and high lactate (LTBL). Brain Dev 38, 857-861.
33. Taskin, B.D., Karalok, Z.S., Gurkas, E., Aydin, K., Aydogmus, U., Ceylaner, S., Karaer, K., Yilmaz, C., and Pearl, P.L. (2016). Early-Onset Mild Type Leukoencephalopathy Caused by a Homozygous EARS2 Mutation. J Child Neurol 31, 938-941.
34. Kevelam, S.H., Klouwer, F.C., Fock, J.M., Salomons, G.S., Bugiani, M., and van der Knaap, M.S. (2016). Absent Thalami Caused by a Homozygous EARS2 Mutation: Expanding Disease Spectrum of LTBL. Neuropediatrics 47, 64-67.
35. Biancheri, R., Lamantea, E., Severino, M., Diodato, D., Pedemonte, M., Cassandrini, D., Ploederl, A., Trucco, F., Fiorillo, C., Minetti, C., et al. (2015). Expanding the Clinical and Magnetic Resonance Spectrum of Leukoencephalopathy with Thalamus and Brainstem Involvement and High Lactate (LTBL) in a Patient Harboring a Novel EARS2 Mutation. JIMD Rep 23, 85-89.
36. Talim, B., Pyle, A., Griffin, H., Topaloglu, H., Tokatli, A., Keogh, M.J., Santibanez-Koref, M., Chinnery, P.F., and Horvath, R. (2013). Multisystem fatal infantile disease caused by a novel homozygous EARS2 mutation. Brain 136, e228.
37. Krenke, K., Szczaluba, K., Bielecka, T., Rydzanicz, M., Lange, J., Koppolu, A., and Ploski, R. (2019). FARSA mutations mimic phenylalanyl-tRNA synthetase deficiency caused by FARSB defects. Clin Genet 96, 468-472.
38. Antonellis, A., Oprescu, S.N., Griffin, L.B., Heider, A., Amalfitano, A., and Innis, J.W. (2018). Compound heterozygosity for loss-of-function FARSB variants in a patient with classic features of recessive aminoacyl-tRNA synthetase-related disease. Human mutation 39, 834-840.
39. Zadjali, F., Al-Yahyaee, A., Al-Nabhani, M., Al-Mubaihsi, S., Gujjar, A., Raniga, S., and Al-Maawali, A. (2018). Homozygosity for FARSB mutation leads to Phe-tRNA synthetase-related disease of growth restriction, brain calcification, and interstitial lung disease. Human mutation 39, 1355-1359.

40. Elo, J.M., Yadavalli, S.S., Euro, L., Isohanni, P., Gotz, A., Carroll, C.J., Valanne, L., Alkuraya, F.S., Uusimaa, J., Paetau, A., et al. (2012). Mitochondrial phenylalanyl-tRNA synthetase mutations underlie fatal infantile Alpers encephalopathy. Hum Mol Genet 21, 4521-4529.
41. Yang, Y., Liu, W., Fang, Z., Shi, J., Che, F., He, C., Yao, L., Wang, E., and Wu, Y. (2016). A Newly Identified Missense Mutation in FARS2 Causes Autosomal-Recessive Spastic Paraplegia. Human mutation 37, 165-169.
42. Raviglione, F., Conte, G., Ghezzi, D., Parazzini, C., Righini, A., Vergaro, R., Legati, A., Spaccini, L., Gasperini, S., Garavaglia, B., et al. (2016). Clinical findings in a patient with FARS2 mutations and early-infantile-encephalopathy with epilepsy. Am J Med Genet A 170, 3004-3007.
43. Finsterer, J., Scorza, F.A., and Scorza, C.A. (2018). Antiepileptic treatment may determine the outcome of FARS2 mutation carriers. Mol Genet Metab Rep 17, 45.
44. Cho, J.S., Kim, S.H., Kim, H.Y., Chung, T., Kim, D., Jang, S., Lee, S.B., Yoo, S.K., Shin, J., Kim, J.I., et al. (2017). FARS2 mutation and epilepsy: Possible link with early-onset epileptic encephalopathy. Epilepsy Res 129, 118-124.
45. Almalki, A., Alston, C.L., Parker, A., Simonic, I., Mehta, S.G., He, L., Reza, M., Oliveira, J.M., Lightowlers, R.N., McFarland, R., et al. (2014). Mutation of the human mitochondrial phenylalanine-tRNA synthetase causes infantile-onset epilepsy and cytochrome c oxidase deficiency. Biochim Biophys Acta 1842, 56-64.
46. McMillan, H.J., Schwartzentruber, J., Smith, A., Lee, S., Chakraborty, P., Bulman, D.E., Beaulieu, C.L., Majewski, J., Boycott, K.M., and Geraghty, M.T. (2014). Compound heterozygous mutations in glycyl-tRNA synthetase are a proposed cause of systemic mitochondrial disease. BMC Med Genet 15, 36.
47. Antonellis, A., Ellsworth, R.E., Sambuughin, N., Puls, I., Abel, A., Lee-Lin, S.Q., Jordanova, A., Kremensky, I., Christodoulou, K., Middleton, L.T., et al. (2003). Glycyl tRNA synthetase mutations in Charcot-Marie-Tooth disease type 2D and distal spinal muscular atrophy type V. Am J Hum Genet 72, 1293-1299.
48. Liao, Y.C., Liu, Y.T., Tsai, P.C., Chang, C.C., Huang, Y.H., Soong, B.W., and Lee, Y.C. (2015). Two Novel De Novo GARS Mutations Cause Early-Onset Axonal Charcot-Marie-Tooth Disease. PLoS One 10, e0133423.
49. Corcia, P., Brulard, C., Beltran, S., Marouillat, S., Bakkouche, S.E., Andres, C.R., Blasco, H., and Vourc'h, P. (2019). Typical bulbar ALS can be linked to GARS mutation. Amyotroph Lateral Scler Frontotemporal Degener, 1-3.
50. Rahane, C.S., Kutzner, A., and Heese, K. (2019). Establishing a human adrenocortical carcinoma (ACC)-specific gene mutation signature. Cancer Genet 230, 1-12.
51. Nan, H., Takaki, R., Hata, T., Ichinose, Y., Tsuchiya, M., Koh, K., and Takiyama, Y. (2018). Novel GARS mutation presenting as autosomal dominant intermediate Charcot-Marie-Tooth disease. J Peripher Nerv Syst.
52. Yu, X., Chen, B., Tang, H., Li, W., Fu, Y., Zhang, Z., and Yan, Y. (2018). A Novel Mutation of GARS in a Chinese Family With Distal Hereditary Motor Neuropathy Type V. Front Neurol 9, 571.
53. Holloway, M.P., DeNardo, B.D., Phornphutkul, C., Nguyen, K., Davis, C., Jackson, C., Richendrfer, H., Creton, R., and Altura, R.A. (2016). An asymptomatic mutation complicating severe chemotherapy-induced peripheral neuropathy (CIPN): a case for personalised medicine and a zebrafish model of CIPN. NPJ Genom Med 1, 16016.
54. Sun, A., Liu, X., Zheng, M., Sun, Q., Huang, Y., and Fan, D. (2015). A novel mutation of the glycyl-tRNA synthetase (GARS) gene associated with Charcot-Marie-Tooth type 2D in a Chinese family. Neurol Res 37, 782-787.

55. Kawakami, N., Komatsu, K., Yamashita, H., Uemura, K., Oka, N., Takashima, H., and Takahashi, R. (2014). [A novel mutation in glycyl-tRNA synthetase caused Charcot-Marie-Tooth disease type 2D with facial and respiratory muscle involvement]. Rinsho Shinkeigaku 54, 911-915.
56. Eskuri, J.M., Stanley, C.M., Moore, S.A., and Mathews, K.D. (2012). Infantile onset CMT2D/dSMA V in monozygotic twins due to a mutation in the anticodon-binding domain of GARS. J Peripher Nerv Syst 17, 132-134.
57. Hamaguchi, A., Ishida, C., Iwasa, K., Abe, A., and Yamada, M. (2010). Charcot-Marie-Tooth disease type 2D with a novel glycyl-tRNA synthetase gene (GARS) mutation. J Neurol 257, 1202-1204.
58. Achilli, F., Bros-Facer, V., Williams, H.P., Banks, G.T., AlQatari, M., Chia, R., Tucci, V., Groves, M., Nickols, C.D., Seburn, K.L., et al. (2009). An ENU-induced mutation in mouse glycyl-tRNA synthetase (GARS) causes peripheral sensory and motor phenotypes creating a model of Charcot-Marie-Tooth type 2D peripheral neuropathy. Dis Model Mech 2, 359-373.
59. Abe, A., Numakura, C., Saito, K., Koide, H., Oka, N., Honma, A., Kishikawa, Y., and Hayasaka, K. (2009). Neurofilament light chain polypeptide gene mutations in Charcot-Marie-Tooth disease: nonsense mutation probably causes a recessive phenotype. J Hum Genet 54, 94-97.
60. Dubourg, O., Azzedine, H., Yaou, R.B., Pouget, J., Barois, A., Meininger, V., Bouteiller, D., Ruberg, M., Brice, A., and LeGuern, E. (2006). The G526R glycyl-tRNA synthetase gene mutation in distal hereditary motor neuropathy type V. Neurology 66, 1721-1726.
61. Del Bo, R., Locatelli, F., Corti, S., Scarlato, M., Ghezzi, S., Prelle, A., Fagiolari, G., Moggio, M., Carpo, M., Bresolin, N., et al. (2006). Coexistence of CMT-2D and distal SMA-V phenotypes in an Italian family with a GARS gene mutation. Neurology 66, 752-754.
62. Forrester, N., Rattihalli, R., Horvath, R., Maggi, L., Manzur, A., Fuller, G., Gutowski, N., Rankin, J., Dick, D., Buxton, C., et al. (2020). Clinical and Genetic Features in a Series of Eight Unrelated Patients with Neuropathy Due to Glycyl-tRNA Synthetase (GARS) Variants. J Neuromuscul Dis 7, 137-143.
63. Vester, A., Velez-Ruiz, G., McLaughlin, H.M., Program, N.C.S., Lupski, J.R., Talbot, K., Vance, J.M., Zuchner, S., Roda, R.H., Fischbeck, K.H., et al. (2013). A loss-of-function variant in the human histidyl-tRNA synthetase (HARS) gene is neurotoxic in vivo. Hum Mutat 34, 191-199.
64. Puffenberger, E.G., Jinks, R.N., Sougnez, C., Cibulskis, K., Willert, R.A., Achilly, N.P., Cassidy, R.P., Fiorentini, C.J., Heiken, K.F., Lawrence, J.J., et al. (2012). Genetic mapping and exome sequencing identify variants associated with five novel diseases. PLoS One 7, e28936.
65. Pierce, S.B., Chisholm, K.M., Lynch, E.D., Lee, M.K., Walsh, T., Opitz, J.M., Li, W., Klevit, R.E., and King, M.C. (2011). Mutations in mitochondrial histidyl tRNA synthetase HARS2 cause ovarian dysgenesis and sensorineural hearing loss of Perrault syndrome. Proc Natl Acad Sci U S A 108, 6543-6548.
66. Demain, L.A.M., Gerkes, E.H., Smith, R.J.H., Molina-Ramirez, L.P., O'Keefe, R.T., and Newman, W.G. (2020). A recurrent missense variant in HARS2 results in variable sensorineural hearing loss in three unrelated families. J Hum Genet 65, 305-311.
67. Kopajtich, R., Murayama, K., Janecke, A.R., Haack, T.B., Breuer, M., Knisely, A.S., Harting, I., Ohashi, T., Okazaki, Y., Watanabe, D., et al. (2016). Biallelic IARS Mutations Cause Growth Retardation with Prenatal Onset, Intellectual Disability, Muscular Hypotonia, and Infantile Hepatopathy. Am J Hum Genet 99, 414-422.

68. Schwartzentruber, J., Buhas, D., Majewski, J., Sasarman, F., Papillon-Cavanagh, S., Thiffault, I., Sheldon, K.M., Massicotte, C., Patry, L., Simon, M., et al. (2014). Mutation in the nuclear-encoded mitochondrial isoleucyl-tRNA synthetase IARS2 in patients with cataracts, growth hormone deficiency with short stature, partial sensorineural deafness, and peripheral neuropathy or with Leigh syndrome. Hum Mutat 35, 1285-1289.
69. Moosa, S., Haagerup, A., Gregersen, P.A., Petersen, K.K., Altmuller, J., Thiele, H., Nurnberg, P., Cho, T.J., Kim, O.H., Nishimura, G., et al. (2017). Confirmation of CAGSSS syndrome as a distinct entity in a Danish patient with a novel homozygous mutation in IARS2. Am J Med Genet A 173, 1102-1108.
70. Jabbour, S., and Harissi-Dagher, M. (2016). Recessive Mutation in a Nuclear-Encoded Mitochondrial tRNA Synthetase Associated With Infantile Cataract, Congenital Neurotrophic Keratitis, and Orbital Myopathy. Cornea 35, 894-896.
71. McLaughlin, H.M., Sakaguchi, R., Liu, C., Igarashi, T., Pehlivan, D., Chu, K., Iyer, R., Cruz, P., Cherukuri, P.F., Hansen, N.F., et al. (2010). Compound heterozygosity for loss-of-function lysyl-tRNA synthetase mutations in a patient with peripheral neuropathy. Am J Hum Genet 87, 560-566.
72. McMillan, H.J., Humphreys, P., Smith, A., Schwartzentruber, J., Chakraborty, P., Bulman, D.E., Beaulieu, C.L., Consortium, F.C., Majewski, J., Boycott, K.M., et al. (2015). Congenital Visual Impairment and Progressive Microcephaly Due to Lysyl-Transfer Ribonucleic Acid (RNA) Synthetase (KARS) Mutations: The Expanding Phenotype of Aminoacyl-Transfer RNA Synthetase Mutations in Human Disease. J Child Neurol 30, 1037-1043.
73. Santos-Cortez, R.L., Lee, K., Azeem, Z., Antonellis, P.J., Pollock, L.M., Khan, S., Irfanullah, Andrade-Elizondo, P.B., Chiu, I., Adams, M.D., et al. (2013). Mutations in KARS, encoding lysyl-tRNA synthetase, cause autosomal-recessive nonsyndromic hearing impairment DFNB89. Am J Hum Genet 93, 132-140.
74. Itoh, M., Dai, H., Horike, S.I., Gonzalez, J., Kitami, Y., Meguro-Horike, M., Kuki, I., Shimakawa, S., Yoshinaga, H., Ota, Y., et al. (2019). Biallelic KARS pathogenic variants cause an early-onset progressive leukodystrophy. Brain : a journal of neurology 142, 560-573.
75. Casey, J.P., McGettigan, P., Lynam-Lennon, N., McDermott, M., Regan, R., Conroy, J., Bourke, B., O'Sullivan, J., Crushell, E., Lynch, S., et al. (2012). Identification of a mutation in LARS as a novel cause of infantile hepatopathy. Mol Genet Metab 106, 351-358.
76. Pierce, S.B., Gersak, K., Michaelson-Cohen, R., Walsh, T., Lee, M.K., Malach, D., Klevit, R.E., King, M.C., and Levy-Lahad, E. (2013). Mutations in LARS2, encoding mitochondrial leucyl-tRNA synthetase, lead to premature ovarian failure and hearing loss in Perrault syndrome. Am J Hum Genet 92, 614-620.
77. Gonzalez, M., McLaughlin, H., Houlden, H., Guo, M., Yo-Tsen, L., Hadjivassilious, M., Speziani, F., Yang, X.L., Antonellis, A., Reilly, M.M., et al. (2013). Exome sequencing identifies a significant variant in methionyl-tRNA synthetase (MARS) in a family with late-onset CMT2. J Neurol Neurosurg Psychiatry 84, 1247-1249.
78. van Meel, E., Wegner, D.J., Cliften, P., Willing, M.C., White, F.V., Kornfeld, S., and Cole, F.S. (2013). Rare recessive loss-of-function methionyl-tRNA synthetase mutations presenting as a multi-organ phenotype. BMC Med Genet 14, 106.
79. Hadchouel, A., Wieland, T., Griese, M., Baruffini, E., Lorenz-Depiereux, B., Enaud, L., Graf, E., Dubus, J.C., Halioui-Louhaichi, S., Coulomb, A., et al. (2015). Biallelic Mutations of Methionyl-tRNA Synthetase Cause a Specific Type of Pulmonary Alveolar Proteinosis Prevalent on Reunion Island. Am J Hum Genet 96, 826-831.

80. Alzaid, M., Alshamrani, A., Al Harbi, A.S., Alenzi, A., and Mohamed, S. (2019). Methionyl-tRNA synthetase novel mutation causes pulmonary alveolar proteinosis. Saudi Med J 40, 195-198.
81. Bayat, V., Thiffault, I., Jaiswal, M., Tetreault, M., Donti, T., Sasarman, F., Bernard, G., Demers-Lamarche, J., Dicaire, M.J., Mathieu, J., et al. (2012). Mutations in the mitochondrial methionyl-tRNA synthetase cause a neurodegenerative phenotype in flies and a recessive ataxia (ARSAL) in humans. PLoS Biol 10, e1001288.
82. Webb, B.D., Wheeler, P.G., Hagen, J.J., Cohen, N., Linderman, M.D., Diaz, G.A., Naidich, T.P., Rodenburg, R.J., Houten, S.M., and Schadt, E.E. (2015). Novel, compound heterozygous, single-nucleotide variants in MARS2 associated with developmental delay, poor growth, and sensorineural hearing loss. Hum Mutat 36, 587-592.
83. Vanlander, A.V., Menten, B., Smet, J., De Meirleir, L., Sante, T., De Paepe, B., Seneca, S., Pearce, S.F., Powell, C.A., Vergult, S., et al. (2015). Two siblings with homozygous pathogenic splice-site variant in mitochondrial asparaginyl-tRNA synthetase (NARS2). Hum Mutat 36, 222-231.
84. Finsterer, J. (2018). Management of NARS2-Related Mitochondrial Disorder is Complex. Pediatr Neurol.
85. Seaver, L.H., DeRoos, S., Andersen, N.J., Betz, B., Prokop, J., Lannen, N., Jordan, R., and Rajasekaran, S. (2018). Lethal NARS2-Related Disorder Associated With Rapidly Progressive Intractable Epilepsy and Global Brain Atrophy. Pediatr Neurol 89, 26-30.
86. Mizuguchi, T., Nakashima, M., Kato, M., Yamada, K., Okanishi, T., Ekhilevitch, N., Mandel, H., Eran, A., Toyono, M., Sawaishi, Y., et al. (2017). PARS2 and NARS2 mutations in infantile-onset neurodegenerative disorder. J Hum Genet 62, 525-529.
87. Simon, M., Richard, E.M., Wang, X., Shahzad, M., Huang, V.H., Qaiser, T.A., Potluri, P., Mahl, S.E., Davila, A., Nazli, S., et al. (2015). Mutations of human NARS2, encoding the mitochondrial asparaginyl-tRNA synthetase, cause nonsyndromic deafness and Leigh syndrome. PLoS Genet 11, e1005097.
88. Sofou, K., Kollberg, G., Holmstrom, M., Davila, M., Darin, N., Gustafsson, C.M., Holme, E., Oldfors, A., Tulinius, M., and Asin-Cayuela, J. (2015). Whole exome sequencing reveals mutations in NARS2 and PARS2, encoding the mitochondrial asparaginyl-tRNA synthetase and prolyl-tRNA synthetase, in patients with Alpers syndrome. Mol Genet Genomic Med 3, 59-68.
89. Zhang, X., Ling, J., Barcia, G., Jing, L., Wu, J., Barry, B.J., Mochida, G.H., Hill, R.S., Weimer, J.M., Stein, Q., et al. (2014). Mutations in QARS, encoding glutaminyl-tRNA synthetase, cause progressive microcephaly, cerebral-cerebellar atrophy, and intractable seizures. Am J Hum Genet 94, 547-558.
90. Nafisinia, M., Sobreira, N., Riley, L., Gold, W., Uhlenberg, B., Weiss, C., Boehm, C., Prelog, K., Ouvrier, R., and Christodoulou, J. (2017). Mutations in RARS cause a hypomyelination disorder akin to Pelizaeus-Merzbacher disease. Eur J Hum Genet 25, 1134-1141.
91. Mendes, M.I., Green, L.M.C., Bertini, E., Tonduti, D., Aiello, C., Smith, D., Salsano, E., Beerepoot, S., Hertecant, J., von Spiczak, S., et al. (2020). RARS1-related hypomyelinating leukodystrophy: Expanding the spectrum. Annals of clinical and translational neurology 7, 83-93.
92. Matsumoto, N., Watanabe, N., Iibe, N., Tatsumi, Y., Hattori, K., Takeuchi, Y., Oizumi, H., Ohbuchi, K., Torii, T., Miyamoto, Y., et al. (2019). Hypomyelinating leukodystrophy-associated mutation of RARS leads it to the lysosome, inhibiting oligodendroglial morphological differentiation. Biochem Biophys Rep 20, 100705.

93. Edvardson, S., Shaag, A., Kolesnikova, O., Gomori, J.M., Tarassov, I., Einbinder, T., Saada, A., and Elpeleg, O. (2007). Deleterious mutation in the mitochondrial arginyl-transfer RNA synthetase gene is associated with pontocerebellar hypoplasia. Am J Hum Genet 81, 857-862.
94. Luhl, S., Bode, H., Schlotzer, W., Bartsakoulia, M., Horvath, R., Abicht, A., Stenzel, M., Kirschner, J., and Grunert, S.C. (2016). Novel homozygous RARS2 mutation in two siblings without pontocerebellar hypoplasia - further expansion of the phenotypic spectrum. Orphanet J Rare Dis 11, 140.
95. Li, Z., Schonberg, R., Guidugli, L., Johnson, A.K., Arnovitz, S., Yang, S., Scafidi, J., Summar, M.L., Vezina, G., Das, S., et al. (2015). A novel mutation in the promoter of RARS2 causes pontocerebellar hypoplasia in two siblings. J Hum Genet 60, 363-369.
96. Musante, L., Puttmann, L., Kahrizi, K., Garshasbi, M., Hu, H., Stehr, H., Lipkowitz, B., Otto, S., Jensen, L.R., Tzschach, A., et al. (2017). Mutations of the aminoacyl-tRNA-synthetases SARS and WARS2 are implicated in the etiology of autosomal recessive intellectual disability. Hum Mutat 38, 621-636.
97. Belostotsky, R., Ben-Shalom, E., Rinat, C., Becker-Cohen, R., Feinstein, S., Zeligson, S., Segel, R., Elpeleg, O., Nassar, S., and Frishberg, Y. (2011). Mutations in the mitochondrial seryl-tRNA synthetase cause hyperuricemia, pulmonary hypertension, renal failure in infancy and alkalosis, HUPRA syndrome. Am J Hum Genet 88, 193-200.
98. Theil, A.F., Botta, E., Raams, A., Smith, D.E.C., Mendes, M.I., Caligiuri, G., Giachetti, S., Bione, S., Carriero, R., Liberi, G., et al. (2019). Bi-allelic TARS Mutations Are Associated with Brittle Hair Phenotype. American journal of human genetics 105, 434-440.
99. Diodato, D., Melchionda, L., Haack, T.B., Dallabona, C., Baruffini, E., Donnini, C., Granata, T., Ragona, F., Balestri, P., Margollicci, M., et al. (2014). VARS2 and TARS2 mutations in patients with mitochondrial encephalomyopathies. Hum Mutat 35, 983-989.
100. Wang, Y., Zhou, X.L., Ruan, Z.R., Liu, R.J., Eriani, G., and Wang, E.D. (2016). A Human Disease-causing Point Mutation in Mitochondrial Threonyl-tRNA Synthetase Induces Both Structural and Functional Defects. J Biol Chem 291, 6507-6520.
101. Okur, V., Ganapathi, M., Wilson, A., and Chung, W.K. (2018). Biallelic variants in VARS in a family with two siblings with intellectual disability and microcephaly: case report and review of the literature. Cold Spring Harb Mol Case Stud 4.
102. Stephen, J., Nampoothiri, S., Banerjee, A., Tolman, N.J., Penninger, J.M., Elling, U., Agu, C.A., Burke, J.D., Devadathan, K., Kannan, R., et al. (2018). Loss of function mutations in VARS encoding cytoplasmic valyl-tRNA synthetase cause microcephaly, seizures, and progressive cerebral atrophy. Hum Genet 137, 293-303.
103. Friedman, J., Smith, D.E., Issa, M.Y., Stanley, V., Wang, R., Mendes, M.I., Wright, M.S., Wigby, K., Hildreth, A., Crawford, J.R., et al. (2019). Biallelic mutations in valyl-tRNA synthetase gene VARS are associated with a progressive neurodevelopmental epileptic encephalopathy. Nat Commun 10, 707.
104. Siekierska, A., Stamberger, H., Deconinck, T., Oprescu, S.N., Partoens, M., Zhang, Y., Sourbron, J., Adriaenssens, E., Mullen, P., Wiencek, P., et al. (2019). Biallelic VARS variants cause developmental encephalopathy with microcephaly that is recapitulated in vars knockout zebrafish. Nat Commun 10, 708.
105. Taylor, R.W., Pyle, A., Griffin, H., Blakely, E.L., Duff, J., He, L., Smertenko, T., Alston, C.L., Neeve, V.C., Best, A., et al. (2014). Use of whole-exome sequencing to determine the genetic basis of multiple mitochondrial respiratory chain complex deficiencies. JAMA 312, 68-77.

106. Nowaczyk, M.J., Huang, L., Tarnopolsky, M., Schwartzentruber, J., Majewski, J., Bulman, D.E., Forge Canada Consortium, C.R.C.C., Hartley, T., and Boycott, K.M. (2017). A novel multisystem disease associated with recessive mutations in the tyrosyl-tRNA synthetase (YARS) gene. Am J Med Genet A 173, 126-134.
107. Ma, K., Xie, M., He, X., Liu, G., Lu, X., Peng, Q., Zhong, B., and Li, N. (2018). A novel compound heterozygous mutation in VARS2 in a newborn with mitochondrial cardiomyopathy: a case report of a Chinese family. BMC Med Genet 19, 202.
108. Alsemari, A., Al-Younes, B., Goljan, E., Jaroudi, D., BinHumaid, F., Meyer, B.F., Arold, S.T., and Monies, D. (2017). Recessive VARS2 mutation underlies a novel syndrome with epilepsy, mental retardation, short stature, growth hormone deficiency, and hypogonadism. Hum Genomics 11, 28.
109. Tsai, P.C., Soong, B.W., Mademan, I., Huang, Y.H., Liu, C.R., Hsiao, C.T., Wu, H.T., Liu, T.T., Liu, Y.T., Tseng, Y.T., et al. (2017). A recurrent WARS mutation is a novel cause of autosomal dominant distal hereditary motor neuropathy. Brain 140, 1252-1266.
110. Theisen, B.E., Rumyantseva, A., Cohen, J.S., Alcaraz, W.A., Shinde, D.N., Tang, S., Srivastava, S., Pevsner, J., Trifunovic, A., and Fatemi, A. (2017). Deficiency of WARS2, encoding mitochondrial tryptophanyl tRNA synthetase, causes severe infantile onset leukoencephalopathy. Am J Med Genet A 173, 2505-2510.
111. Wortmann, S.B., Timal, S., Venselaar, H., Wintjes, L.T., Kopajtich, R., Feichtinger, R.G., Onnekink, C., Muhlmeister, M., Brandt, U., Smeitink, J.A., et al. (2017). Biallelic variants in WARS2 encoding mitochondrial tryptophanyl-tRNA synthase in six individuals with mitochondrial encephalopathy. Hum Mutat 38, 1786-1795.
112. Hubers, A., Huppertz, H.J., Wortmann, S.B., and Kassubek, J. (2020). Mutation of the WARS2 Gene as the Cause of a Severe Hyperkinetic Movement Disorder. Mov Disord Clin Pract 7, 88-90.
113. Williams, K.B., Brigatti, K.W., Puffenberger, E.G., Gonzaga-Jauregui, C., Griffin, L.B., Martinez, E.D., Wenger, O.K., Yoder, M.A., Kandula, V.V.R., Fox, M.D., et al. (2019). Homozygosity for a mutation affecting the catalytic domain of tyrosyl-tRNA synthetase (YARS) causes multisystem disease. Hum Mol Genet 28, 525-538.
114. Nakajima, J., Eminoglu, T.F., Vatansever, G., Nakashima, M., Tsurusaki, Y., Saitsu, H., Kawashima, H., Matsumoto, N., and Miyake, N. (2014). A novel homozygous YARS2 mutation causes severe myopathy, lactic acidosis, and sideroblastic anemia 2. J Hum Genet 59, 229-232.
115. Sasarman, F., Nishimura, T., Thiffault, I., and Shoubridge, E.A. (2012). A novel mutation in YARS2 causes myopathy with lactic acidosis and sideroblastic anemia. Hum Mutat 33, 1201-1206.
116. Riley, L.G., Cooper, S., Hickey, P., Rudinger-Thirion, J., McKenzie, M., Compton, A., Lim, S.C., Thorburn, D., Ryan, M.T., Giege, R., et al. (2010). Mutation of the mitochondrial tyrosyl-tRNA synthetase gene, YARS2, causes myopathy, lactic acidosis, and sideroblastic anemia--MLASA syndrome. Am J Hum Genet 87, 52-59.
117. Lee, E.Y., Kim, S., and Kim, M.H. (2018). Aminoacyl-tRNA synthetases, therapeutic targets for infectious diseases. Biochem Pharmacol 154, 424-434.
118. Ognjenovic, J., and Simonovic, M. (2018). Human aminoacyl-tRNA synthetases in diseases of the nervous system. RNA Biol 15, 623-634.
119. Rajendran, V., Kalita, P., Shukla, H., Kumar, A., and Tripathi, T. (2018). Aminoacyl-tRNA synthetases: Structure, function, and drug discovery. Int J Biol Macromol 111, 400-414.
120. Retterer, K., Juusola, J., Cho, M.T., Vitazka, P., Millan, F., Gibellini, F., Vertino-Bell, A., Smaoui, N., Neidich, J., Monaghan, K.G., et al. (2016). Clinical application of

whole-exome sequencing across clinical indications. Genetics in medicine : official journal of the American College of Medical Genetics 18, 696-704.
121. Harripaul, R., Vasli, N., Mikhailov, A., Rafiq, M.A., Mittal, K., Windpassinger, C., Sheikh, T.I., Noor, A., Mahmood, H., Downey, S., et al. (2018). Mapping autosomal recessive intellectual disability: combined microarray and exome sequencing identifies 26 novel candidate genes in 192 consanguineous families. Mol Psychiatry 23, 973-984.
122. Li, H., and Durbin, R. (2009). Fast and accurate short read alignment with Burrows-Wheeler transform. Bioinformatics (Oxford, England) 25, 1754-1760.
123. McKenna, A., Hanna, M., Banks, E., Sivachenko, A., Cibulskis, K., Kernytsky, A., Garimella, K., Altshuler, D., Gabriel, S., Daly, M., et al. (2010). The Genome Analysis Toolkit: a MapReduce framework for analyzing next-generation DNA sequencing data. Genome research 20, 1297-1303.
124. Wang, K., Li, M., and Hakonarson, H. (2010). ANNOVAR: functional annotation of genetic variants from high-throughput sequencing data. Nucleic acids research 38, e164.

Section 6: Consortia and networks involved in this study

The Synaptopathies and Paroxysmal Syndromes (SYNaPS) Study Group (http://neurogenetics.co.uk/synaptopathies-synaps/)

Study Group Members:

Prof Stanislav Groppa
Affiliation: Department of Neurology and Neurosurgery, Institute of Emergency Medicine, Chisinau, Republic of Moldova.

Dr. Blagovesta Marinova Karashova
Affiliation: Department of Paediatrics, Medical University of Sofia, Sofia 1431, Bulgaria

Dr. Wolfgang Nachbauer
Affiliation: Department of Neurology, Medical University Innsbruck, Anichstrasse 35, Innsbruck 6020, Austria

Prof. Sylvia Boesch
Affiliation: Department of Neurology, Medical University Innsbruck, Anichstrasse 35, Innsbruck 6020, Austria

Dr. Larissa Arning
Affiliation: Department of Human Genetics, Ruhr-University Bochum, Bochum 44801, Germany

Prof. Dagmar Timmann
Affiliation: Braun Neurologische Universitätsklinik Universität Essen, Hufelandstr 55, Essen D-45122, Germany

Prof. Bru Cormand
Affiliation: Department of Genetics, Universitat de Barcelona, Barcelona 08007, Spain

Dr. Belen Pérez-Dueñas
Affiliation: Hospital Sant Joan de Deu, Esplugues de Llobregat 08950, Barcelona, Spain

Dr Gabriella Di Rosa, MD, PhD
Affiliation: Department of Pediatrics, University of Messina, Messina 98123, Italy

Prof. Jatinder S. Goraya, MD, FRCP
Affiliation: Division of Paediatric Neurology, Dayanand Medical College & Hospital, Ludhiana, Punjab 141001, India

Prof. Tipu Sultan
Affiliation: Division of Paediatric Neurology, Children's Hospital of Lahore, Lahore 381-D/2, Pakistan

Affiliation: IRCCS Foundation, Neurological Institute “Carlo Besta”, Molecular Neurogenetics, 20126 Milan, Italy

Dr. Eugenia Borgione
Affiliation: Laboratorio di Neuropatologia Clinica, U.O.S. Malattie, Neuromuscolari Associazione OASI Maria SS. ONLUS – IRCCS, Via Conte Ruggero 73, 94018 Troina, Italy

Dr. Simona Portaro
Affiliation: IRCCS Centro Neurolesi "Bonino Pulejo", SS113, c.da Casazza, 98124 Messina, Italy

Dr. Benigno Monteagudo Sanchez
Affiliation: Hospital Arquitecto Marcide, Avenida de la Residencia S/N, Ferrol (A Coruña), 15401 Spain

Dr. Richard Boles
Affiliation: Courtagen Life Sciences, 12 Gill Street Suite 3700, Woburn, MA 01801 USA

Prof. Savvas Papacostas
Affiliation: Neurology Clinic B, The Cyprus Institute of Neurology and Genetics, 6 International Airport Road, 1683 Nicosia, Cyprus

Dr. Michail Vikelis
Affiliation: Iatreio Kefalalgias Glyfadas, 8 Lazaraki str, 3rd floor, 16675, Athens, Greece

Prof Eleni Zamba Papanicolaou
Affiliation: The Cyprus Institute of Neurology & Genetics, Nicosia, Cyprus

Dr Efthymios Dardiotis
Affiliation: UNIVERSITY HOSPITAL OF LARISSA, NEUROLOGY Department, Greece

Prof Shazia Maqbool
Affiliation: Department of Developmental and Behavioral Pediatrics, CH&ICH, Lahore, Pakistan

Prof Shahnaz Ibrahim
Affiliation: Department of Pediatrics and child health, Aga Khan University, Karachi, Pakistan

Prof Salman Kirmani
Affiliation: Department of Paediatrics & Child Health, The Aga Khan University, Karachi , Pakistan

Dr. Nuzhat Noureen Rana
Affiliation: Department of Paediatric Neurology, Children Hospital Complex and ICH, Multan, Pakistan

Dr. Osama Atawneh
Affiliation: Hilal Pediatric Hospital Hebron, Hebron West Bank, Palestine

Prof George Koutsis
Affiliation: Neurogenetics Unit, Neurology Department, Eginition Hospital, National and Kapodistrian University, Athens, Greece

Prof Salvatore Mangano
Affiliation: Unità di Neuropsichiatria Infantile, AOUP "P.Giaccone" Palermo, Italy

Dr Carmela Scuderi
Affiliation: Associazione Oasi Maria SS, 94018 Troina, Italy

Dr Eugenia Borgione
Affiliation: Associazione Oasi Maria SS, 94018 Troina, Italy

Dr Giovanna Morello
Affiliation: Institute of Neurological Sciences, National Research Council, Mangone, Italy

Dr Tanya Stojkovic
Affiliation: Institute of Myology, Hôpital La Pitié Salpêtrière, Paris, France

Prof Massimo Zollo
Affiliation: CEINGE, Biotecnologie Avanzate S.c.a.rl., Naples, Italy

Dr Gali Heimer
Affiliation: University Hospital of Tel Aviv, Tel Aviv, Israel

Prof Yves A. Dauvilliers
Affiliation: University Hospital Montpellier, Montpellier, France

Prof Pasquale Striano
Affiliation: Institute “Giannina Gaslini”, Genova, Italy

Dr Issam Al-Khawaja
Affiliation: Albashir University Hospital, Amman, Jordan

Dr Fuad Al-Mutairi
Affiliation: King Saud University, Riyadh, Saudi Arabia

Prof Sherifa Ahmed Hamed
Affiliation: Assiut University Hospital, Assiut, Egypt

Prof. Mohamed A. Abd El Hamed
Affiliation: Department of Neurology and Psychiatry, Assuit University Hospital, Assiut, Egypt.

Dr. Samson Khachatryan

Affiliation: "Somnus" Neurology Clinic Sleep and Movement Disorders Center, Yerevan, Armenia

Dr. Ulviyya Guliyeva
Affiliation: Mediclub clinic, Baku, Azerbaijan

Dr. Sughra Guliyeva
Affiliation: Mediclub clinic, Baku, Azerbaijan

Dr. Kamran Salayev
Affiliation: Azerbaijan State Medical University, Baku, Azerbaijan

Dr. Georgia Xiromerisiou
Affiliation: Department of Neurology, Medical School, University of Thessaly, Larissa, Greece

Dr. Liana Fidani
Affiliation: Department of Biology, Medical School, Aristotle University, Thessaloniki, Greece

Dr. Cleanthe Spanaki
Affiliation: Department of Neurology, Medical School, University of Crete, Heraklion, Greece

Prof. Mhammed Aguennouz
Affiliation: Department of Clinical and Experimental Medicine, University of Messina, Messina 98123, Italy

Prof. Gabriella Silvestri
Affiliation: Institute of Neurology, Università Cattolica del Sacro Cuore, Rome, Italy

Dr. Chingiz Shashkin
Affiliation: Kazakh National State University, Almaty, Kazakhstan

Dr. Nazira Zharkynbekova
Affiliation: Shymkent Medical Academy, Kazakhstan

Dr. Kairgali Koneyev
Affiliation: Kazakh National State University, Almaty, Kazakhstan

Prof. Abdullah Al-Ajmi
Affiliation: Neurology Unit, Department of Medicine, Al-Jahra Hospital, Kuwait

Prof. Shen-Yang Lim
Affiliation: Department of Biomedical Science, Faculty of Medicine, University of Malaya, Malaysia

Dr. Farooq Shaikh
Affiliation: Jeffrey Cheah School of Medicine and Health Sciences, Monash University Malaysia

Prof. Mohamed El Khorassani
Affiliation: Children's Hospital of Rabat, University of Rabat, Rabat 6527, Morocco

Prof. Arn M J M van den Maagdenberg
Affiliation: Leiden University Medical Center, Albinusdreef 2, Leiden 2333, Netherlands

Prof. Njideka U. Okubadejo
Affiliation: College of Medicine, University of Lagos (CMUL) & Lagos University Teaching Hospital, Idi Araba, Lagos State, Nigeria

Dr. Oluwadamilola O. Ojo
Affiliation: College of Medicine, University of Lagos, (CMUL) & Lagos University Teaching Hospital (LUTH), Idi Araba, Lagos State, Nigeria.

Prof. Kolawole Wahab
Affiliation: University of Ilorin Teaching Hospital (UITH), Ilorin, Kwara State, Nigeria.

Dr. Abiodun H. Bello
Affiliation: University of Ilorin Teaching Hospital (UITH), Ilorin, Kwara State, Nigeria.

Prof. Sanni Abubakar
Affiliation: Ahmadu Bello University, Zaria, Kaduna State, Nigeria.

Dr. Yahaya Obiabo
Affiliation: Delta State University Teaching Hospital, Oghara, Delta State, Nigeria.

Dr. Ernest Nwazor
Affiliation: Federal Medical Centre, Owerri, Imo State, Nigeria.

Dr. Oluchi Ekenze
Affiliation: University of Nigeria Teaching Hospital, Ituku-Ozalla, Enugu State, Nigeria.

Dr. Uduak Williams
Affiliation: University of Calabar Teaching Hospital, Calabar, Cross Rivers State, Nigeria.

Dr. Alagoma Iyagba
Affiliation: University of Port Harcourt Teaching Hospital, Port Harcourt, Rivers State, Nigeria.

Dr. Lolade Taiwo
Affiliation: Babcock University, Ilishan, Remo & Federal Medical Centre, Abeokuta, Ogun State, Nigeria.

Prof. Morenikeji Komolafe
Affiliation: Obafemi Awolowo University Teaching Hospital (OAUTH), Ile-Ife, Osun State, Nigeria.

Dr. Olapeju Oguntunde
Affiliation: Lagos University Teaching Hospital (LUTH), Nigeria.

Dr. Konstantin Senkevich
Affiliation: Almazov Medical Research Centre and Pavlov First Saint Petersburg State Medical University, Saint-Petersburg, Russia

Prof. Fowzan S Alkuraya
Affiliation: King Faisal Specialist Hospital and Research Center, Riyadh, Saudi Arabia

Dr. Ganieva Manizha
Affiliation: Avicenna Tajik State Medical University, Dushanbe, Tajikistan

Dr. Maksud Isrofilov
Affiliation: Avicenna Tajik State Medical University, Dushanbe, Tajikistan

Dr. Erin Torti
Affiliation: GeneDX, Gaithersburg, Maryland, USA.